NTNU
Norwegian University of
Science and Technology

Residual Strength of Composite Hulls after Impact

Pål Duus

Norwegian University of Science and Technology
Department of Engineering Design and Materials

Abstract

Norsafe MILPRO boats operates in different waters at high speeds. The chance of hitting unknown objects e.g. floating logs is present. Being able to judge the damages and the residual strengths to these impacts are desirable. To reach this goal, the first step is to focus on the basics of how flat panels of glass reinforced polymer composites will behave.

The composite hulls on the Norsafe MILPRO boats are made out of a sandwich structure which consists of two glass reinforced polymer composite skins separated by a lightweight core. Post-impact analysis of the composite skins will be studied with focus on the residual strength properties.

Low-velocity impact events by an impactor of a hemispherical tip on composite specimen supported by a rigid substrate will be performed. The damage tolerance of the impact event has been investigated through tensile-, compression- and flexural tests.

Two laminates have been studied. A cross-ply laminate with layup $[0/90]_5$ and a quasi-isotropic laminate with layup $[(0/90/\pm 45)_2 0/90]$. Both laminates show a reduction in the residual strength in tension, compression and bending.

A quantitative damage model of predicting the impact damage out of the size of a clean circular hole has been utilized.

Sammendrag

Norsafe MILPRO båter opererer i ulike farvann ved høye hastigheter. Sjansen for å treffe ulike gjenstander f.eks. flytende tømmerstokker, vil være til stede. Å kunne bedømme skaden og reststyrken etter en slik hendelse vil være ønskelig. Det første skrittet for å nå et slikt mål, vil være å fokusere på slagstyrken til flate paneler av glassfiber.

Komposittskrogene på Norsafe MILPRO skrog består av en sandwichstruktur av to glassfiberlag adskilt av en lett kjerne. En analyse av disse komposittlagene vil bli undersøkt med fokus på reststyrkeegenskaper.

Slag ved bruk av en halvkuleformet sylindrisk annslagsinnretning vil bli utført på flere komposittprøver. Reststyrken etter disse hendelsene vil bli undersøkt gjennom strekk-, kompresjons og bøyetester.

To laminater har blitt undersøkt. Ett med opplegget $[0/90]_5$ og et annet laminat med opplegget $[(0/90/\pm 45)_2 0/90]$. Begge laminater viser en reduksjon i reststyrken i strekk, kompresjon og bøying.

En kvantitativ metode for å forutsi reststyrken av slagskaden er gjennomført. Den tar utgangspunkt i å måle omfanget av selve skaden og sammenligne med reststyrken til et sirkulært hull.

Preface

This master thesis is written in the spring of 2016 as a part of fulfilment of the Master of Science degree at the Norwegian University of Science and Technology, under the supervision of Professor *Andreas T. Echtermeyer*.

The work is a collaboration between NTNU and Norsafe AS as a part of further investigation on Norsafe MILPRO boat hulls.

The present work was performed at the Department of Engineering Design and Materials, Faculty of Engineering Science and Technology (NTNU).

I would like to thank my supervisor Andreas Echtermeyer for his guidance and help, Carl-Magnus Midtbø for support in connection with the experimental work and my supervisor at Norsafe AS, Gunnar Semb, for good advices during this project.

Pål Thomas Ribe Duus

Trondheim, 10.06.2016

Table of Contents

List of Tables

List of Figures

Abbreviations

Symbol	=	definition
E_{1t}	=	Tensile Young's Modulus in longitudinal direction
E_{2t}	=	Tensile Young's Modulus in transverse direction
E_{3t}	=	Tensile Young's Modulus in out-of-plane direction
ν_{12}	=	Longitudinal Poisson's ratio
ν_{13}	=	Through thickness Poisson's ratio
ν_{23}	=	Out-of-plane Poisson's ratio
G_{12}	=	In-plane shear moduli
G_{13}	=	Through thickness shear moduli
G_{23}	=	Out-of-plane shear moduli
X^T	=	Longitudinal tensile strength
X^C	=	Longitudinal compressive strength
Y^T	=	Transverse tensile strength
Y^C	=	Transverse compressive strength
S^L	=	Longitudinal shear strength
S^T	=	Transverse shear strength
G_{ft}^C	=	Fiber Tensile Fracture Energy
G_{fc}^C	=	Fiber Compressive Fracture Energy
G_{mt}^C	=	Matrix Tensile Fracture Energy
G_{mc}^C	=	Matrix Compressive Fracture Energy
$\eta_L^{T,C}$	=	Viscosity coefficient for longitudinal (fiber) tensile, compression
$\eta_T^{T,C}$	=	Viscosity coefficient for transverse (matrix) tensile, compression
$ALLCD$	=	Energy associated during viscous regularization
$ALLSE$	=	Energy associated with elastic strain energy
2σ	=	Two standard deviations

Chapter 1

Introduction

Composite materials are commonly used in marine applications. These materials have generally a good fatigue resistance and corrosion suppression. However, they have some challenges in their ability to resist damages, such as damages due to low-velocity impact. Metallic structures, have the ability of absorbing energy caused by an impact through plastic deformation. For brittle materials, such as glass-fiber reinforced plastic composites, impact-induced damages will be more critical. Energy will only be absorbed through elastic deformations and through damage modes. Impact damages on composite laminates could cause a significant reduction in strength, even barely visible ones. Such an impact damage might also be close to invisible due to painting and coating. The types of composite material and their applications varies widely so that no single test could represent their subsequent effect. This itself tells the importance of post-impact investigation of this type of composite laminates.

Given the scenario; A Norsafe Munin high speed patrol vessel is on a mission at night. Due to bad visibility it suddenly hits a log floating in the sea. The crew aboard are uncertain on the extent of the damage. In order to continue the mission, they need to know if the vessel could be operated with its full functionality or not. Therefore, the Munin S1200 docks at a shipyard nearby. They will do some simple inspections of the damage and give a feedback if the vessel is operational or not and more important the safety of the boat.

Figure 1.1: Norsafe's Munin S1200 (Photo courtesy of Norsafe).

The residual strength might have a significant reduction due to these damages. Being able to judge the damage tolerance which is related to the safety of the boat, is therefore desirable.

The hulls consist of two skins of glass reinforced polymer composites separated by a lightweight core. The damage tolerance by impact-induced damages of the composite skin of two different layups will be investigated. A cross-ply and a quasi-isotropic laminate, respectively.

The pre-study of this topic focused on how glass fiber composites responded to different impact-induced damages. Methods on creating impact damages above the damage initiation threshold and performing successfully tensile tests on composite materials were studied. This master thesis will focus on creating larger impact damages including all damage modes in order to get a wider knowledge of the damage tolerance on glass reinforced composites.

Investigations of a quantitative method judging the residual strength after e.g. the impact damage induced in the scenario given above, will be done. Low-velocity impact of different magnitudes will be conducted on face sheet specimen placed on a rigid substrate by an impactor with a hemispherical tip. Post-impact analysis will be studied with focus on the residual strength properties. An equivalent hole to impact damage will be utilized that quantifies the impact damage in terms of circular hole size.

Chapter 2

Basic Theory

2.1 Low-velocity impact on composites

Fiber reinforced composites are known for their high mechanical properties, with high stiffness-to-weight and strength-to-weight ratios. However, the material is sensitive to many aspects on in-service use as e.g. impact-induced damages which many studies have shown will reduce the strength of the material. Impact is generally divided into low-velocity and high-velocity impact. High-velocity impact or ballistic impact events occur when the structure does not have time to respond which results in very localized damage. The boundary effects could be ignored since the stress waves will not reach the end of the structure before the impact is over. After a low-velocity impact, the structure will have time to respond as the stress waves propagate through the material. This will lead to elastically absorption of the impact energy. High-velocity is characterized as penetration induced fiber breakage of the composite while low-velocity impact will lead to matrix cracking, fiber failure and delamination [13]. This thesis will focus on fiber breakage, matrix cracking and delamination after a low-velocity impact event in the speed range of 1-10 m/s.

The level of impact energies in most test machines are varied by the drop height or the weight of the impactor [9].

2.1.1 Damage modes

The damage modes in low-velocity impact are mainly matrix cracking, delamination and fiber failure. Generally, damage is initiated by matrix cracks which creates delaminations between plies of different fiber orientation.

Matrix cracking

Matrix damage is the first to occur after an impact damage. In unidirectional laminates the matrix damage is usually oriented in planes parallel to the fiber direction [2]. Two different types of matrix cracks are generally observed, shear and tensile cracks. Tensile cracks are introduced when the in-plane normal stress exceed the transverse tensile strength in the ply. Tensile cracks are generally a result of the flexural response. Shear cracks are related to high contact stresses acting between the impactor and the composite plate. They could also be generated by the transverse shear stresses resulting from the flexural deformation during the impact event. The formation of the matrix crack pattern is hard to predict but it is dependent on the thickness of the laminate. Matrix cracks will propagate from the top surface and downwards in a pine tree pattern, due to the high contact stresses acting between the impactor and plate. For a thin plate structure, the opposite occurs. The matrix crack propagation starts at the bottom due to tensile matrix cracks induced by the flexural bending which results in a reverse pine-tree pattern (ref. figure 2.1).

(a)   **(b)**
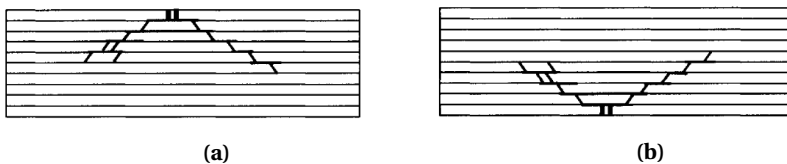
Figure 2.1: Pine tree (a) and pine tree reverse (b) damage patterns [2].

Generally, matrix damages will not significantly contribute to a reduction in the residual properties of the laminate. But an intralaminar matrix crack could initiate delamination.

Delamination

When a crack runs between plies of different fiber orientation and lead to separation between them, delaminations appear. Research show that delaminations occurs only at interfaces between plies of different fiber directions [2]. The shape of the delamination are usually oblong or as a peanut in the fiber direction as figure 2.2. Delamination has a severe effect on the residual compressive properties of the material.
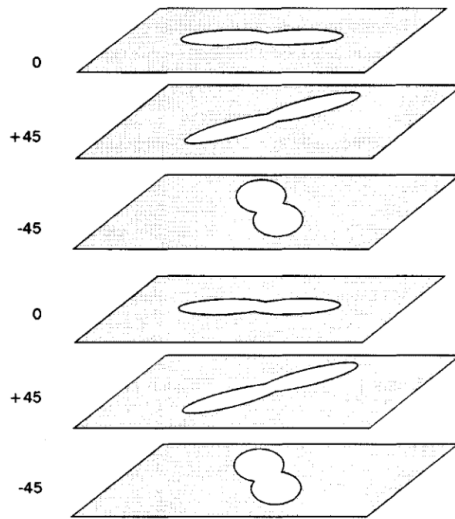
Figure 2.2: Orientations of delaminations.

Fiber failure

Fiber failure occurs after matrix cracking and delamination. It is induced due to high contact forces right below the impactor. Fiber failure could also be initiated by bending stresses at the bottom plies. The role of fiber is significant since this constituent is carrying the majority of the tensile load. Once the threshold for fiber failure is reached the residual strength will reduce remarkably. The fibers ability to absorb energy is a fundamental parameter in determining the impact resistance. Fibers that are able to absorb high elastic energies are more impact resistant than fibers with low energy absorption capacity [4].

2.1.2   Parameters affecting impact damage

Material properties affect the stiffness of the composite and will have a significant effect on the dynamic response of the structure. The thickness, plate size and boundary conditions are parameters that have an influence on the stiffness and will therefore be important parameters affecting the impact damage. Other factors as the size, weight, velocity and incident angle of the impactor need also to be considered [2].

Simply supported beams tend to fail in flexure, whereas short thick specimen tend to fail in an intralaminar mode [3]. In this thesis, the impact test will be conducted by an impactor with hemispherical tip on a specimen supported by a rigid substrate.

Stacking sequence of multidirectional laminates are strongly dependent on specific orientations of the plies. Damage appears to be greatest in crossply laminates with a 90° orientation [4].

The rigid substrate support will avoid deflections of the specimen and will act as a thick specimen without support. The target will act as a stiff structure and cause matrix damages in a pine tree pattern from the impact face at the top and downwards (figure 2.1a). The high contact force between the impactor and the local target will cause fiber breakage at the top plies if the threshold for fiber initiation failure is reached. Yigit and Christoforou [21] showed the effect of laminate thickness impacted on specimen supported by a rigid substrate. The impact force remains the same, but the damage decreases with increasing thickness of the target. JM Koo et. al. [10] used similar boundary condition in their studies resulting in mainly local deformations rather than deflections of the specimen.

Mitrevski, Marshall and Thomson [11] have investigated on the effect on impactor shape on the resulting damage. By using impactors with a tip of hemispherical, ogival and conical shape. They were showing that the hemispherical impactor produced the largest damage area by delamination, whereas more fiber breakage was found in the specimen impacted by the conical impactor.
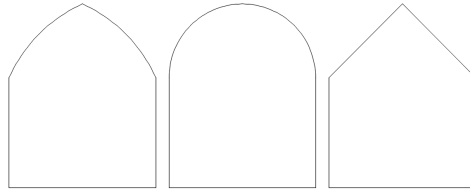
Figure 2.3: From left to right; Ogival, hemispherical and conical shape.

2.2   Residual strength

The general trend for the strength reduction after impact is that low impact energies creates little or no damages without any effect. When the energy increases, strength reduces more significantly and then levels off. Impact damages containing matrix cracks, delaminations and fiber failures have a complex damage pattern and are difficult to predict in detail.

Several investigators have suggested that the stress distribution around an impact damaged zone shows the same distribution around a crack, a clean hole or a softer inclusion loaded in tension.

2.2.1   Whitney and Nuismer's model

Whitney and Nuismer [20] proposed two failure criteria based on stress distribution around holes and cracks. These would predict the uniaxial tensile strength of laminated composites with a through the thickness discontinuity of a general shape. The criteria uses two parameters, the unnotched tensile strength and a characteristic distance. The characteristic distance is used as a free parameter to be fixed at best fitting the experimental data. The two criteria are called the point stress- and the average stress criterion.

Point stress criterion

This criterion assumes that the stress at a characteristic distance d_0 from the hole, first reaches the unnotched tensile strength of the material. For an infinite wide anisotropic plate with a circular hole of radius R under uniform uniaxial tension, the notch strength is given by

$$\frac{\sigma_N^\infty}{\sigma_0} = (1 - \xi_1^2)^{1/2} \tag{2.1}$$

where $\xi_1 = R/(R + d_0)$ and σ_N^∞ is the far-field notch strength.

Average stress criterion

The average stress criterion assumes that failure occurs when the average of the stress over some distance a_0 ahead of the hole reaches the unnotched tensile strength. For an infinite wide anisotropic plate with a circular hole of radius R under uniform uniaxial tension, the notch strength is given by

$$\frac{\sigma_N^\infty}{\sigma_0} = \left(\frac{1 - \xi_2}{1 + \xi_2}\right)^{1/2} \tag{2.2}$$

where $\xi_2 = R/(R + a_0)$.

Whitney and Nuismer found that the average stress criterion gave a better fit to experimental data for glass-epoxy composites than did the point stress criterion.

For a finite-width specimen, a correction factor are given

$$\frac{K_T}{K_T^{\infty}} = \frac{2 + (1 - 2R/W)^3}{3(1 - 2R/W)} \tag{2.3}$$

where W is the finite width of the specimen.

2.2.2 Caprino's model

Caprino [5], [6] proposed a similar model to Whitney and Nuismer. He did a comparison with this model and showed that Whitney and Nuismer's model is reliable when small holes or notches are considered, while his model is more effective estimating the residual strength for larger notches and holes.

$$\frac{\sigma_R}{\sigma_0} = \left(\frac{L_0}{L}\right)^m \tag{2.4}$$

where σ_R is the residual strength, σ_0 is the strength of the unnotched material, L_0 is the dimension of the characteristic defect and $2L$ is the length of the notch or hole. m and L_0 must be experimentally determined. Equation 2.4 is only valid when $L \geq L_0$. From a physical point of view, L_0 represents a notch that will not affect the residual strength.

Through experimental results, Caprino also showed that the parameter m seems to be independent of the material system, type of laminate and shape of discontinuity for fiber dominated materials [6].

Caprino suggested a model for predicting the residual strength for holes or notches. He made a correlation between the impact energy and the equivalent notch size, which adequately not only fits the experimental results for residual tensile strength but also the compressive strength of laminate composites.

$$\frac{\sigma_R}{\sigma_0} = \left(\frac{E_{th}}{E_i}\right)^{\alpha} \tag{2.5}$$

where σ_R is the residual strength, σ_0 is the strength of the unnotched material, E_{th} and E_i is the threshold and the incident impact energy, respectively.

Several investigators have used this model for the analysis of the experimental results. JM Koo [10] used Caprino's model in his study on CFRP composites and showed that it worked well for impactors with a hemispherical tip performed on specimen supported by a rigid supported by rigid plane.

2.3 Finite element modelling

2.3.1 Hashin damage criterion

The Hashin failure criterion has been used to simulate initial damage creation in unidirectional fiber composites in Abaqus/Standard [1]. It has been used to predict fiber failure and matrix failure modes. The criteria are presented below.

Fiber tension ($\hat{\sigma}_{11} \geq 0$) :

$$F_f^t = \left(\frac{\hat{\sigma}_{11}}{X^T}\right)^2 + \alpha\left(\frac{\hat{\tau}_{12}}{S^L}\right)^2 \tag{2.6}$$

Fiber compression ($\hat{\sigma}_{11} < 0$) :

$$F_f^c = \left(\frac{\hat{\sigma}_{11}}{X^C}\right)^2 \tag{2.7}$$

Matrix tension ($\hat{\sigma}_{22} \geq 0$) :

$$F_m^t = \left(\frac{\hat{\sigma}_{22}}{Y^T}\right)^2 + \left(\frac{\hat{\tau}_{12}}{S^L}\right)^2 \tag{2.8}$$

Matrix compression ($\sigma_{22} < 0$) :

$$F_m^t = \left(\frac{\hat{\sigma}_{22}}{2S^T}\right)^2 + \left[\left(\frac{Y^C}{S^T}\right)^2 - 1\right]\left(\frac{\hat{\sigma}_{22}}{Y^C}\right) + \left(\frac{\hat{\tau}_{12}}{S^L}\right)^2 \tag{2.9}$$

$\hat{\sigma}_{11}$, $\hat{\sigma}_{22}$ and $\hat{\tau}_{12}$ are components of the effective stress tensor, $\hat{\sigma}$. X^T, X^C, Y^T, Y^C, S^L and S^T denotes the longitudinal tensile and compressive strengths, the transverse tensile and compressive strengths and the longitudinal and transverse shear strengths, respectively.
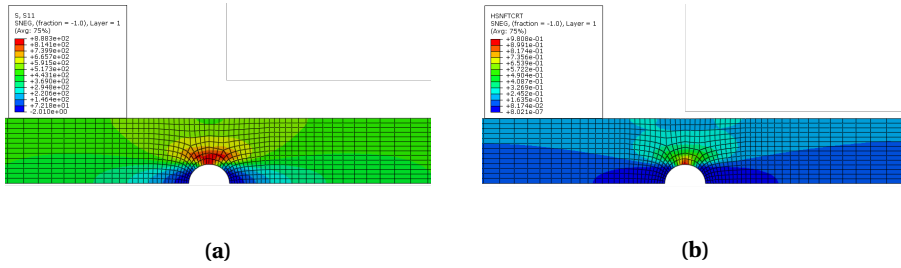
Figure 2.4: Hashin fiber tension criteria (a) and the stress state at the equivalent time increment (b).

Once one of the failure criteria reaches the value of one, the stiffness properties of the element reaches zero. Figure 2.4a shows a notch model of the Hashin fiber tension criteria were some elements have reached the value of one (the red elements), while figure 2.4b shows the stress in the longitudinal direction at the same time increment.

2.3.2 Viscous regularization

For materials that exhibit e.g. stiffness degradation, the model often leads to convergence difficulties in implicit analysis programs, such as Abaqus/Standard. Viscous regularization is one such parameter that introduces localized damping to overcome convergence difficulties. It is an iterative procedure to overcome any convergence issues. Using a small value of the viscosity parameter (small compared to the characteristic time increment) will improve the convergence of the model without compromising the results.

2.3.3 Damage evolution

To describe the post-damage initiation behavior, the damage evolution model is used. The stress is in this stage described as $\sigma = \mathbf{C}_d \epsilon$, where ϵ is the strain and $\mathbf{C}_d$ is the damaged elasticity matrix on the form

$$\mathbf{C}_d = \frac{1}{D} \begin{bmatrix} (1-d_f)E_1 & (1-d_f)(1-d_m)v_{21}E_1 & 0 \\ (1-d_f)(1-d_m)v_{12}E_2 & (1-d_m)E_2 & 0 \\ 0 & 0 & (1-d_s)G \end{bmatrix} \tag{2.10}$$

where $D = 1 - (1-d_f)(1-d_m)v_{12}v_{21}$, d_f, d_m and d_s reflects the current state of fiber damage, matrix damage and shear damage, respectively.

The damage variables d_f, d_m and d_s are derived from damage variables d_f^t, d_f^c, d_m^t and d_m^c corresponding to the four failure modes.

For each failure mode, the energy dissipated due to failure, G^c, must be specified. This corresponds to the area under the curve, shown in figure 2.5. Four parameters are set where G_{ft}^C, G_{fc}^C, G_{mt}^C and G_{mc}^C represents energy dissipated during damage for fiber tension, fiber compression, matrix tension and matrix compression respectively. The positive slope of the curve show the stress-strain prior to damage initiation and corresponds to the linear elastic behavior while the negative slope corresponds to the damage evolution after the damage initiation [1].
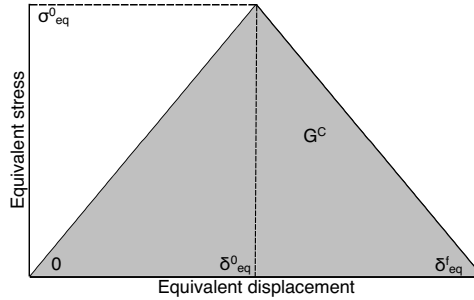
Figure 2.5: Linear damage evolution.

Chapter 3

Experimental work

3.1 Material Production

Fabrication of the composite laminate were done at Norsafe AS. The laminates produced are representative of a panel from a boat hull. The composite consists of biaxial knitted E-glass fabrics with chopped strand mat (figure 3.1). A single mat of the E-glass fabrics contains of two individual plies. One mat with [0/90°] plies and one mat with [±45°].

Two different panels were made by vacuum assisted resin infusion, *Laminate A* with layup $[0/90]_5$ and *Laminate B* with $[(0/90/\pm45)]_2/0/90]$ and cured at room temperature for more than one week. Both panels with dimensions of $1200x1500$ mm and two different thicknesses with an average of 4.0 ± 0.2 mm and 3.6 ± 0.2 mm for Laminate A and B, respectively. The average dimensions of the coupons are listed in table 3.1 Specimen were then cut out by a CNC water-jet cutting system with average dimensions of 27.0 ± 0.2 mm width and length of 244.0 ± 0.6 mm into a total number of approximately 240 specimens. By this fully automated cutting method, the coupons got approximately the equivalent dimensions and ensured straight cuts and fiber alignment.

By cutting the plate into this large amount of coupons prior to the impact testing, the efficiency of mechanical testing will increase drastically while ensuring the equivalent dimensions on each testing coupon. If the impact testing where conducted on a bigger plate and then cut into smaller coupons, it would require higher precision in the cutting process and the cutting process itself might affect the impact damage. A misalignment of the fibers relative to the coupon of 1 degree can reduce the measured strength of a unidirectional laminate by over 30% [9].

This will result in more consistent testing results and the economic aspect is also present since less material is used per experimental test.

The mechanical properties of the E-glass vinylester composite with a fiber volume fraction of 50 % are listed in 3.2.

(a)   (b)
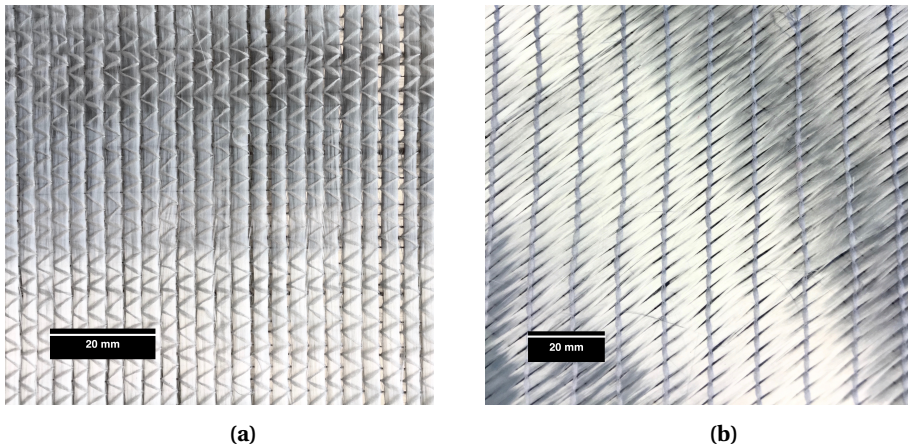
Figure 3.1: [0/90] fabric (a) and [+45/-45] fabric (b).

Table 3.1: Average coupon dimensions, based on a random population of 30 coupons.

Dimensions	Laminate A	Laminate B
Length, L (mm)	244.3	244.3
Width, w (mm)	27.6	27.6
Thickness, t (mm)	4.0	3.6
Cross section area (mm^2)	108.7	99.1

Table 3.2: Mechanical properties of E-glass vinylester (data from Norsafe).

Property	Unit	Mean value
v_f	%	50
ρ	g/mm^3	0.00186322
E_{1t}	GPa	42.28
E_{2t}	GPa	9.65
E_{3t}	GPa	9.65
v_{12}	-	0.27
v_{13}	-	0.27
v_{23}	-	0.43
G_{12}	GPa	3.62
G_{13}	GPa	3.62
G_{23}	GPa	3.43
X^T	MPa	1133.42
X^C	MPa	755.78
Y^T	MPa	64.83
Y^C	MPa	194.50
S^{12}	MPa	96.10

3.1.1 Quality

Out of the populations of coupons, a representative selection of specimen from each laminate where visually inspected for voids, presence of delamination on the cutting edges, matrix absorption and surface smoothness. The results from the inspection are listed in the Appendix (tables 3 - 6). Voids on a selection were inspected in microscopy. Coupons with obvious bad surface smoothness or other visual defects, were excluded from testing. Figure 3.2a shows microscopy image of an airbuble detected visually.

| (a) | (b) |
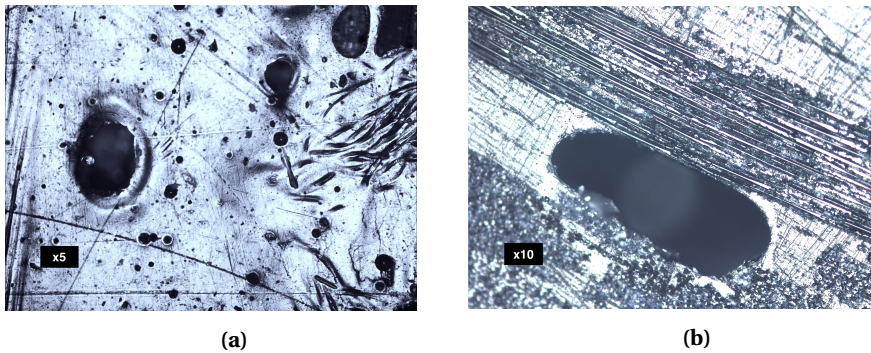
Figure 3.2: Air bubbles at outer surface (x5 scaling) (a), Microvoid at the cross section surface at Laminate B, x10 scaling (b).

3.1.2 Fiber fraction through burn-off

The volume fraction can be calculated from the initial weight of composite and fiber's weight. Burn-off tests were conducted to estimate the volume fraction of fibers, V_f. Volume fraction could be determined when the densities are known. By measuring the weight of the coupon before and after burning, the weight of both the fibers and the matrix was determined (table 3.3).

Table 3.3: Weight on fibers and vinylester

Measured data	Laminate A	Laminate B
Vinylester weight	12.6 g	13.4 g
Fiber weight	31.6 g	31.4 g

3.2 Equivalent hole

In order to investigate the possibility of utilizing an equivalent hole to impact damage, specimen with drilled circular central holes were tested in tension and compression to compare with the residual strength of the impact damage once. Clean circular holes with radius of 1.5, 2.0, 3.0 and 4.0 mm were drilled in specimens with groups of 3 specimens per hole size, located at the center of the specimen. This procedure was done on both laminates.

Figure 3.3: Coupons with circular holes (here, R = 4.0 mm).

3.3   Impact drop test

3.3.1   Experimental setup

Impact tests were carried out by an impactor with a mass of 8.25 kg and hemispherical tip of 100 mm in diameter through a guiding tube with inside diameter 110 mm. Different impact energies were selected by varying the falling height. Four different heights 350, 850, 1350 and 1750 mm with corresponding impact energy of 28, 69, 109 and 142 J respectively. Frictional forces between the tube and impactor, drag and other minor effects are neglected. These energy levels would most likely produce a specter of impact damages.

The specimen was placed on a steel foundation with thickness of 7.0 mm, preventing out of plane motion. This test method will obviously increase the flexural rigidity resulting in a higher impact energy for the specified damage initiation and propagation, compared to a simple supported beam [14]. This type of test could be compared to the damages initiated on a thick composite laminate where deflection could be neglected. The steel foundation was moved after each impact test avoiding damage effects due to the dented region on the steel foundation caused by the impactor. The impactor was guided to hit the center of the specimen. Repeated impacts were prevented. In order to keep the variables to a minimum, the same impact drop tests were performed on both laminates.

Figure 3.4: Impact drop tower.
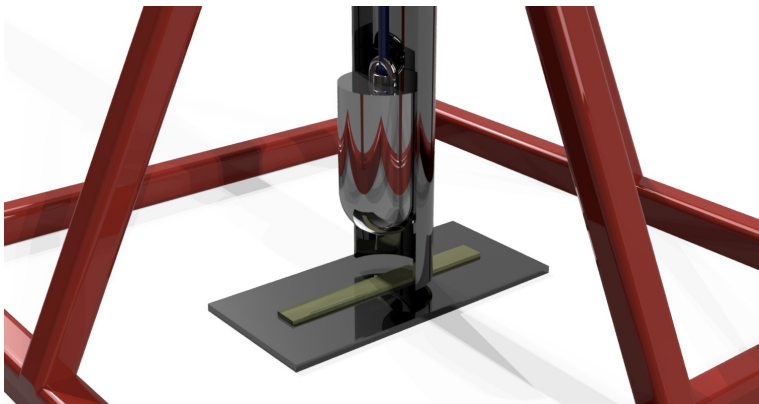
Figure 3.5: Drop tower, close.

3.4 Mechanical testing

Tensile, compression and flexural tests were conducted to measure the residual strength of the two composite layups. All tests were conducted on an Instron 8800 hydraulic machine with pneumatic side action grips and a maximum load capacity of 100 kN. In order to get reasonable results, series of 5 specimens each impact damage in addition to undamaged coupons (as a reference) were tested in each mechanical test. For the circular hole specimen, series of 3 specimens were tested. The following procedures have been carried in similar manner on all coupons from both laminates.
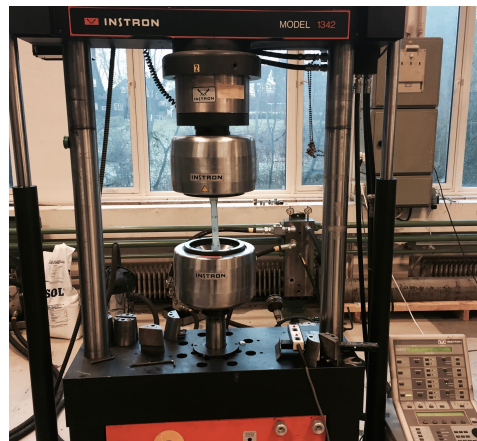
Figure 3.6: Mechanical test machine, Instron 8800.

Each load-displacement curve is found in the Appendix. Each coupon was labeled with an unique code, and each series was conducted at the same day. Pictures and videos were captured during the tensile test to investigate the development of the impacted damage zone, initiation of fracture and after the test to investigate the failure modes.

3.5   Tensile testing

3.5.1   Test procedure

The tensile tests were carried out with ASTM D3039 as a guiding reference with a constant cross-head speed of 2.0 mm/min, at room temperature. Catman Data Acquisition software were used to record load and displacement, calibrated ahead of the tests. The specimens were gripped with hydraulic grips with cross-cut pattern and a gripping cloth of 320 grit (product name *Lion's cloth*) where a pressure of 1400 psi was applied. This will ensure the specimen to be held at the maximum load without slippage and thereby not causing local damage in the grip section. Care was taken when placing the specimen into the testing machine. A misalignment of the coupon within the test machine could lead to a scatter of the results [9]. The coupons were therefore carefully aligned in the grips to obtain correct loading results. It was also important to align the grips parallel to each other. A rotation about the loading axis will exert torsion moments in the specimen and cause premature failure.

Mode and location of failure were recorded by using a standard three-part failure code for each specimen according to ASTM D3039 for impact damaged coupons, while ASTM 5766 for coupons with circular holes. The ultimate stress was calculated by using the following equation

$$\sigma_{tu} = \frac{P_{max}}{A} \tag{3.1}$$

where σ_{tu} is ultimate strength (MPa), P_{max} is the maximum force before failure (N), A is the average cross-sectional area at the gauge (mm^2).

The notched strength, σ_N is calculated as the tensile strength of the laminate based on the far-field stress

$$\sigma_N = \frac{P_{max}}{bd} \tag{3.2}$$

where P_{max} is the maximum force before failure (N), b is the specimen width (mm), d is the specimen thickness (mm).

3.6 Compression testing

3.6.1 Test procedure

The compression tests were carried out using ASTM D6641 and ASTM D7137 as guiding references. To avoid buckling, an anti-buckling guide of hardened stainless steel was used to prevent macro buckling. The assembly is illustrated in figure 3.7a.

The plates are held in place by four bolts, hand-tightened to allow the coupon to compress freely. Placed in similar grips as for the tensile test with a pressure of 1400 psi. The tests were conducted with a constant cross-head speed of 2.0 mm/min, at room temperature. In case of minor bucklings, each test was monitored and a selection was captured using timelapse to investigate. All compression tests were performed until failure.

(a)   **(b)**
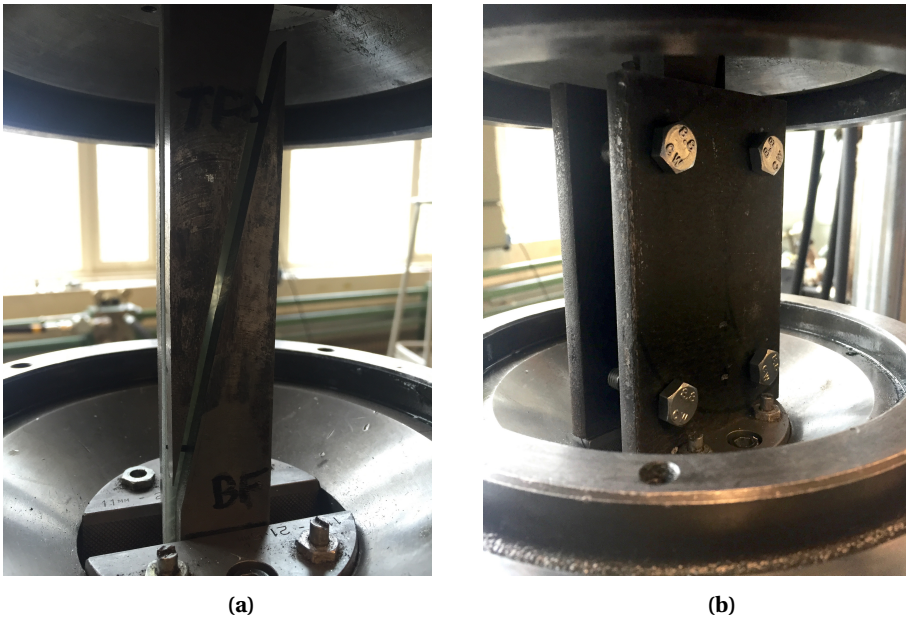
Figure 3.7: Inner anti-buckling (a) and outer-buckling plates (b).

3.7 Flexural testing

3.7.1 Test procedure

The flexural tests were conducted in accordance to ASTM 7264 by a four-point bending test. By doing a four-point bending test, loads will be applied outside the impacted damage area, in comparison to a three-point bending test. The impact damage zone will be the weakest point if the damage initiation threshold is reached. The major difference between a three- and a four-point bending test is that the bending moment is constant between the force application members, shown in figure 3.8, while for a three-point configuration, the maximum bending moment is located right under the center force application member. Another difference, is the presence of the shear force. In the four-point configuration there are no shear force in between the two force application members.
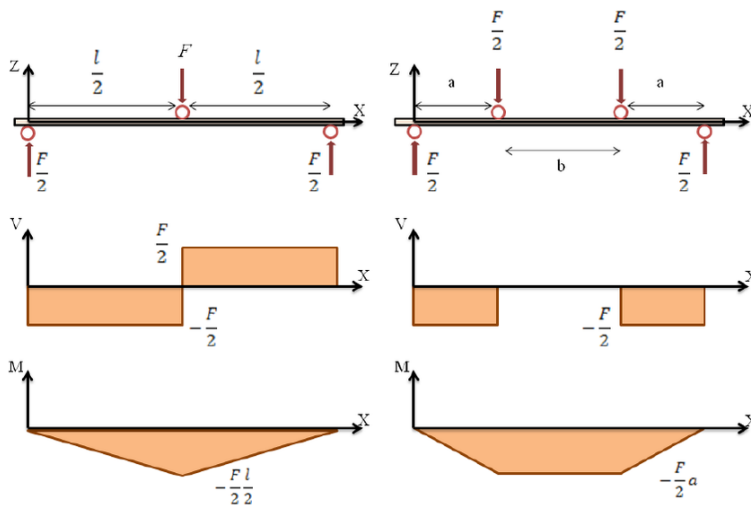
Figure 3.8: Three-point versus four-point bending test [12].

From ASTM 7264, the span-to-thickness ratio should be 32:1. Resulting in a supporting span L = 128.0 mm and a load span of 64.0 mm between the loading noses. The specimen was then shortened to a length of 180.0 mm to avoid collision between the coupon and the machine. The loading noses may be fixed, rotatable or rolling. In this case, the loading and supporting noses are fixed with a radius of 5.0 mm.
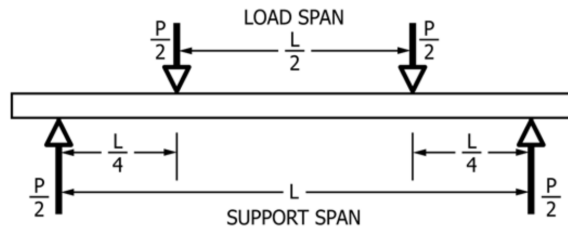
Figure 3.9: Loading diagram, four-point bending test.

A pressure of 1400 psi was applied on the hydraulic grips, clamping the support and the loading noses. The coupons were placed so that the impact damage area was centered in the middle of the loading noses and with the impact damage surface facing towards the loading noses. The axes of the cylindrical surfaces of the loading noses are parallel and aligned. Valid flexural strength is achieved when failure occurs on either one of its outer surface, without a preceding interlaminar shear failure or a crushing failure under a support or loading nose [18]. The tests were conducted at room temperature with a constant cross-head speed of 30.0 mm/min, until failure. Force and displacement of the support are recorded. The deflection is not of major importance in this case so the deflection at the center of the coupon will not be recorded. A three-part failure identification code was recorded for each test in accordance to ASTM D7264.

The residual strength is calculated using this equation,

$$\sigma = \frac{3PL}{4bh^2} \tag{3.3}$$

where σ is the stress at the outer surface in the load span region (MPa), P is the applied load (kN), L is the support span (mm), b is the width of the coupon (mm) and h is the thickness of the coupon (mm).
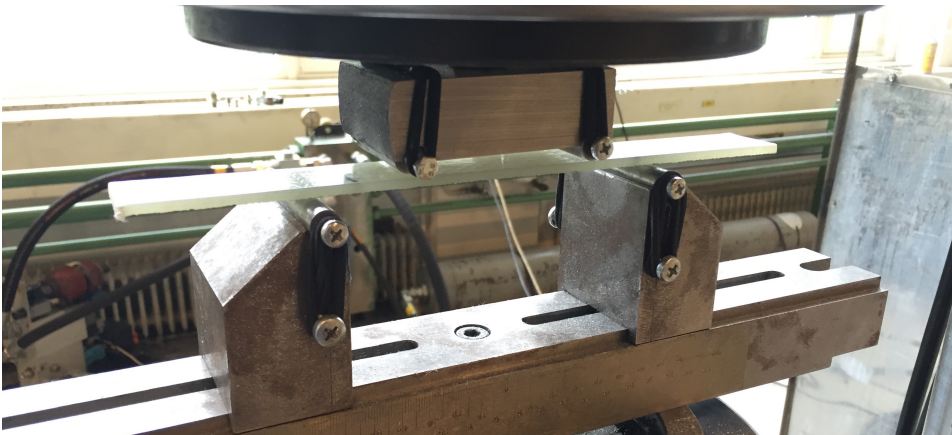
Figure 3.10: Flexural setup.

3.8   Numerical simulations

A numerical model has been made for the coupons with circular holes. This will be simulated in tension to compare with experimental data. This will show how a simplified model could simulate composite materials and how well the simulations represent the experimental data. This will give an indication on how this type of prediction could be used on further work. It would also be used to simulate hole sizes below 1.5 mm in radius to give a better predicting curve for the residual strength reduction.

The coupon is modeled in Abaqus/Standard using a 3D deformable planar shell with appropriate dimensions as the coupons conducted in the experimental tests. Due to symmetry, only one-fourth of the model needs to be modeled with appropriate symmetric boundary conditions. The coupons are loaded in tension by displacement control. The numerical simulations are performed by static analysis with a maximum of 1000 increments and increment size ranging from 1E-6 to 1E-1. The composite material with its respective parameters are listed in table 3.4 in addition to the failure initiation stresses in Hashin failure criteria. The model was assigned a composite layup, each ply with a thickness of 0.4 mm, giving a total thickness of 4.0 mm. The stack plot for the respective laminates are shown in figure 3.12. The viscosity parameters are as mentioned in theory (section 2.3) a material damping factor to avoid convergence issues. This was also an iterative process to fit with the experimental data. A mesh of 4-node doubly curved thin shell with reduced and hourglass control elements (S4R) was used.
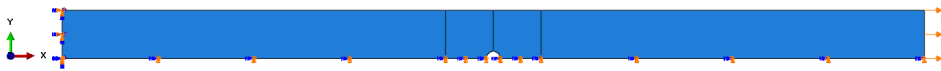
Figure 3.11: Numerical model with boundary conditions.

Table 3.4: Material parameters in FE model.

| Property	Value
General composite parameters	
Elastic modulus (MPa)	$E1 = 42279$, $E2 = E3 = 9649$
Shear modulus (MPa)	$G12 = G13 = 3260$, $G23 = 3428$
Poison's ratio (mm/mm)	$NU12 = NU13 = 0.266$, $NU23 = 0.43$
Density (kg/mm^3)	$1.86E - 006$
Hashin failure parameters	
Failure initiation stress (MPa)	$X_T = 1133$, $X_C = 756$, $Y_T = 64.8$, $Y_C = 194.5$ $S_{12} = S_{13} = 96.1$
Fiber fracture energy (Nmm^{-1})	$G_{ft}^C = 450$, $G_{fc}^C = 150$
Matrix fracture energy (Nmm^{-1})	$G_{mt}^C = G_{mc}^C = 0.83$
Viscosity coefficient	$\eta_L^{T,C} = 1E - 4$, $\eta_T^{T,C} = 0.1$
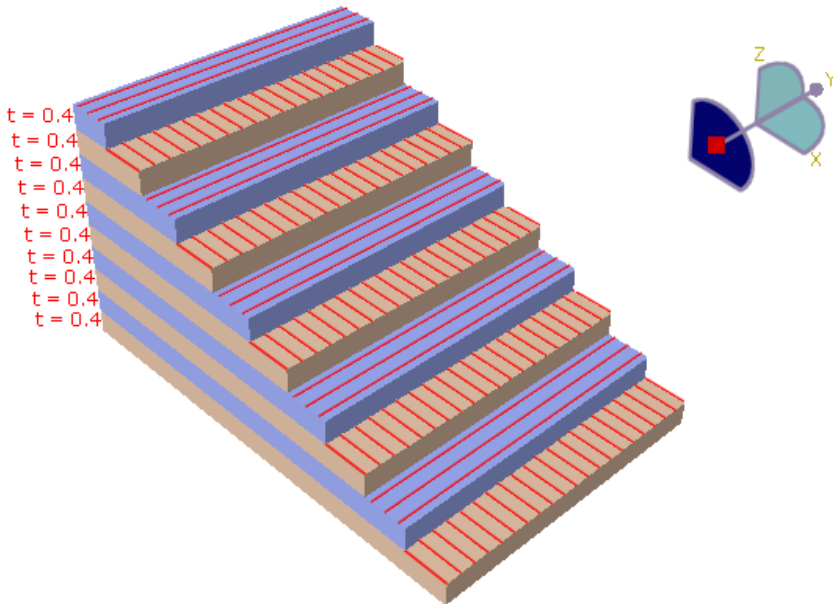
Figure 3.12: Ply stack plot of numerical model.

3.8.1 Mesh refinement

A mesh sensitivity analysis has been conducted in order to get accurate results and an acceptable computational time. The mesh used should be linear quadratic with reduced integration and hourglass control. The angles of the elements should be between 10 and 160 degrees and an aspect ratio greater than 10 in order to sustain a good quality. The meshing around the two smallest holes, is most critical. The hole with a radius of 2.0 mm is chosen for the analysis and the results will be conducted on the other hole sizes. The model is reduced to analyze the closest area around the hole (ref. figure 3.13) and applied a displacement of 1.0 mm. Figure 3.14 shows the coarsest and finest mesh analyzed.
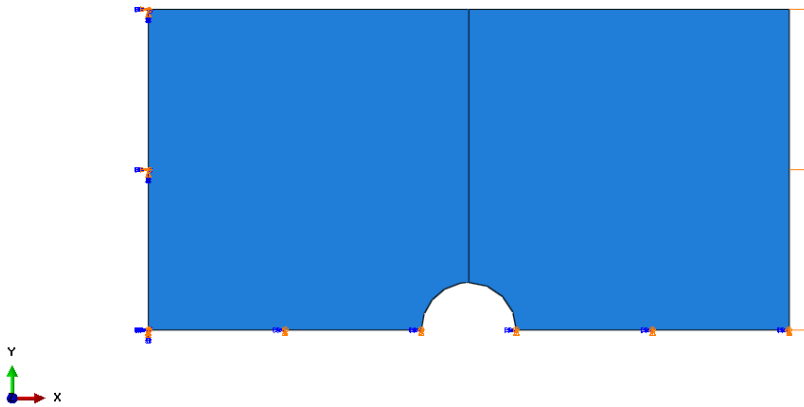

Figure 3.13: Mesh analysis model with boundary conditions.

**(a)**   **(b)**
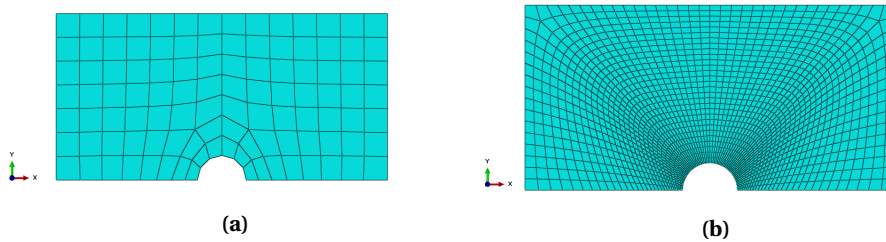
Figure 3.14: Coarse mesh with 108 elements (a) and fine mesh with 1829 elements (b).

The peak stress at the hole varies with the mesh size, shown in figure 3.16. The coarsest mesh has an equivalent ultimate stress but the stiffness degradation differs from the finer meshes (figure 3.17). Only seven nodes along a path of 12 mm gives inaccurate calculations compared to 58 nodes at the finest mesh.

The peak stress at the hole converges at 426 elements shown in 3.17. An element number of 690 around the hole is chosen which is elements with an edge size of approximately 0.2 mm around the hole and gradually increases to 2 mm at the ends. The peak stress at the hole tip and maximum force is acceptable compared to the finest mesh. The computational time is significantly lower compared to the finest mesh which require 4 times more time. This is therefore chosen as the mesh quality for each hole coupon, shown in 3.15.
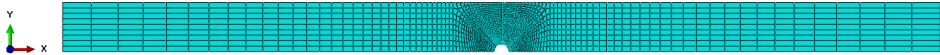
**Figure 3.15:** Final mesh of numerical model.
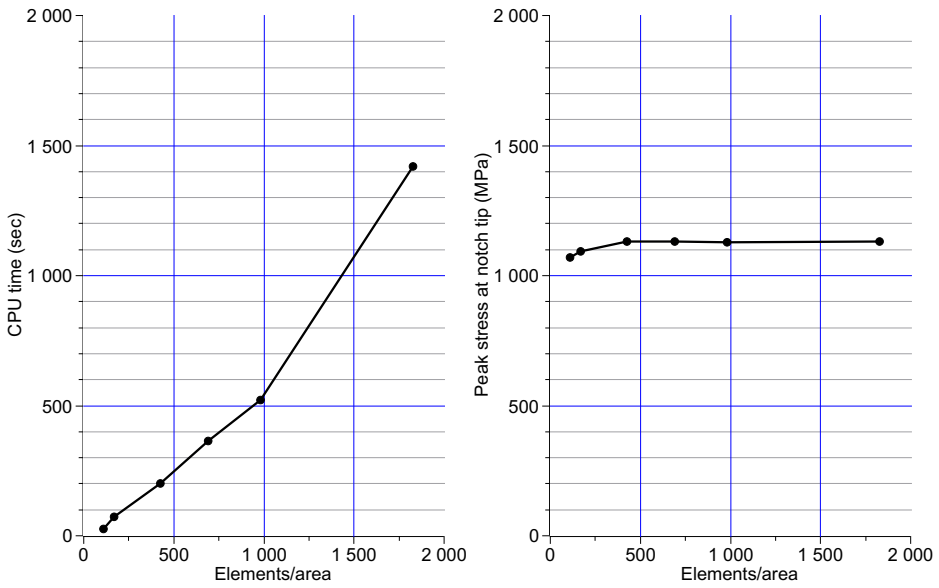
Figure 3.16: Computational time versus number of elements per unit area and peak stress at hole tip versus number of elements per unit area.
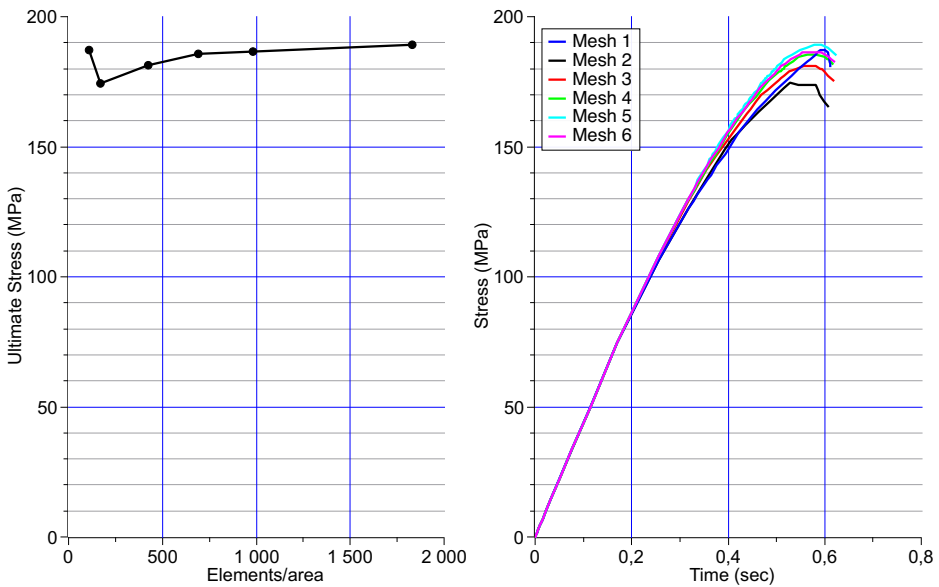

Figure 3.17: Ultimate stress versus number of elements per unit area and force-displacement where *Mesh 1* is the coarsest and *Mesh 6* is the finest mesh.

3.8.2 Choosing proper values of the damage parameters

Choosing the proper viscosity parameters ($\eta_L^{T,C}$ and $\eta_T^{T,C}$) and the energy dissipated at fracture (G_{ft}^C, G_{fc}^C, G_{mt}^C and G_{mc}^C) is an iterative process. As mentioned in section 2.3, the viscosity parameters are used to overcome convergence issues. The smaller the viscosity parameter, the more abrupt the failure is. If the coefficient becomes too large, the material gets overdamped. Figure 3.18 gives the stress-time curves for different viscosity parameters. As the plot indicates, when $\eta_L^T = 1E-6$ the simulation do not converge. $\eta_L^T = 1E-2$ becomes too large and the material gets overdamped and an unrealistic force-displacement curve. The chosen longitudinal viscosity parameter is $\eta_L^T = 1E-4$ which both represent the experimental results well and the energy dissipated due to the viscosity (as output ALLCD) is relatively small compared to the elastic strain energy (as output ALLSE) shown in the right plot in figure 3.18.

The fracture energy parameters were unavailable. As a starting point, the parameters used by Skaar [15] for his filament wounded GFRP was chosen. Generally, failure of the matrix involves low fracture energies while fiber failure result in significantly greater energy dissipation [4]. The fiber compressive fracture energies does not have an impact on the stress-displacement curve in the tensile simulation while the matrix energies are assumed to be $0.83 Nmm^{-1}$. By doing an iterating process to fit with the experimental data, the fracture energy properties were obtained as listed in table 3.4.
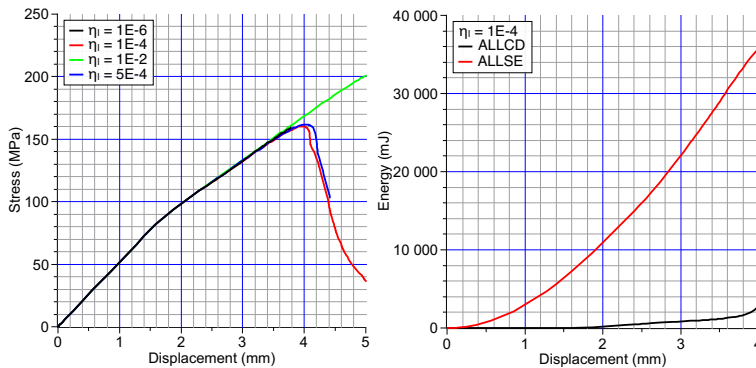

Figure 3.18: Convergence analysis with longitudinal tensile viscosity parameter (left side) and elastic strain energy (ALLSE) compared to energy dissipated due to viscosity (ALLCD) (right side).

Chapter 4

Results

4.1 Impact damage

After the drop test the impacted damage size on all coupons were inspected using backlight to get a clear view of the damaged area. By using this method, the damage is more easy to inspect visually and to measure the extent of the damage in terms of size. The backlight provides a projection of all the damaged surfaces into one plane (figure 4.1 and 4.2. The white areas that occurs on the surface is delamination. This area is measured by the width and height for each coupon at the impacted surface, giving the damage area.

The average damage area of all impacted coupons are shown in figure 4.3 and 4.4. Earlier studies indicate that the total area varies linearly with the initial kinetic energy of the projectile [2] which also is the case for Laminate A and B.

It should be noted that finding this damage on a 27 mm wide, clear and unpainted specimen is relatively simple compared to a painted panel on a boat's hull where this damage would barely be visible or even invisible.

The result from all impact damaged coupons could be found in the Appendix.
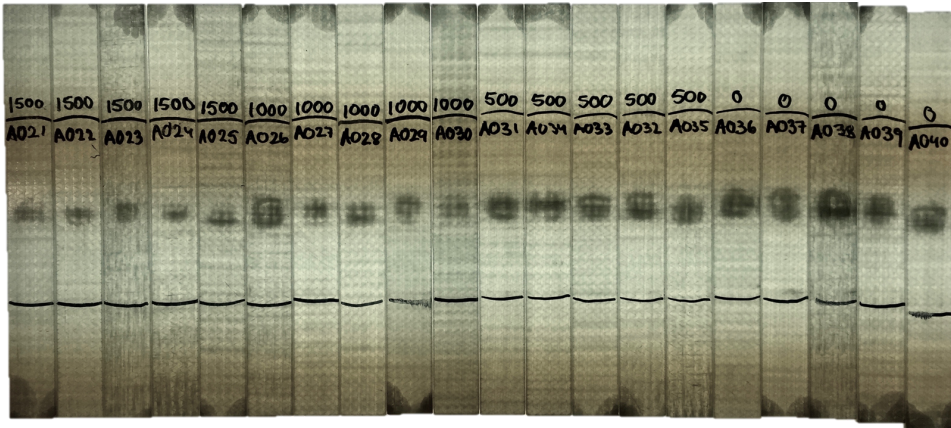
**Figure 4.1:** Visual inspection of impact damage size using backlight, Laminate A.
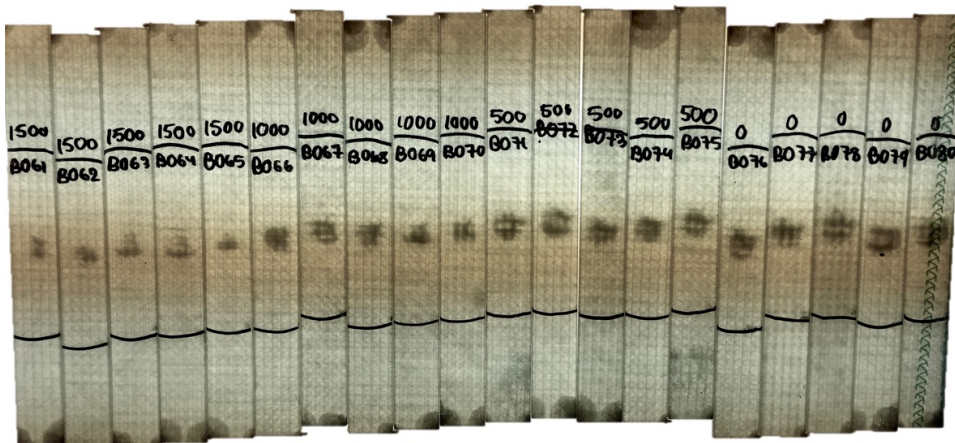
**Figure 4.2:** Visual inspection of impact damage size using backlight, Laminate B.
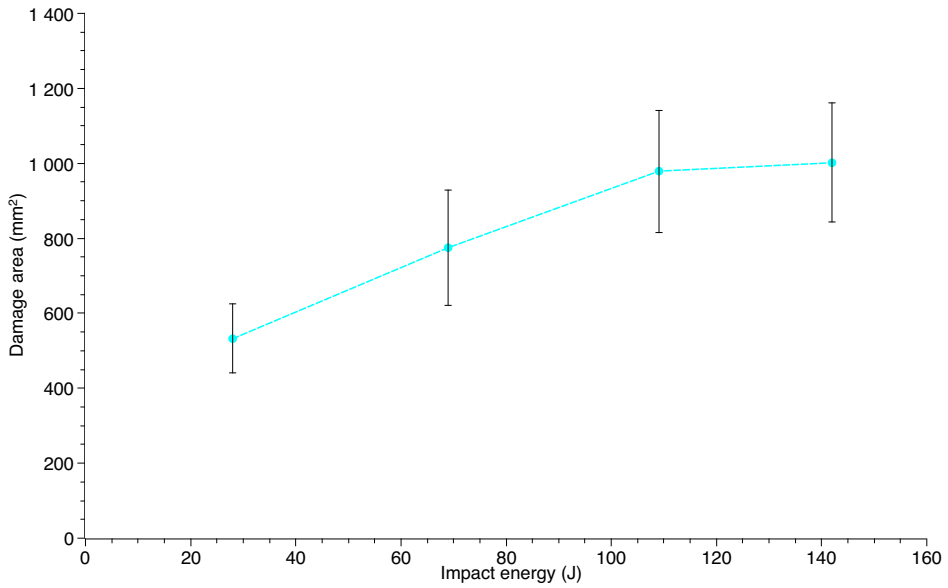
Figure 4.3: Coupons of Laminate A.
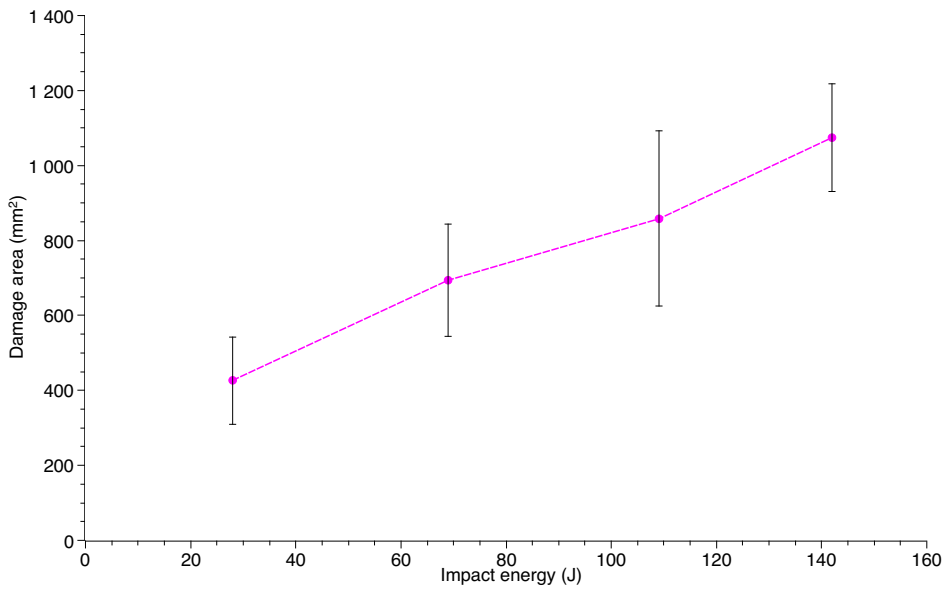
Figure 4.4: Coupons of Laminate B.

4.1.1 Delamination

By visual inspection, delamination is relatively easy to detect from the top surface. It occurs as white areas. As mentioned in section 2.1.1, the debonding occurs between plies with different fiber orientation. The peanut-shape damage area occurs in the respective direction of the fibers. Laminates with abrupt fiber orientations will have the greatest effect on delamination after impact [4], such as a crossply laminate. This effect does not have an influence on the laminates tested in these experiments. The average damage size of the two laminates are approximately the same. Although the delamination area of laminate A is wider relatively to the height, compared to laminate B, indicates that debonding has occurred in the transverse direction of the coupon, while for laminate B, the debonding has occurred in the direction of ±45°.

By inspecting the back side of the specimen induced by the lowest impact energy, the measured damage size is smaller compared to the area at the impact surface, which implies that the extent of delamination decreases through the thickness.

4.1.2 Matrix cracks and fiber failure

Matrix cracks and fiber fracture is not easy to detect by the naked eye. To detect these damage mechanisms, burn-off test and microscopy inspection of the damaged cross section were conducted. Coupons were cut across the width using a water cut blade and mounted in epoxy and grounded by finer abrasive silicon carbide grinding paper (grit 80, 120, 220, 500, 1000 and 4000) Figure 4.5 shows images captured with a microscope, model *Leica Optical Microscopy DFC245* at x5 and x10 scaling. Even with a bad grounded surface, delaminations and matrix cracks could be detected. The red arrows indicates matrix cracks and delaminations. Image 4.5a shows a coupon of Laminate A conducted by 142 J with a 10 times scaling. Image 4.5b shows the cross section of a 28 J induced damage on Laminate B with a 5 times scaling.

By conducting burn-off tests on specimen impacted by 28 J and 142 J (two coupons per impact energy from each laminate), fiber failure could easily be detected. Out of the coupons from the lowest impact energy, the extent of fiber failure varied. For Laminate A, fiber failure were only detected at one of the coupons (at ply 7 and 9). For Laminate

B, also only one out of two coupons had fiber failure at the two bottom plies.

For the greatest impact energy, fiber failure were detected at the two bottom and the four bottom plies for the coupons from Laminate A respectively. For Laminate B, only one of the coupons had fiber failure at ply 9 and 10.

Figure 4.6 shows fiber failure at the highest impact energy induced at Laminate A. The extent of fiber failure increase towards the bottom plies.

(a)   **(b)**
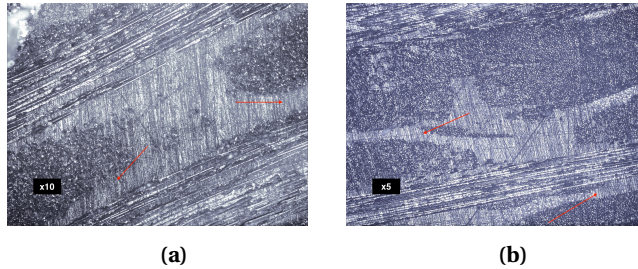
Figure 4.5: Cross section of the damage area on Laminate B with 28 J (a) and Laminate A with 142 J (b).

**(a)**   **(b)**

(c)   **(d)**
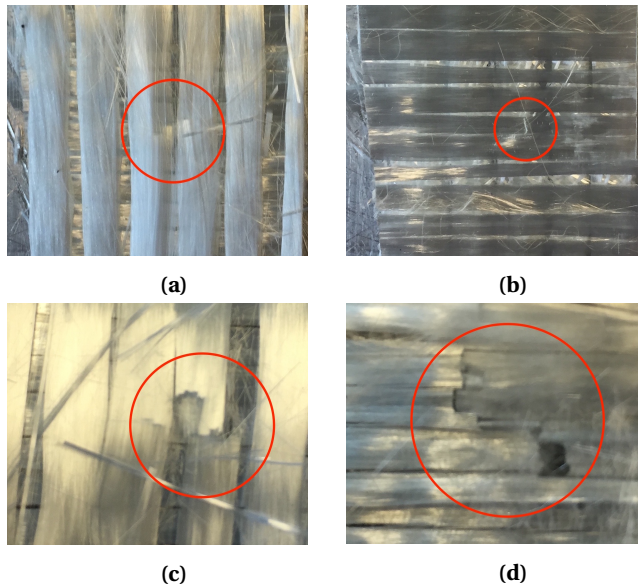
Figure 4.6: Laminate A after a impact damage of 142 J. Ply 7 (a), ply 8 (b), ply 9 (c) and ply 10 (d).

4.2 Residual tensile strength properties

Table 4.1 and 4.2 gives the tensile strength properties of the two laminates with the associate impact energy, damage area and the three-part failure code. The failure codes are explained in figure 4.7. *AXXX* and *BXXX* are the labels of the coupons with impact damage, while *ATXXX* and *BTXXX* are the labels of the undamaged coupons. Valid test results are only when failure occurs within the gauge section. The associate standard deviation and average residual tensile strength are calculated only from the valid coupons. Noting the difficulties on getting failure within the gauge section for undamaged coupons more than 10 coupons needed to be tested in order to get valid tensile strength properties of the laminates. To increase the success rate, tabs are recommended to avoid local failure at the grips [7]. The tensile strength is calculated according to equation (3.1), using the associate specimen data listed in table 3.1. The distribution of residual tensile strength versus impact energy are plotted in figure 4.8 and 4.9 for Laminate A and Laminate B, respectively. The black scatter plot represents the strength of each individual coupon and the cyan and magenda represents the average strength from each impact energy series. The invalid coupons are plotted as red diagonal crosses. The relative residual tensile strength for both laminates are shown in figure 4.10.

Table 4.1: Tensile coupons, Laminate A.

Coupon	Impact energy (J)	Damage area, (mm, mm^2)			Failure code	Residual stress (MPa)
		w	h	Area (wxh)		
A021	28	16	14	703.7	LGM	425.7
A022	28	16	11	552.9	LGM	340.1
A023	28	13	12	490.1	AIT	432.1
A024	28	16	12	603.2	LGM	345.8
A025	28	18	11	622.0	LGM	313.0
A026	69	19	19	1134.1	LGM	322.2
A027	69	14	14	615.8	LGM	278.2
A028	69	18	12	678.6	LGM	354.6
A029	69	15	18	848.2	LGM	365.5
A030	69	17	14	747.7	LGM	440.3
A031	109	18	15	848.2	LGM	353.5
A032	109	17	17	907.9	LGM	277.3
A033	109	19	18	1074.4	LGM	342.9
A034	109	20	19	1193.8	LGM	163.7
A035	109	18	19	1074.4	LGM	377.3
A036	142	20	18	1131.0	LGM	276.2
A037	142	19	21	1253.5	LGM	340.1
A038	142	18	18	1017.9	LGM	216.3
A039	142	17	17	907.9	LGM	233.4
A040	142	19	17	1014.7	LGM	335.2
AT001	-	-	-	-	LGM	469.6
AT002	-	-	-	-	AGM	459.4
AT003	-	-	-	-	LGM	495.1
AT004	-	-	-	-	AIB	415.4
AT005	-	-	-	-	LAB	478.9
AT006	-	-	-	-	LIB	387.0
AT007	-	-	-	-	LAT	448.4
AT008	-	-	-	-	LGM	494.6
AT09	-	-	-	-	LIB	442.0
AT10	-	-	-	-	LIB	419.4

Table 4.2: Tensile coupons, Laminate B.

Coupon	Impact energy (J)	Damage area, (mm, mm^2)			Failure code	Residual stress (MPa)
		w	h	Area (wxh)		
B021	28	10	12	377.0	AGM	377.2
B022	28	11	11	380.1	LIT	403.6
B023	28	10	11	345.6	LIT	336.2
B024	28	12	12	452.4	LGM	412.8
B025	28	13	13	530.9	LGM	353.2
B026	69	18	15	848.2	LGM	376.7
B027	69	15	15	706.9	AGM	315.2
B028	69	17	16	854.5	LGM	402.1
B029	69	15	15	706.9	LGM	411.4
B030	69	18	16	904.8	LGM	331.8
B031	109	16	15	754.0	LGM	349.1
B032	109	19	23	1372.9	AGM	293.3
B033	109	13	15	612.6	LGM	231.9
B034	109	18	19	1074.4	LGM	317.2
B035	109	20	21	1319.5	LGM	348.4
B036	142	20	20	1256.6	LGM/AGM	328.5
B037	142	18	18	1017.9	LIB	318.0
B038	142	20	19	1193.8	LGM/AGM	314.9
B039	142	20	21	1319.5	LGM/AGM	253.6
B040	142	19	20	1193.8	LGM/AGM	305.3
BT01	-	-	-	-	LIB	404.8
BT02	-	-	-	-	LIB	347.5
BT03	-	-	-	-	LIB	369.8
BT04	-	-	-	-	AIB	365.0
BT05	-	-	-	-	AIB	375.0
BT06	-	-	-	-	LIB	365.9
BT07	-	-	-	-	LAT	400.6
BT08	-	-	-	-	LGM	439.0
BT09	-	-	-	-	LGM	392.7
BT10	-	-	-	-	LIT	400.3

Figure 4.7: Failure codes for tensile tests [16].
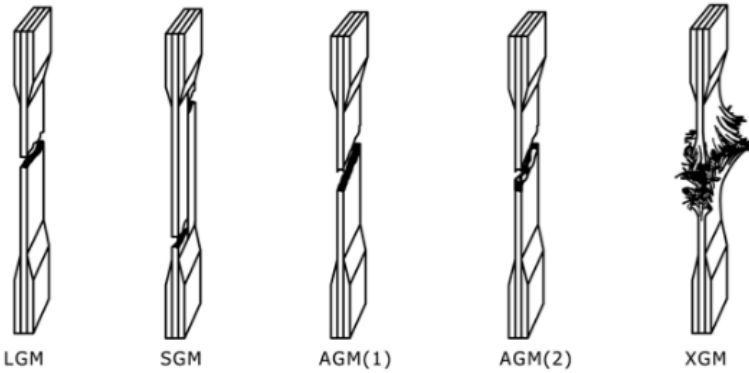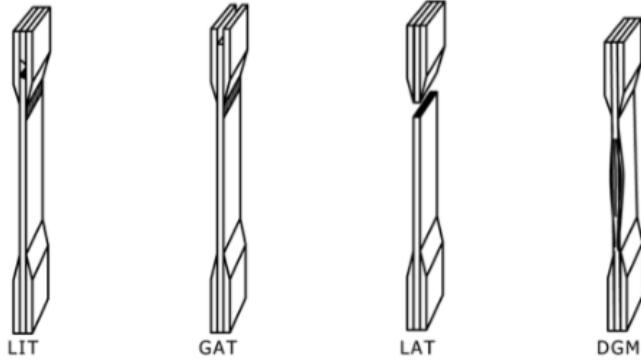
First Character	
Failure Type	Code
Angled	A
edge Delamination	D
Grip/tab	G
Lateral	L
Multi-mode	M(xyz)
long. Splitting	S
eXplosive	X
Other	O

Second Character	
Failure Area	Code
Inside grip/tab	I
At grip/tab	A
<1W from grip/tab	W
Gage	G
Multiple areas	M
Various	V
Unknown	U

Third Character	
Failure Location	Code
Bottom	B
Top	T
Left	L
Right	R
Middle	M
Various	V
Unknown	U
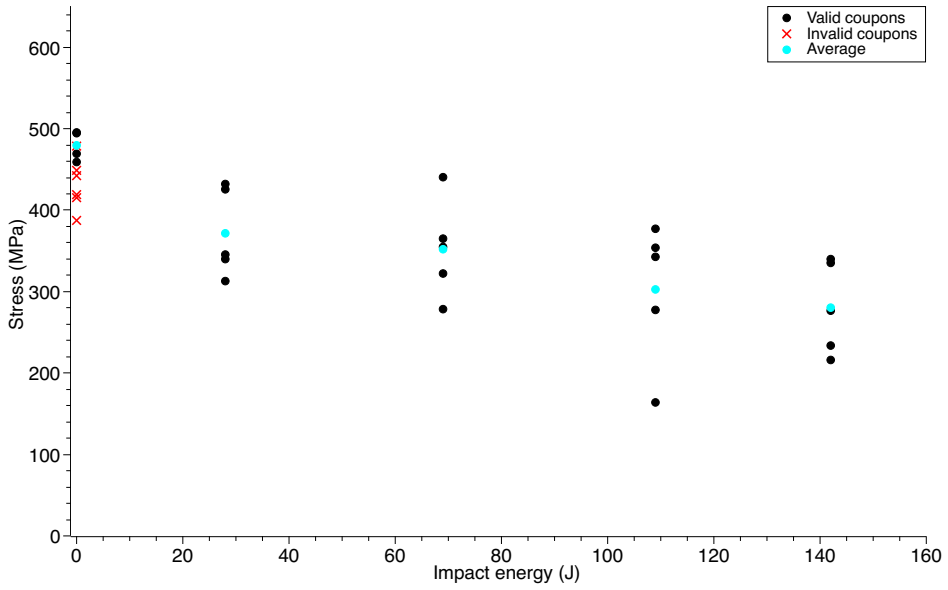
Figure 4.8: Residual tensile strength, Laminate A.
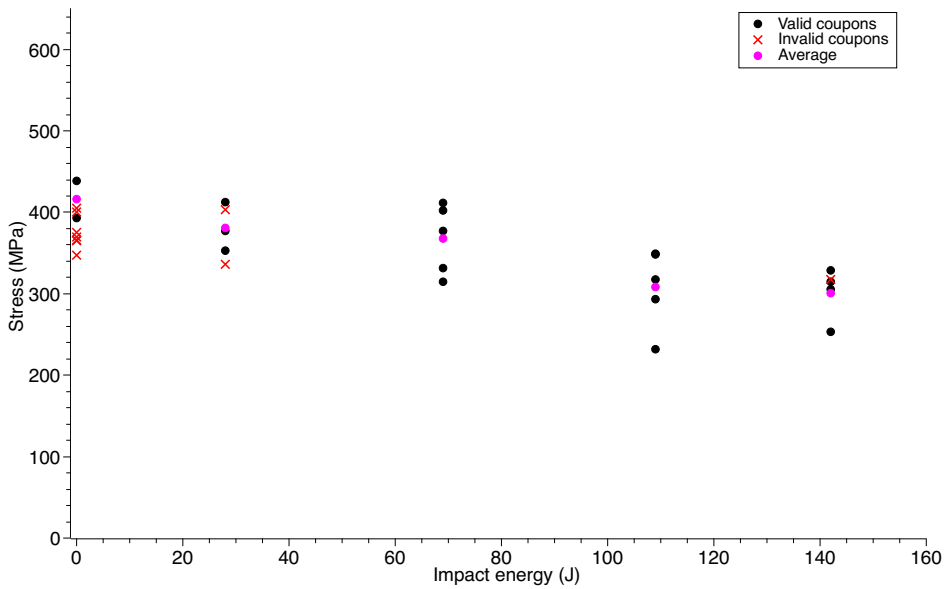
Figure 4.9: Residual tensile strength, Laminate B.
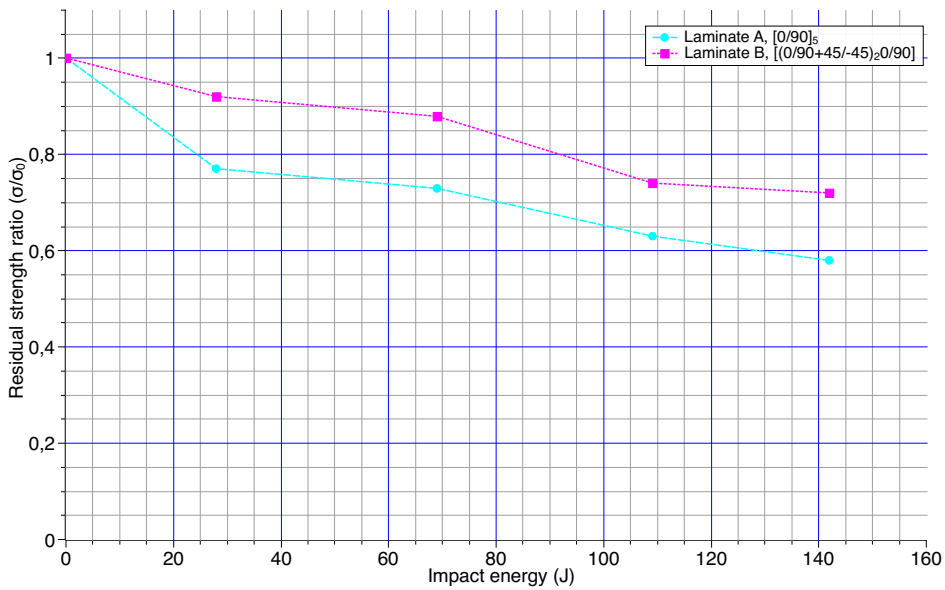
Figure 4.10: Relative tensile strength reduction Laminate A and B.

Both laminates have almost the same relative reduction from the lowest impact energy to the highest. Lamina A has exceeded the damage initiation threshold after first impact, which the plot in figure 4.10 indicates. The strength drops rapidly and levels off. The reduction after the lowest impact energy (28 J) is 20% and degrades almost linearly to a total reduction of approximately 42% at the highest impact energy (142 J). For Laminate B, the reduction of the residual tensile strength is modest until the energy reaches 64 J, where the reduction is more significant. The reduction after the larges impact damage is approximately 28%.

4.3   Residual compressive strength properties

Compression usually gives the largest reduction in strength for impact damaged composites. The residual compressive strength of the test coupons are represented in table 4.3 and 4.4 with the associated impact energy, damage area and three-part failure code. Explanation of the failure codes are shown in figure 4.11. The standard deviation and average residual strength are calculated only from the valid tests. Valid results are obtained when failure occurs within the gauge section at the damaged region for the damaged coupons. As for the other residual strength test, *AXXX* and *BXXX* are labels on the impact damaged coupons while *ACXX* and *BCXX* for the undamaged once. The distribution of residual compressive strength versus impact energy are plotted in figure 4.12 and 4.13 for Laminate A and Laminate B, respectively.

Table 4.3: Compression coupons, Laminate A.

Coupon	Impact energy (J)	Damage area, (mm, mm^2)			Failure code	Residual stress (MPa)
		w	**h**	**Area (wxh)**		
A041	28	12	11	414.7	HGM	309.8
A042	28	14	14	615.8	BGM	249.1
A043	28	14	10	439.8	HGM	263.5
A044	28	15	10	471.2	HGM	204.6
A045	28	11	17	587.5	BGM/OIR	362.0
A046	69	16	14	703.7	BGM	230.5
A047	69	14	16	703.7	BGM	215.7
A048	69	14	18	791.7	BGM	251.4
A049	69	18	19	1074.4	HGM	315.5
A050	69	17	15	801.1	BGM	272.6
A051	109	21	18	1187.5	BGM	193.3
A052	109	19	19	1134.1	BGM	206.2
A053	109	19	19	1134.1	BGM	253.7
A054	109	19	19	1134.1	HGM	237.3
A055	109	18	18	1017.9	HGM	223.1
A056	142	19	18	1074.4	BGM	280.8
A057	142	18	19	1074.4	BGM	188.3
A058	142	20	18	1131.0	BGM	174.3
A059	142	18	20	1131.0	HGM/OIR	286.5
A060	142	20	18	1131.0	HGM	159.6
AC04	-	-	-	-	BGM	307.3
AC05	-	-	-	-	BGM	356.1
AC06	-	-	-	-	BGM	281.5
AC07	-	-	-	-	BGM	313.4
AC08	-	-	-	-	HGM	374.3

Table 4.4: Compression coupons, Laminate B.

Coupon	Impact energy (J)	Damage area, (mm, mm^2)			Failure code	Residual stress (MPa)
		w	h	Area (wxh)		
B041	28	11	12	414.7	BGM	273.6
B042	28	15	15	706.9	BGB/OIR	260.7
B043	28	14	11	483.8	BGM/OIR	362.4
B044	28	13.0	13	530.9	BGM/OIR	271.8
B045	28	10.0	10	314.2	BGM/OIR	321.1
B046	69	14.0	18	791.7	BGM/OIR	288.2
B047	69	15.0	15	706.9	BGM	221.9
B048	69	15.0	18	848.2	BGM	277.2
B049	69	17.0	14	747.7	BGM	224.1
B050	69	16.0	15	754.0	HGM	280.2
B051	109	14.0	12	527.8	BGM	227.4
B052	109	20.0	16	1005.3	BGM	220.9
B053	109	15.0	18	848.2	BGM	216.7
B054	109	13.0	17	694.3	HGM	256.5
B055	109	15.0	15	706.9	BGM	234.9
B056	142	18.0	18	1017.9	BGM	250.0
B057	142	18.0	20	1131.0	BGM	257.0
B058	142	20.0	17	1068.1	BGM	205.0
B059	142	20.0	20	1256.6	BGM	245.0
B060	142	18.0	18	1017.9	HGM	188.7
BC01	-	-	-	-		310.2
BC02	-	-	-	-		259.7
BC03	-	-	-	-		359.0
BC04	-	-	-	-		329.8
BC05	-	-	-	-		267.3

TAT   BGM   HAT   SGV   DTT   HIT   CIT   DIT

Acceptable Failure Modes and Areas   **Unacceptable Failure Modes and Areas**

First Character	
Failure Mode	Code
Angled	A
Brooming	B
end-Crushing	C
Delamination	D
Euler buckling	E
tHrough-thickness	H
Kink bands	K
Lateral	L
Multi-mode	M(xyz)
long.-Splitting	S
Transverse shear	T
eXplosive	X
Other	O

Second Character	
Failure Area	Code
Inside grip/tab	I
At grip/tab	A
Gage	G
Multiple Areas	M
Tab adhesive	T
Various	V
Unknown	U

Third Character	
Failure Location	Code
Bottom	B
Top	T
Left	L
Right	R
Middle	M
Various	V
Unknown	U

Figure 4.11: Failure codes for compression tests [17].
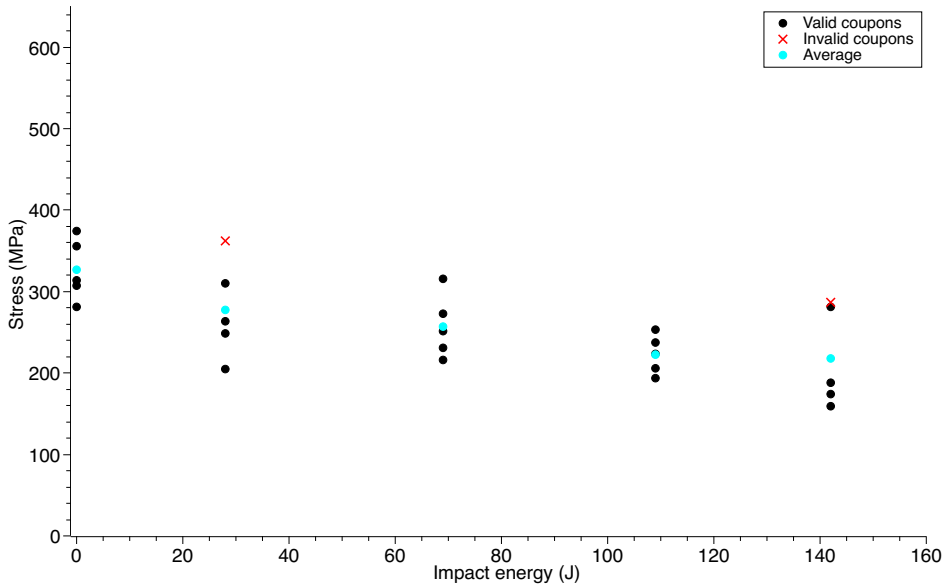
Figure 4.12: Residual compressive strength, Laminate A.
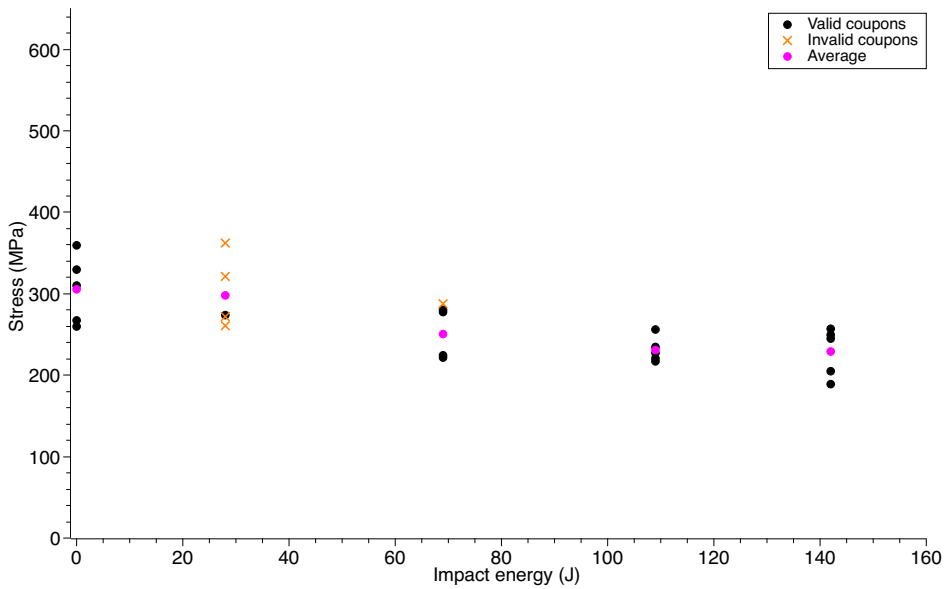
Figure 4.13: Residual compressive strength, Laminate B.

The black scatter plot represents the strength of individual each coupon and the cyan and pink represents the average strength from each impact-series, for Laminate A and B respectively. The red diagonal crosses indicates invalid coupons, while the orange indicates coupons where the failure at compression was outside the impacted area. Meaning, the impacted area did not affect the strength of the material. For Laminate B, close to no strength reduction has occurred as the impact energy is below the threshold to initiation of damage. This threshold is reached after 28 J. For laminate A on the other hand, this threshold is reached at 28 J. Delaminations and matrix cracks are more of a concern in compression than tensile.

The relative residual compressive strength of both laminates are shown in figure 4.14.
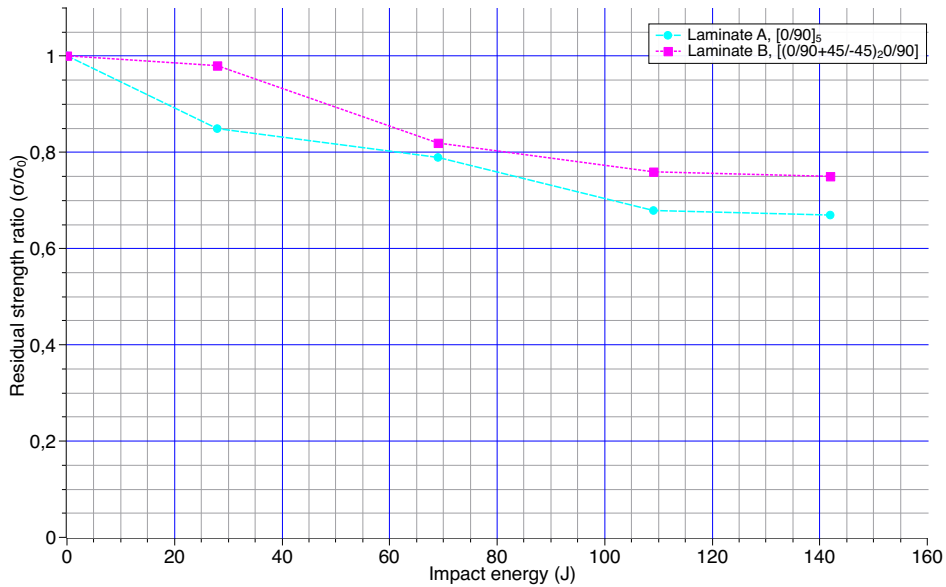
Figure 4.14: Relative tensile strength reduction Laminate A and B.

4.4 Residual flexural strength properties

Table 4.5 and 4.6 lists the information on the measured impacted area, with the corresponding three-part failure identification code and residual flexural strength. The residual strength is calculated using equation (3.3).

Figure 4.17 and 4.18 show the distribution of the residual flexural strength of valid tested coupons (black scatter) and average strength (cyan and pink scatter) versus the impacted energy. It could be noted that the initiation of damage threshold is not reached at energies below 69 J for both laminates. The majority of the coupons in the impact range below initiation of damage, fail in shear at the loading noses rather than in bending at the impacted area which also indicates that the extent of damage does not affect the strength of the material. A selection of coupons with failure areas outside the impacted region are shown in figure 4.20.

(a) (b)
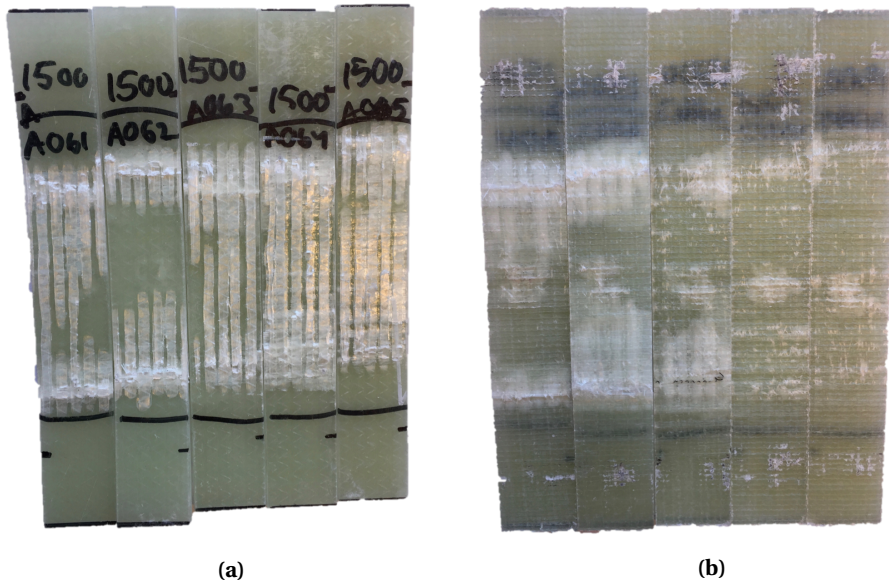
Figure 4.15: Flexural test failure, top surface (a) and back surface (b).

Table 4.5: Flexural testing coupons, Laminate A.

| Coupon | Impact energy (J) | Damage area, (mm, mm^2) | | | Failure code | Residual stress (MPa) |
		w	h	Area (wxh)		
A061	28	13	13	530.9	M(CS)AV	529.5
A062	28	12	15	565.5	M(CS)AV	539.3
A063	28	15	13	612.6	CAT	476.0
A064	28	12	10	377.0	CAT	474.3
A065	28	10	13	408.4	CAT	491.2
A066	69	13	13	530.9	TBB	451.0
A067	69	15	16	754.0	M(CT)BB	551.8
A068	69	17	16	854.5	M(CT)BB	492.1
A069	69	15	15	706.9	TBB	456.4
A070	69	18	12	678.6	TBB	468.0
A071	109	16	15	754.0	TBB	407.4
A072	109	15	18	848.2	TBB	348.7
A073	109	15	16	754.0	M(CT)BB	510.0
A074	109	18	16	904.8	M(CT)BB	514.5
A075	109	15	15	706.9	TBB	462.6
A076	142	15	15	706.9	M(CT)BB	466.2
A077	142	16	17	854.5	TBB	403.0
A078	142	19	18	1074.4	TBB	293.2
A079	142	18	14	791.7	TBB	262.2
A080	142	18	13	735.1	TBB	336.1
AF03	-	-	-	-	CAT	444.8
AF04	-	-	-	-	C/BAT	559.0
AF07	-	-	-	-	M(C/BS)AV	474.3
AF08	-	-	-	-	C/BAT	542.0

Table 4.6: Flexural testing coupons, Laminate B.

Coupon	Impact energy (J)	Damage area, (mm, mm^2)			Failure code	Residual stress (MPa)
		w	h	Area (wxh)		
B061	28	8.0	12	301.6	CAT	525.1
B062	28	11.0	10	345.6	CAT	513.3
B063	28	13.0	13	530.9	CAT	528.4
B064	28	12.0	12	452.4	CAT	561.5
B065	28	12.0	6	226.2	CAT	558.3
B066	69	13.0	15	612.6	M(CS)AV	488.4
B067	69	12.0	15	565.5	M(BT)BV	510.0
B068	69	12.0	12	452.4	CAT	516.5
B069	69	12.0	12	452.4	TBB	526.2
B070	69	13.0	11	449.2	TBB	538.9
B071	109	17.0	15	801.1	TBB	358.2
B072	109	16.0	18	904.8	TBB	455.0
B073	109	17.0	14	747.7	TBB	456.1
B074	109	16.0	16	804.2	TBB	376.5
B075	109	15.0	15	706.9	TBB	377.6
B076	142	15.0	17	801.1	TBB	426.1
B077	142	18.0	18	1017.9	TBB	329.3
B078	142	18.0	16	904.8	TBB	501.4
B079	142	19.0	15	895.4	TBB	470.1
B080	142	17.0	19	1014.7	TBB	373.3
BF01	-	-	-	-	M(CS)AV	600.4
BF02	-	-	-	-	M(CS)AV	547.5
BF04	-	-	-	-	M(CS)AV	541.0
BF05	-	-	-	-	M(CS)AV	550.7
BF06	-	-	-	-	M(CS)AV	534.6

Figure 4.16: Failure codes for flexural tests [18].

First Character

Failure Mode	Code
Tension	T
Compression	C
Buckling	B
interlaminar Shear	S
Multi-mode	M(xyz)
Other	O

Second Character

Failure Area	Code
At loading nose	A
Between loading noses	B
at Support nose	S
between Load and support nose	L
Unknown	U

Third Character

Failure Location	Code
Top	T
Bottom	B
Left	L
Right	R
Middle	M
Various	V
Unknown	U
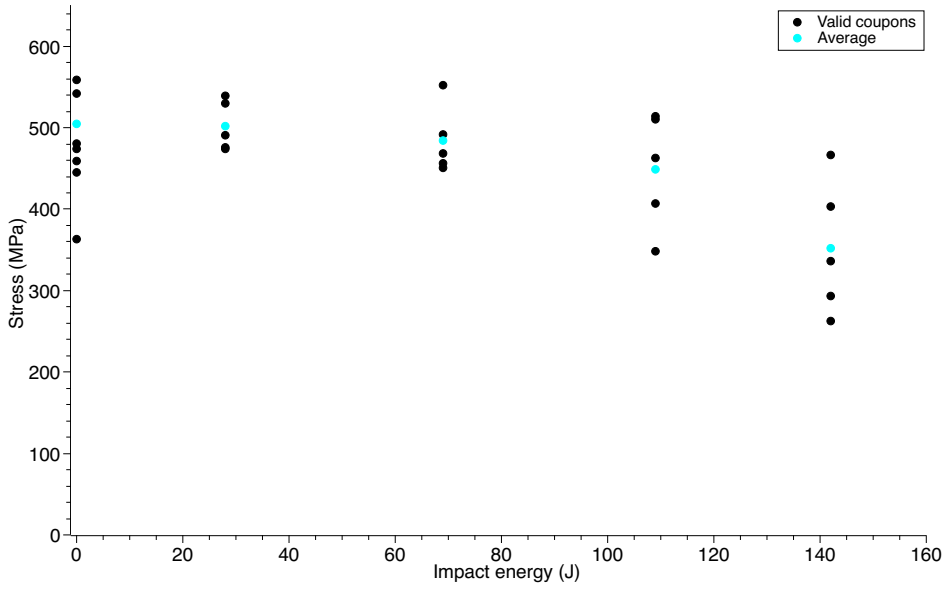
Figure 4.17: Residual flexural strength, Laminate A.
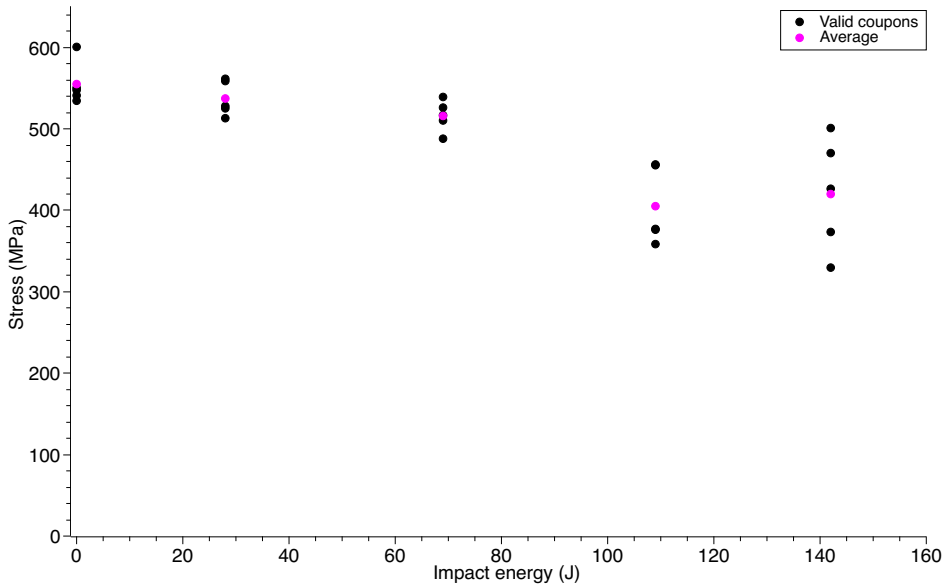
Figure 4.18: Residual flexural strength, Laminate B.

After the damage initiation threshold, laminate B decreases rapidly and smooths out at higher energies. For laminate A, the significant reduction appears at 109 J. A comparison of the strength reduction of both laminates are shown in figure 4.19. The residual strength for both laminates ends up at less than 80% of the undamaged material.
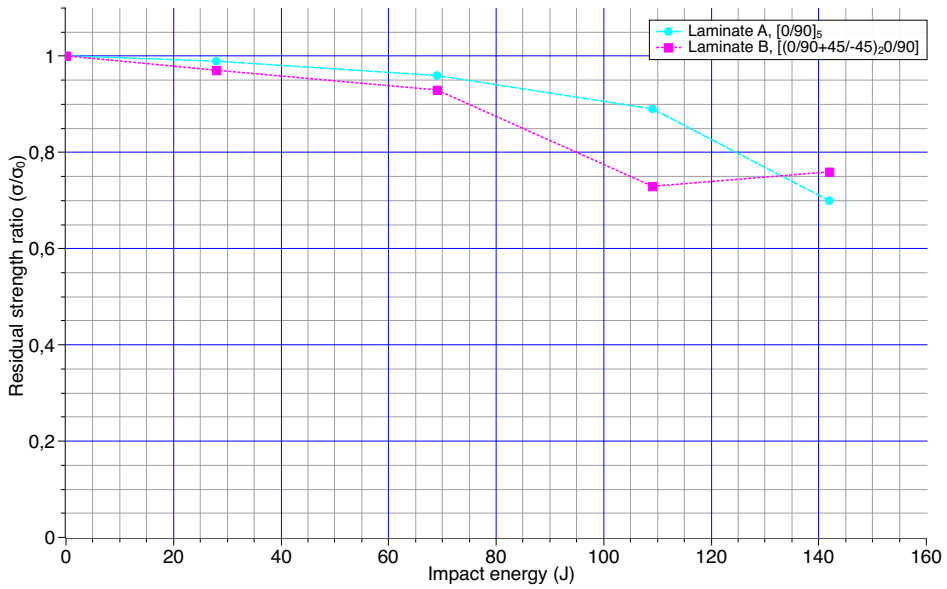
Figure 4.19: Flexural strength comparison of laminate A and B.

It is also important to notice that the deflection at failure is relatively large for the coupons. For Laminate A, it ranges from 17.2 mm to 36.9 mm measured at the loading nose (Note: Not at the middle of the coupon). In this case, it is necessary to take account of the horizontal forces when calculating the real flexural strength. ASTM D 790, BSI 2782 and ISO-14125 each consider what correction should be applied to the stress equation if the beam experiences large deflections (greater than 10% of the support span) [9]. ASTM D790 [19] recommends the following equation for correcting for large deflections

$$\sigma = \frac{3PL}{4bh^2}\left(1 - \frac{10.9hD}{L^2}\right) \tag{4.1}$$

where D is the deflection at the centerpoint. Since the deflection of the centerpoint is not recorded in this thesis, and only relatively values are evaluated, the correction for large deflections will not be considered. ASTM D7264 [18], makes no comment on this correction.

(a)   (b)
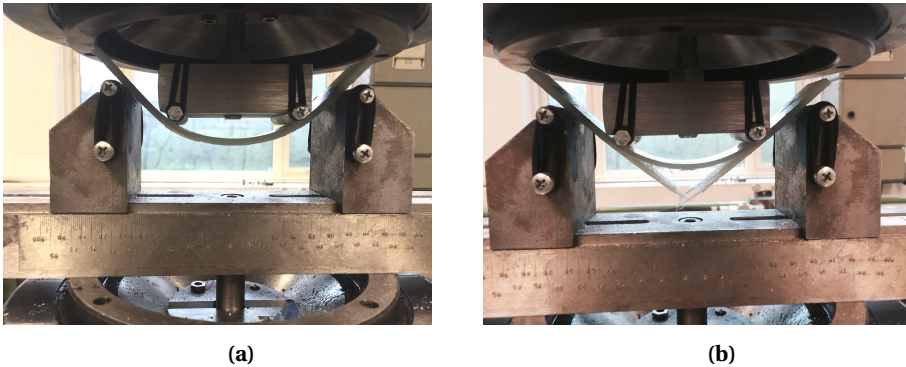
Figure 4.20: Coupon A070 rigth before (a) and after failure (b).

4.5 Numerical results

The stress displacement curve for the tensile tests are shown in figure 4.21 and 4.22. The deformation after the maximum stress is reached for the model, it is unrealistic and is not plotted in the stress-displacement curves. The stress-displacement of importance is until the ultimate stress is reached and this is the only range that will be evaluated. As the plot indicates, the numerical curve fits with the experimental data quite well by a deviation ranging between 1.1% to 9.3%, listed in 4.7. The simulation for the two biggest holes correlates the best to the experimental data. This may be due to the fiber bundle cut-out that will be discussed in section 5.3. For the two small holes the deviation is larger relatively to the two bigger holes.

Table 4.7: Deviation between numerical simulations and experimental results.

Coupons	Average (MPa)	Abaqus (MPa)	Deviation (%)
AH1	359.4	381.1	6.0
AH2	356.1	352.2	1.1
AH3	291.6	264.6	9.3
AH4	293.0	268.0	8.5
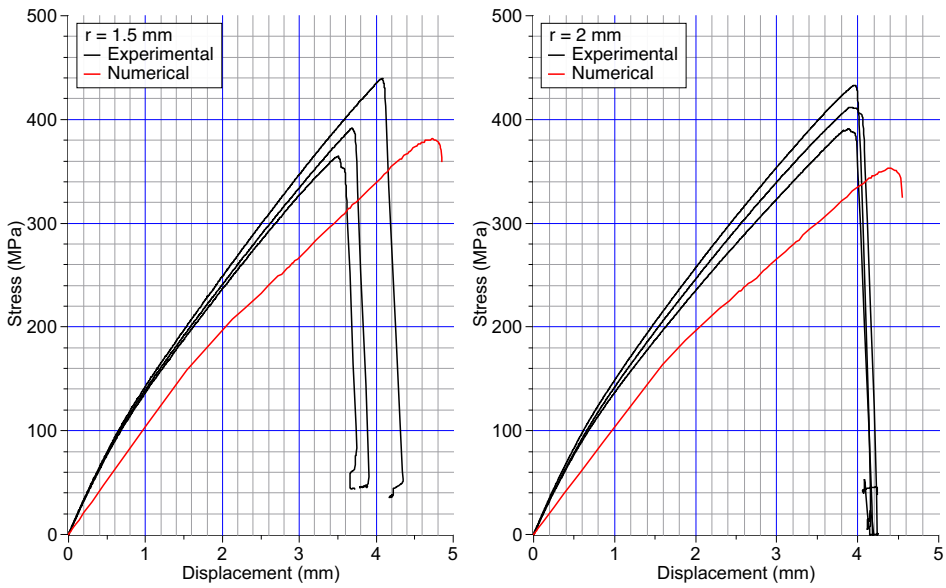
Figure 4.21: Numerical simulations compared with experimental results. Holes with r = 1.5 mm and r = 2.0 mm.
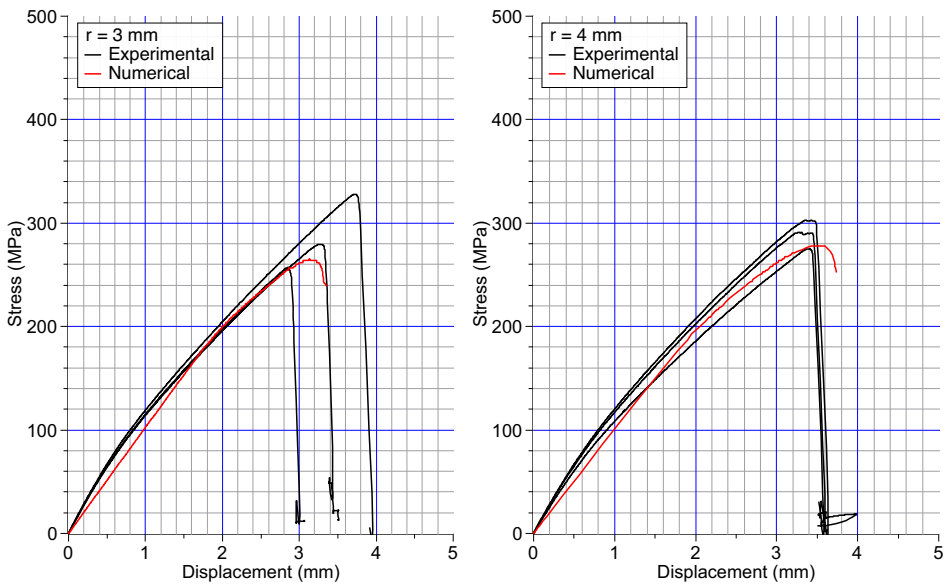
Figure 4.22: Numerical simulations compared with experimental results. Holes with r = 3.0 mm and r = 4.0 mm.
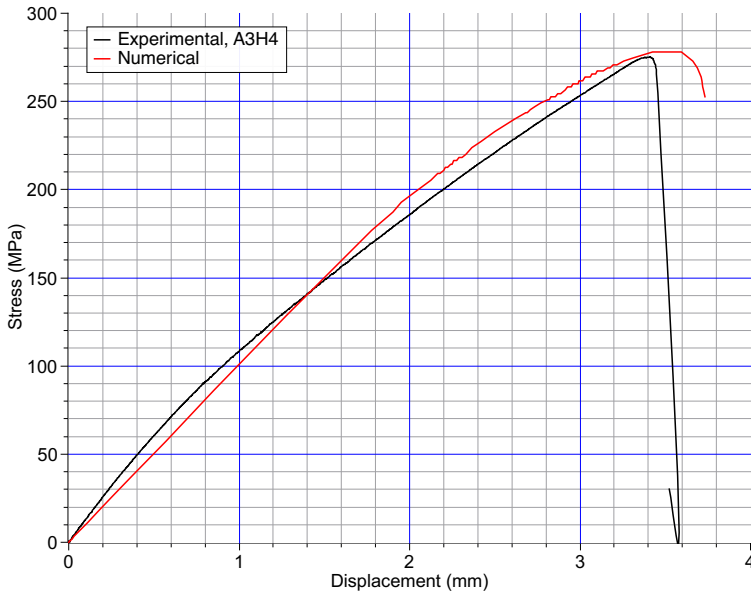
Figure 4.23: Numerical simulations compared with experimental results for r = 4.0 mm.
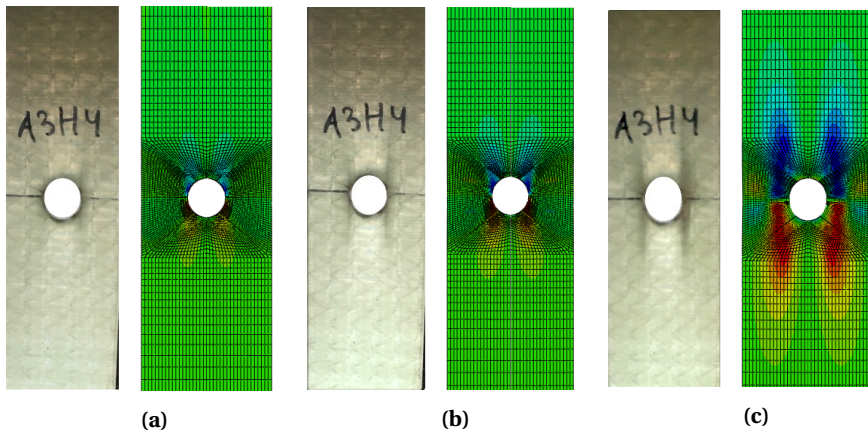
Figure 4.24: Laminate A loaded in tension. Comparison between experimental and numerical simulation, showing the shear stress propagation at 90 MPa (a), 180 MPa (b) and 270 MPa (c).

Chapter 5

Discussion

5.1 Factors affecting the residual strength

The area of delamination on Laminate A is a bit larger compared to Laminate B. As mentioned in section 2.1.2, an abrupt fiber orientation will create larger delaminations. By this reason, the delamination area is larger for the cross-ply laminate. Comparison of the damage area of Laminate A and B are shown in figure 5.1

In tensile strength, fibers carry the most of the tensile load. Fiber failure will therefore have a significant effect to the residual tensile strength properties. Experiments with laminates having the similar fiber reinforcement but with different matrix materials indicates that the matrix have little effect to the residual tensile strength of the material [2]. The strength of the cross-ply laminate is higher than for the quasi-isotropic (ref. table 4.1 and 4.2).

The tensile strength of Laminate A shows a great reduction just after the first impact damage and continues to decrease as the impact energy increases. At 142 J, the residual strength has been reduced by over 40%. As the fibers carries the majority of the tensile loading, this great reduction implies that fiber failure has occurred. From the damage inspection (section 4.1), fiber failures were detected both at 28 J and 142 J, but the extent varied. This confirms that fiber failure occurs at impact damages for 28 J, but this could
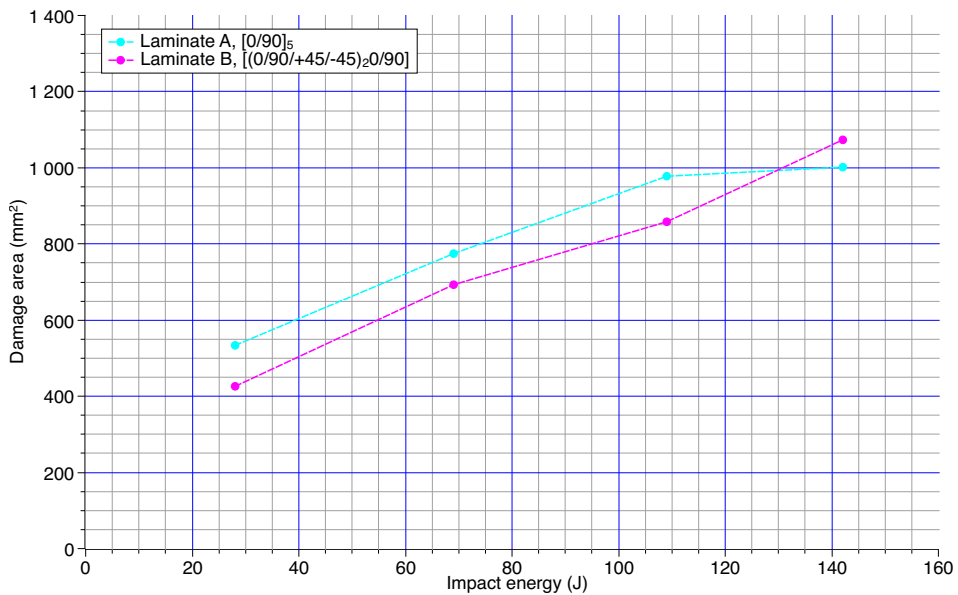
Figure 5.1: Comparison of damage area for Laminate A and B, juster fontstørrelse etc.

not be generalized. Out of two coupons only one confirmed the presence of fiber failure, visually. This were also the case for Laminate B.

For Laminate B, the tensile strength reduction after the first impact energy are modest, but decreases more rapidly after the second impact energy. The extent of fiber failure varied for the different impact energies inspected.

The residual compression strength is more affected by delamination and matrix cracking than fiber failure due to local instability from the delaminations [13].

For Laminate B, threshold for initiation of damage is not reached until the impact energy exceeds 28 J. The delamination area increases linearly with increasing impact energy. Higher impact energies induce more matrix cracks which leads to more delaminations. When the damage threshold is reached (somewhere between 28 J and 69 J), the compressive residual strength drops and levels off at a strength of 75% of the undamaged strength.

Laminate A, reaches the threshold of damage initiation somewhere between 0 and 28 J. From this, the compressive strength of Laminate A reduces significantly until it levels off at 109 J and just under 70% of the undamaged specimen strength. Due to larger

delaminations in Laminate A, a greater compressive reduction will apply compared to Laminate B. Figure 4.14 correlates well with figure 5.1.

S. Abrate [2] states that compression is critical for impact-damaged specimen because under this type of loading, strength reductions are the largest. The tensile and compressive strength of Laminate B shows a similar reduction for the relative point of view. However, the tensile strength reduction of Laminate A is greater than the compressive strength reduction, shown in figure 5.2.

In a four-point bending test, the top plies (at the loading nose surface) are subjected to a compression force while tension forces will act at the bottom surface (the surface in contact with the supporting noses). As investigated, fiber failures were detected at the bottom plies of the coupons. This is also where the failure at the flexural tests for the higher impact energies appear.

Figure 5.2 shows that the flexural strength properties are more impact resistant than the properties of both tensile and compression. The flexural strength is much higher than the residual tension and compression strength. In tension and compression, the whole cross-section is subjected to the maximum stress while the location for maximum stress in flexure is at the outer plies.

It could also be noted that Laminate A has the greatest reduction for tensile and compression strength but the flexural strength remains with the highest strength until it is induced by the highest impact energy.
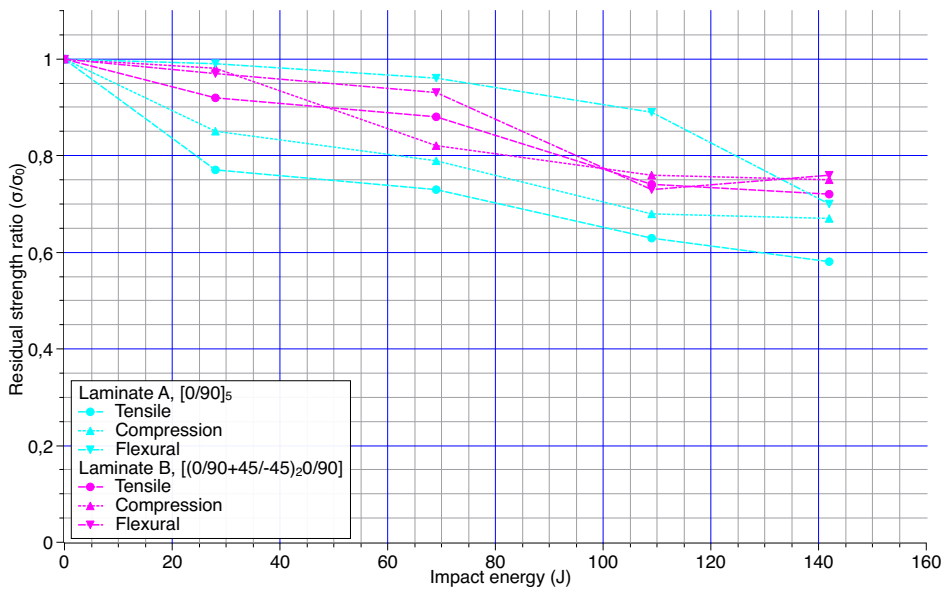
Figure 5.2: Comparison of residual tensile, compressive and flexural strength.

5.2   Relation between damage size and residual strength

Figures 5.3 - 5.8 show the scatter of damage area versus residual strength. As mentioned in section 4.1, the measured area is done through backlighting providing the projection of all delamination surfaces. The extent of fiber failure and matrix cracking is not quantitatively measured through this method. The plotted damage area is therefore the extent of delaminations on the specimen. The slope of the trendlines are negative, indicating a reduction in the residual strength with increasing damage area. Due to the large variance giving a low coefficient of determination (listed in table 1 for all plots), a prediction model of the damage size versus residual strength will not have an effect.
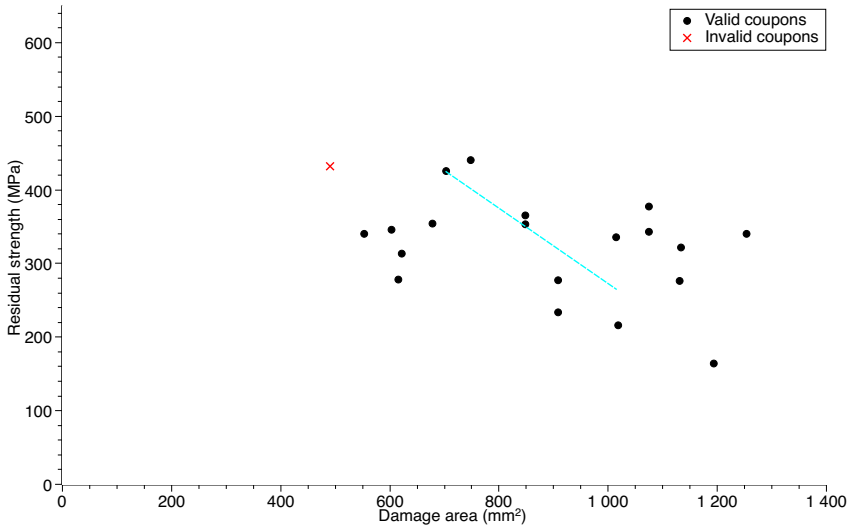
Figure 5.3: Damage size versus tensile strength, Laminate A.
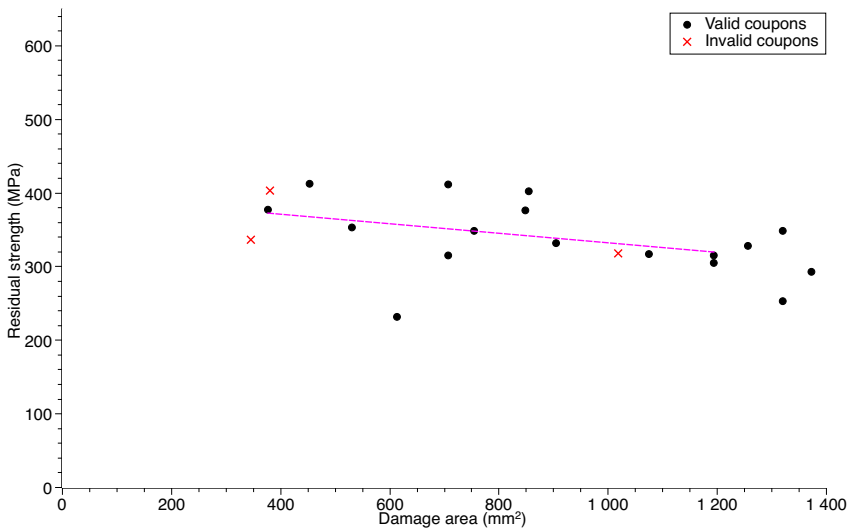
Figure 5.4: Damage size versus tensile strength, Laminate B.

Figure 5.5: Damage size versus compressive strength, Laminate A.
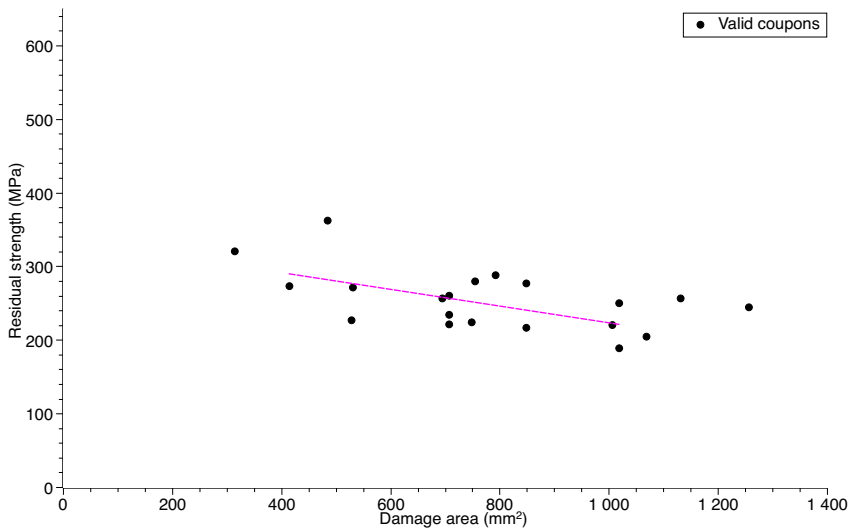
Figure 5.6: Damage size versus compressive strength, Laminate B.
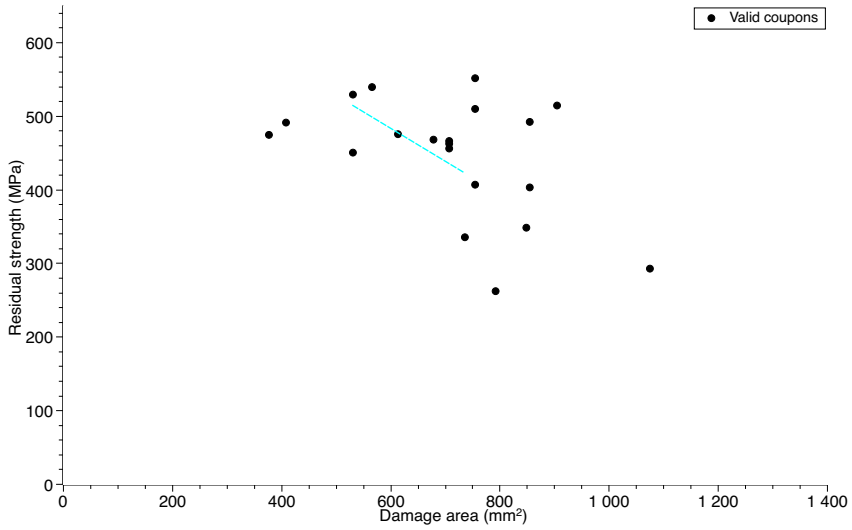
Figure 5.7: Damage size versus flexural strength, Laminate A.
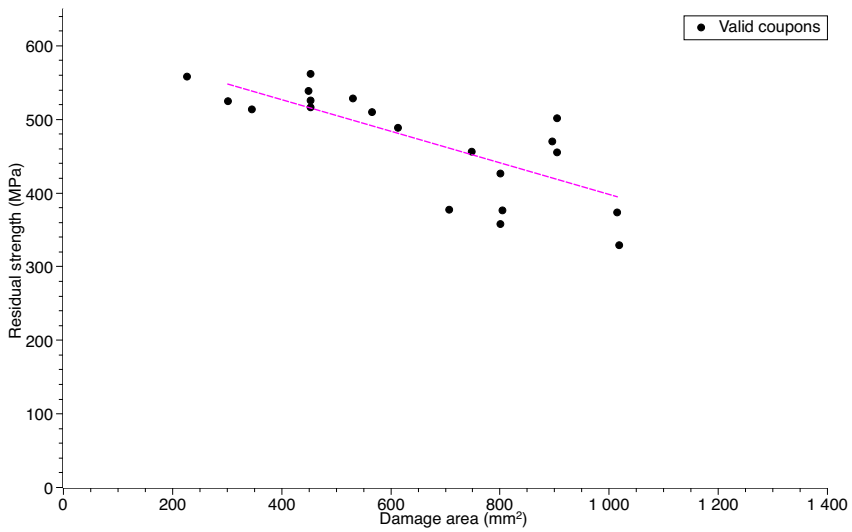
Figure 5.8: Damage size versus flexural strength, Laminate B.

5.2.1 Accuracy of results

It is worth evaluating the variance of the results. The tensile test of the undamaged specimen, shows a low variation for both Laminate A and B. This gives an indication that the test itself is relatively precise. Having this in mind, the variations that occurs when the specimen is subjected to impact might imply that the impact damage itself gives the large variation. The results from the burn-off tests showed this in particular. Within the same impact energy induced, some specimen had fiber failure, some did not. This explains some of the variations.

For the compression test on the other hand, the undamaged coupons show a relatively large variation. This gives an indication that the test setup itself gives variations. This might be due to the anti-buckling device. There is a small friction force acting between the device and the coupon and there were minor bucklings for some coupons during the test that might give variations in the residual strength. Therefore, when the impact damages were induced the variations were not only due to variations in the damage, it might be due to the strength test itself.

For the flexural test, the impact damages did not affect the strength until after energies exceeded 69 J. Large variations were stalled for the coupons below the damage initiation threshold. This tells us that the test setup itself is relatively precise. After the threshold was reached, the variations arose. This indicates again that the impact damages vary.

Generally, a coefficient of variance (CV) below 5% indicates a very good correlation of the data, 10% is a good correlation, while greater than 15% shows a bad correlation of the data set. Utilizing models with a large deviation will give a low value of significance and will not have any effect. Tables of the CV could be found in the Appendix.

For the damage size versus impact energy plots, all plots have a CV greater than 15%, except for the greatest impact energy conducted on Laminate B. It should be noticed that drop heights were performed using measuring tape to mark points along the rope. This will obviously give an uncertainty for the test as well, but the deviation was not possible to be measured quantitatively.

Voids could also cause variations. Out of the selection of 30 specimen of the pop-

ulation of 240, Laminate A 13% had bubbles, 37% had dry zones and 3% had wrinkles and for Laminate B none with bubbles, 3% with dry zones and 7% with wrinkles. The coupons were as mentioned inspected ahead of the experimental tests to detect defected ones. There is always a possibility of missing this detection. Even though there is a low probability of the combination of both missing to inspect the coupon as well as one of the selected coupons is defect, the likelihood is present.

Other affecting factors worth mentioning causing the variations in result is the rigid substrate supporting the specimen when the impact was induced. In addition, both impact and strength experiments were conducted on different days. The lack of personal routines and experience might have an effect to the accuracy of the results as well.

5.3 Equivalent hole models

The residual strength in tension and compression for the specimen with central circular holes are plotted in the figures 5.9 - 5.12. The specimen noted as invalid were specimen with a failure outside the hole. The two laminates are compared in figure 5.13 and 5.14. In both tensile and compression both laminates have almost equivalent strength reduction.

The smaller hole sizes show a bigger variance than the bigger holes. Coupons with the holes of 4.0 mm in radius show almost no variation. The variation in the smaller holes might be due to the misalignment of the holes relative to the centerline causing nonsymmetrical loads. One other reason might be due to the variations of the fiber bundles in the laminate. The relative positioning of the fiber bundles in the specimens will vary (figure 3.1). There is a small space between each bundle in the E-glass mats. When drilling the small holes, one might hit the space between the bundles, which would break less fibers than hitting the bundle right in the middle. Due to the variation of cutting fibers, this might have an effect on the residual strength for the small holes.

A drilled hole through a specimen will of course destroy the load carrying fibers in addition to the matrix. For the case of the impact damages created in this thesis, the fiber failures occurred only at the top plies of the specimen, and will therefore have a less significant effect on the residual strength than for through specimen drilled holes. For compression strength, where delaminations and matrix damage has the most significant effect on the strength (while the fibers have a less effect), the drilled hole will simulate these damage modes through the thickness of the specimen. Even though the impact damage only affects the top plies of the specimen, the stresses around the damage acts in the same manner as for stresses around holes, mentioned in theory.
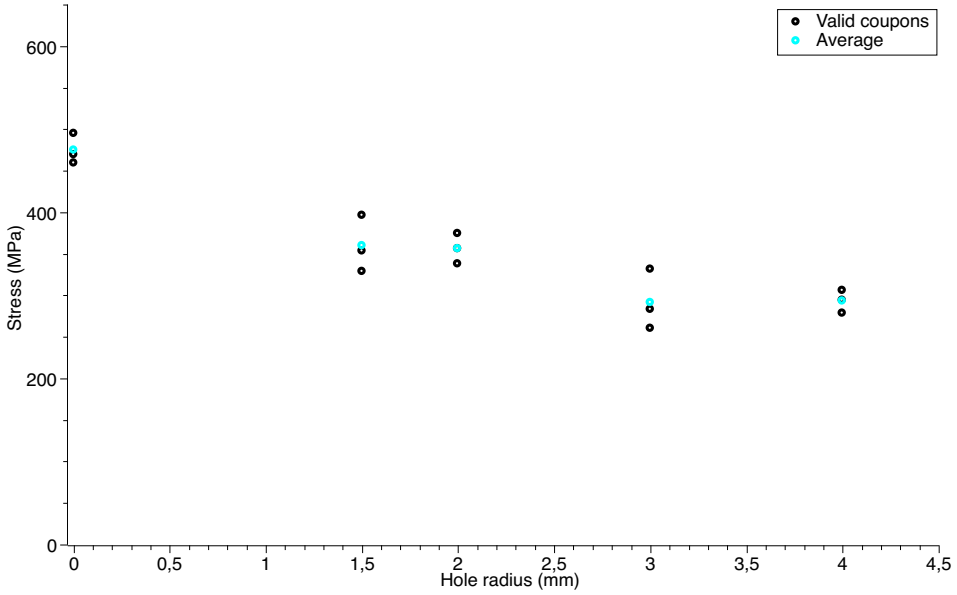
Figure 5.9: Residual tensile strength of Laminate A versus drilled hole size.
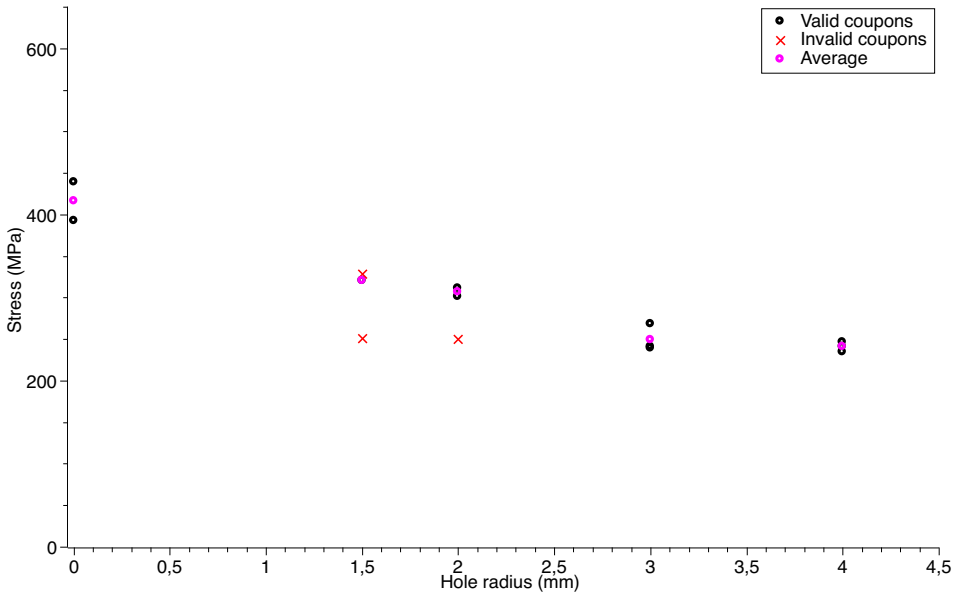
Figure 5.10: Residual tensile strength of Laminate B versus drilled hole size.
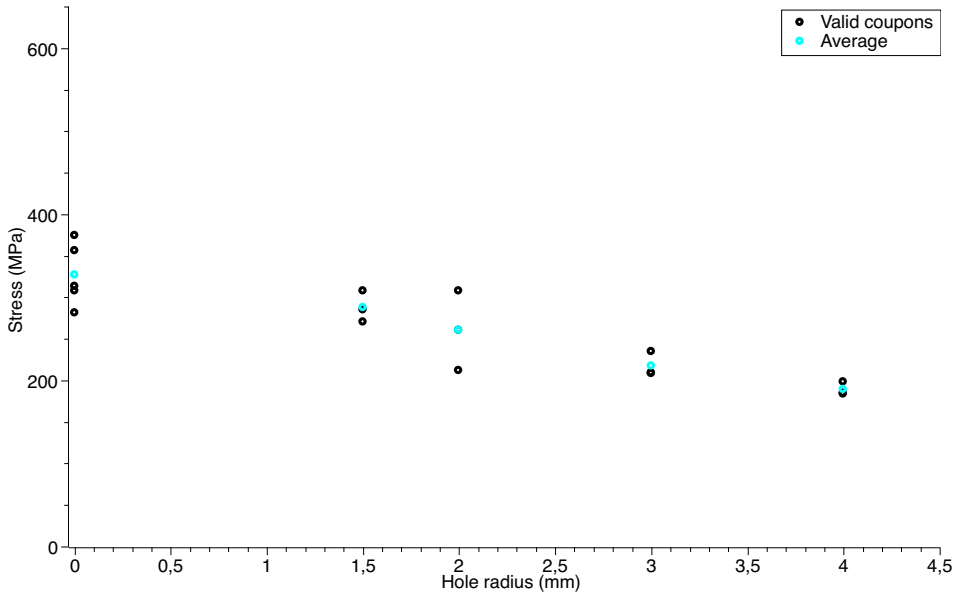
Figure 5.11: Residual compression strength of Laminate A versus drilled hole size.
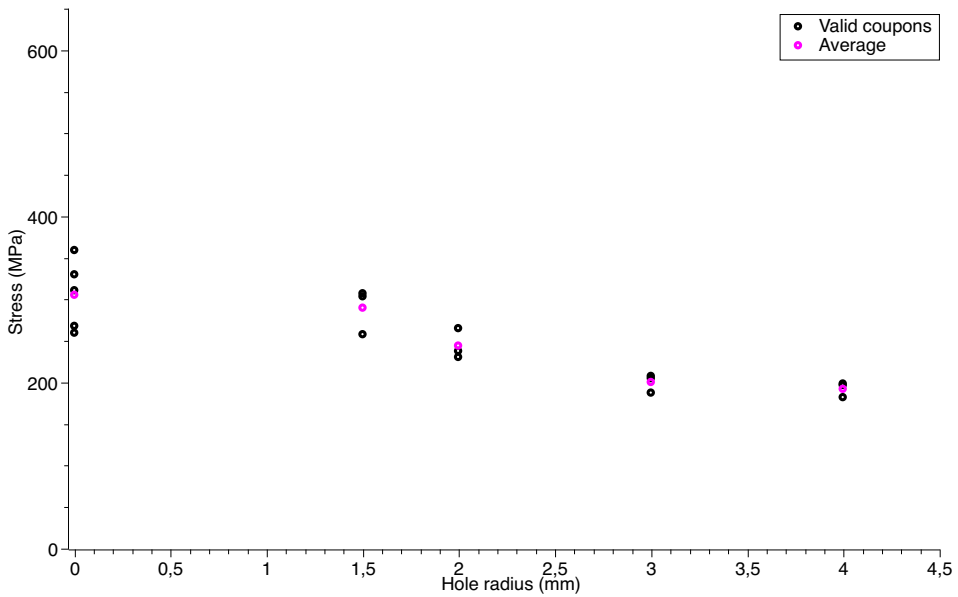
Figure 5.12: Residual compression strength of Laminate B versus drilled hole size.
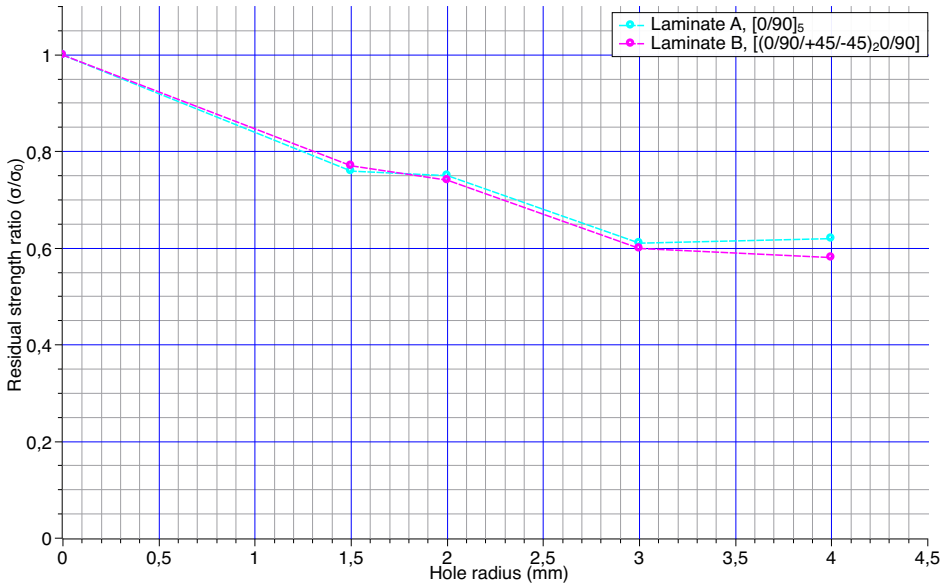
Figure 5.13: Relative residual tensile strength for Laminate A and B.
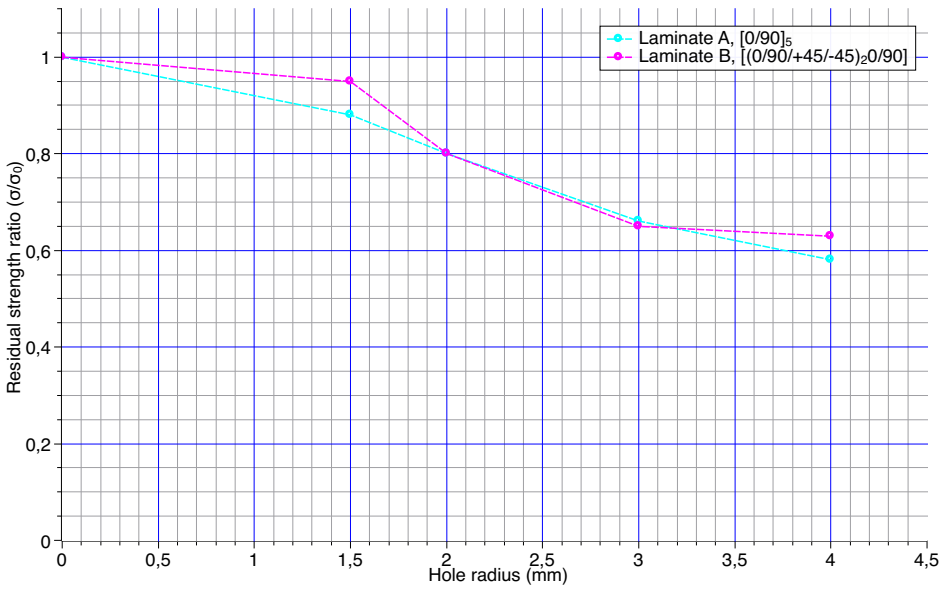
Figure 5.14: Relative residual compression strength for Laminate A and B.

5.3.1 Average stress criterion

As Whitney and Nuismer discovered in their study, the average stress criterion fitted better for glass-epoxy composites than the point stress criterion. Therefore, this model will be considered. The characteristic value of a_0 needs to be determined through experimental data. In figures 5.15 - 5.18, the average stress criterion is plotted with the experimental data of coupons containing circular holes with radii of 1.5, 2.0, 3.0 and 4.0 mm tested in both tension and compression for both laminates.

5.3.2 Caprino's model

To compare with the average stress criteria, the model proposed by Caprino is plotted using the characteristic lengths listed in table 5.1. For the experimental data from the specimen with holes the parameter m is set to a value in the range of 0.30 to 0.42. The two parameters are chosen to give the best fit with the experimental data. The threshold parameter, L_0 is given a value close to zero that correlates good with the experimental data. For the impacted specimen the characteristic parameters α and E_0 were given a best fit value.

An exact value of the threshold for initiation of damage could not be detected. The threshold energies in the prediction models are therefore chosen by approximate values, based on the theory that a characteristic residual strength versus impact energy curve will follow a plateau stage where no damage has occurred for low impact energies and. Once the threshold is reached, the residual strength reduces quickly [13].

5.3.3 Evaluation of the two models

As Caprino stated in his study, his model fits better for relatively large holes than for Whitney and Nuismer's model. The damage initiation threshold could better be described by Caprino's model. Caprino showed in his study [5] through a four-point bending test that the residual compression strength worked well with his predicted model as well.

For the specimen containing circular holes the two follows a different path in the beginning of the plot, and gradually get equal when the hole size increases.

As known, small impact damages will not affect the residual strength. Once the threshold is reached, the strength will reduce. For the experiment conducted for both the cross-ply and the quasi-isotropic laminate, this is the case. Where exactly the threshold is is not known. It is indicated that the threshold is somewhere between 0 and 28 J for both Laminate A and B in tension and compression. The four-point bending test indicated that the significant strength reduction started after 28 J, and should lay somewhere between the present energy and 69 J. Once the threshold is set, the characteristic length of α could be determined. The characteristic parameters are listed in table 5.1.

The predicted curve by Caprino and Whitney and Nuismer in the range between the undamaged strength and the smallest hole is relatively different for both criteria. The further prediction is quite similar.

By using the numerical model, holes of a radii of 0.5 mm and 1.0 mm have been simulated in tension for Laminate A (shown in 5.9 and 5.10. The predicted threshold value seems to fit well, both for the experimental and numerical data. The coefficient of variance in listed in table 2. Due to the equivalent strength reduction in tension for both laminates, the results from the simulation are used for the prediction model of laminate B as well.
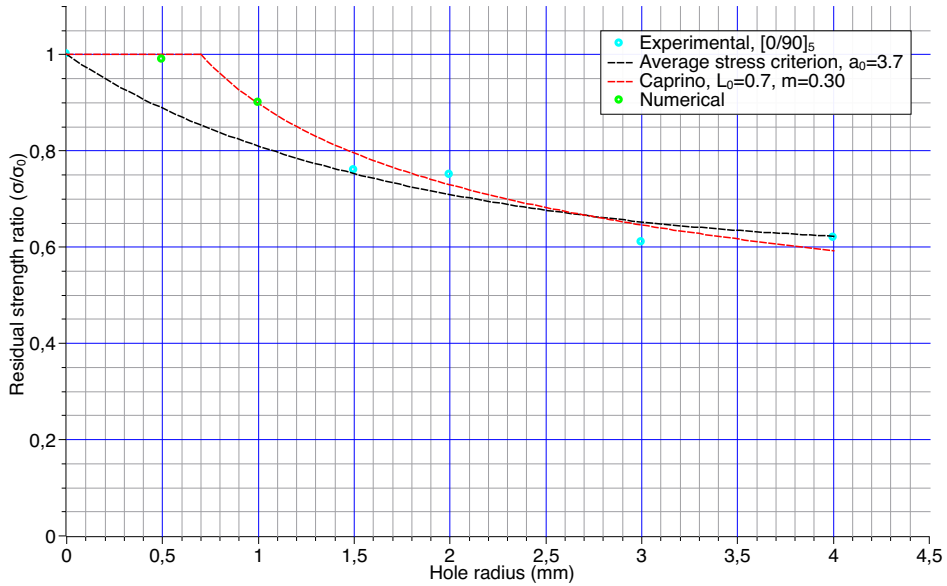
Figure 5.15: Equivalent hole model in tension for Laminate A.
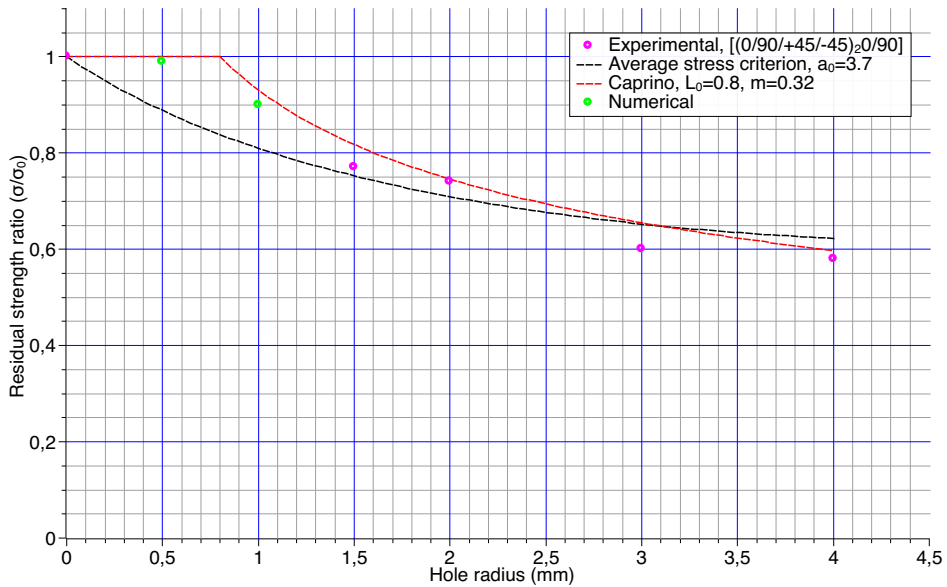
Figure 5.16: Equivalent hole model in tension for Laminate B.
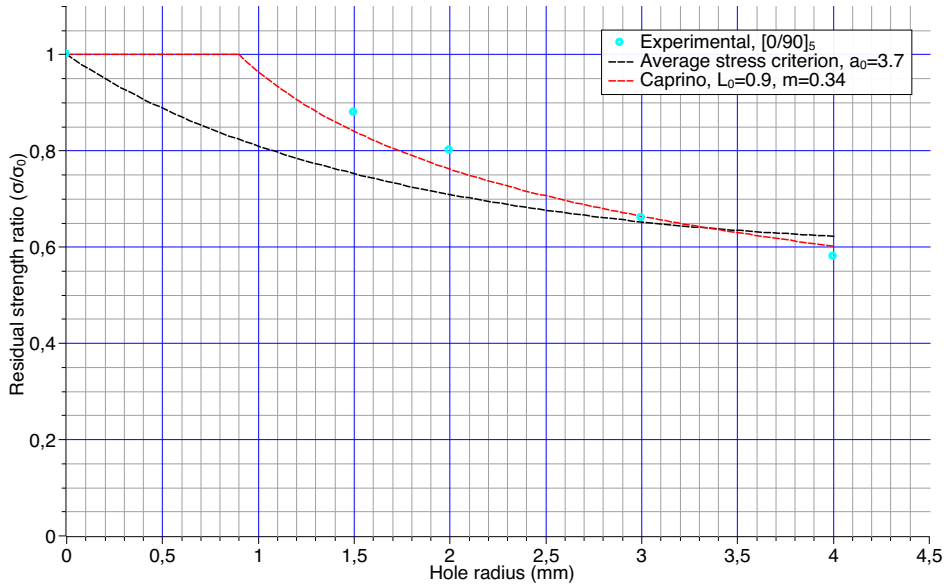
Figure 5.17: Equivalent hole model in compression for Laminate A.
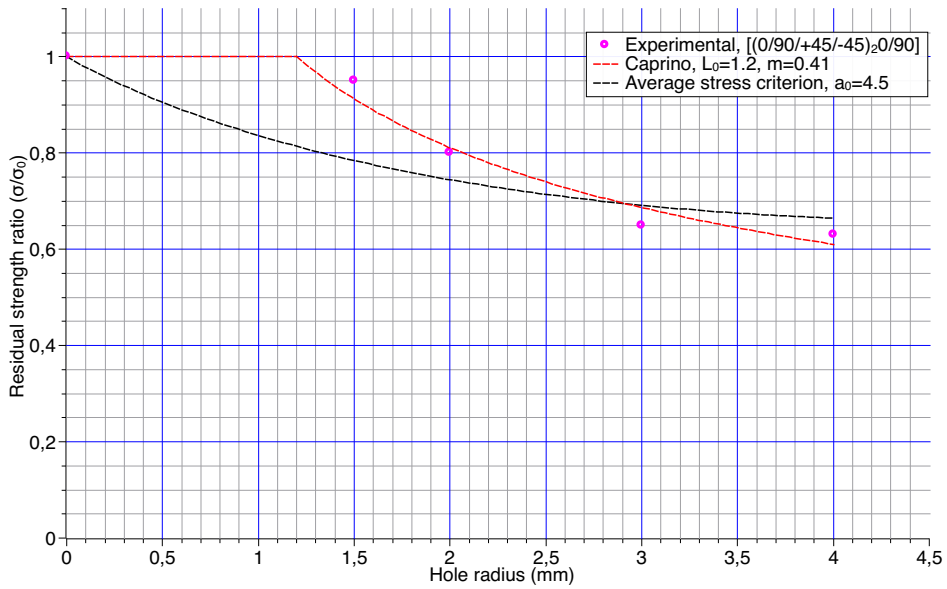
Figure 5.18: Equivalent hole model in compression for Laminate B.

Table 5.1: Parameters to the hole model. L_0 and m are used in Caprino's model, while a_0 are used in the average stress criterion proposed by Whitney and Nuismer.

	Laminate A		**Laminate B**	
	Tension	Compression	Tension	Compression
L_0	0.7	0.9	0.8	1.2
m	0.30	0.34	0.32	0.41
a_0	3.7	3.7	3.7	4.5

Table 5.2: Variation of coefficient for mechanical tests on specimen with holes of Caprino's model.

Coefficient of variation, R^2	**Caprino's model**
0.951	Tensile, Laminate A
0.979	Compression, Laminate A
0.941	Tensile, Laminate B
0.968	Compression, Laminate B

5.4   Residual strength of hole size versus impact damage

A model of comparing the residual strength after impact using the damage size (the size of the delamination area) with an equivalent circular hole size was attempted utilizing. Due to the large variation in the correlation between the damage size and the residual strength (as discussed in section 5.2), such a representation becomes inapplicable.

On the other hand, the impact energy and the circular hole size model had a better correlation. Figure 5.19 and 5.20 shows this relation. As discussed in section 5.3.3, Caprino's prediction model seemed to fit the experimental results the best and are therefore used as the prediction model. There are no experimental results to confirm whether the threshold value or the range from the threshold to the first impact are acceptable or not. The numerical results were used to give an indication on these values.

5.5   Design criteria for damage tolerance

A design criterion for the cross-ply and quasi-isotropic laminate are shown in figure 5.21 and 5.22 using the impact energy with the equivalent hole size. The lower bound are set by using the pooled standard deviation from the impact specimen (which had a larger deviation than the specimen with holes). By multiplying this by two the criterion will apply for 95% of all impact cases. Due to the large deviations in the experimental results, the criterion becomes quite conservative especially for Laminate A.
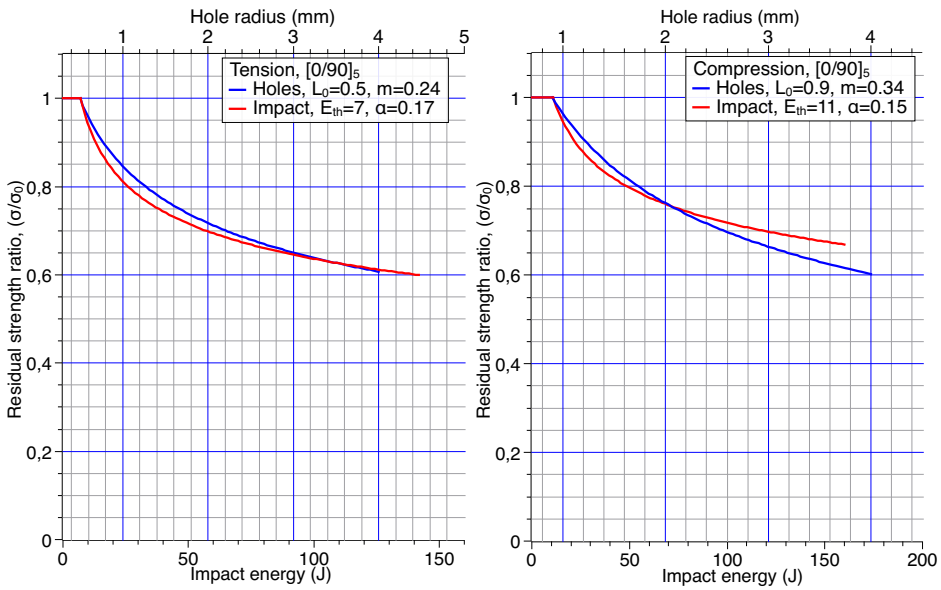
Figure 5.19: Hole size compared with impact damage energy for Laminate A. Tensile strength on the left and compression on the right, respectively.
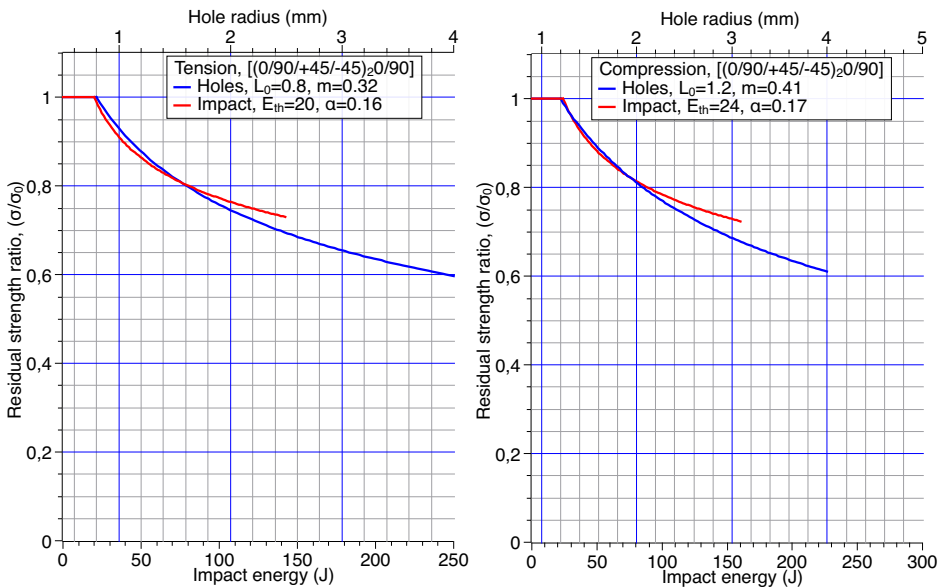
Figure 5.20: Design criteria for Laminate A using two standard deviations. Tensile strength on the left and compression on the right, respectively.
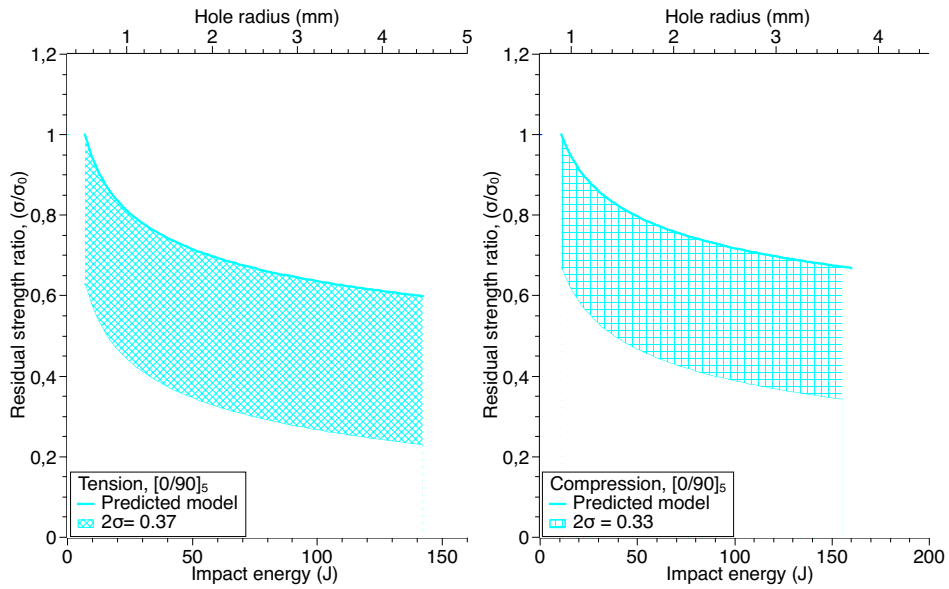
Figure 5.21: Design criteria for Laminate A using two standard deviations. Tensile strength on the left and compression on the right, respectively.
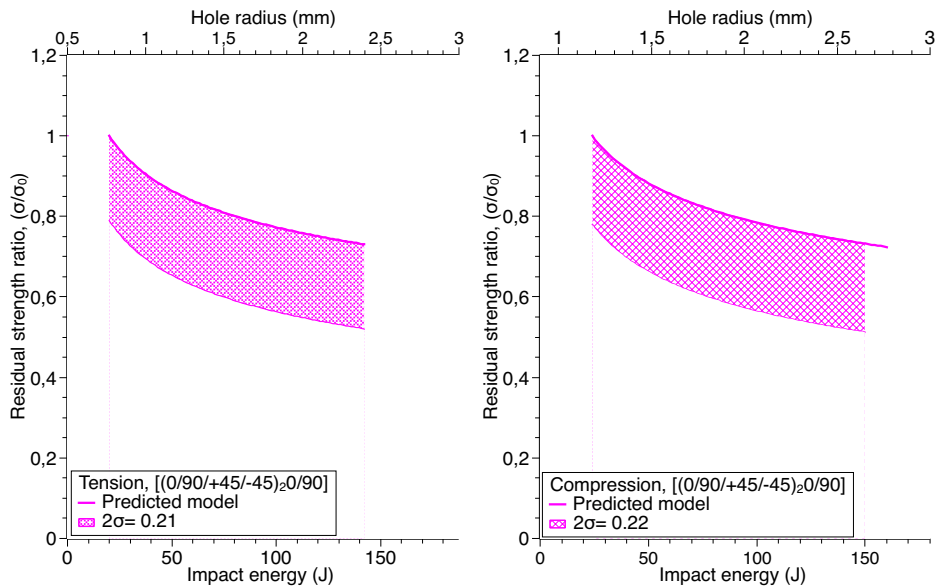
Figure 5.22: Hole size compared with impact damage energy for Laminate B. Tensile strength on the left and compression on the right, respectively.

5.6 Global strength prediction

The models achieved for predicting the residual strength with impact energy for the specimens could be used for predicting the residual strength for a wider panel or in terms of an infinite plate. If the characteristic parameters of the model are unknown experimental tests must be conducted in order to get the characteristic parameters for both models.

As mentioned, the stresses around impact-induced damages could be related to stresses around holes. On a large panel with the impact damages conducted in this thesis will obviously have a less significant effect on the residual strength as seen in the predicted model. It has been noted that the characteristic values in the predicted model by Caprino are influenced by the shape and size of the impactor aswell as the arcitecture and boundary conditions of the specimen or structure [10].

Hayman at *Section for Structural Integrity and Laboratories, Det Norske Veritas AS* developed a damage assessment scheme to investigate how a local impact damage affected the structural performance and functionality in naval ships [8].

The procedure was presented as follows:

- Estimate the strength reduction caused by the damage or defect.

- Determine the allowable strength reduction based on the original design assumptions, operational envelope, etc.

- Compare these. If the residual strength is smaller than the allowable value, consider the possibilities for restricting the operational envelope and/or accepting a lower safety factor until repair can be effected.

- If this is not sufficient carry out an emergency repair or take other emergency measures as necessary.

Damage levels

The damage is divided into 4 levels based on the extent of damage. Level 1 damage covers a small part of the panel stiffness and stresses and the effect could be neglected far away from the damage zone. It is possible to neglect distribution of the stresses in the structure when estimating the influence on the global strength. Level 4 damage is an extensive damage and will affect one or more panels. Will lead to redistribution of the whole structure.

Panel strength reduction

After strength tests, will find a reduction factor for the local damage, R_l. This quantifies the far-field stress/strain at failure. Determine a sensitivity factor S_p that accounts for the location of the damage in relation to the stress field in a real case scenario. Will give $R_p = S_p * R_l$, which is the panel strength reduction.

Global strength reduction

The change in stiffness after damages in Level 1 and 2 could be neglected. The global load reduction Rs is given by $R_s = S_s * R_p$. For levels 3 and 4 the stiffness changes could not be neglected. For level 4, it is normally necessary to remove the hole panel or the equivalent stiffness reduction and do a strength analysis of the whole ship.

The design criteria on the MILPRO boats produced by Norsafe needs to follow the standards by DNV GL. The standards include material type, length of the boat, velocities the boat and so on. When these inputs are set, an allowable strength of panels are given. Usually these criteria are based on a panel subjected to a pressure of a certain value.

The models conducted in this thesis gives answers to the first pin point in the damage assessment scheme. The second point will be given by DNV GLs standards. The two next points will be as a results of the two preceding.

Chapter 6

Conclusion and Further work

6.1   Further work

In order to judge the damages and the residual strength on Norsafe's MILPRO hulls in global scale, some recommendations on further work are highlighted. The predicted model worked well with the small specimen conducted in this thesis. With this study as a foundation, the next step would be conducting tests on larger plates and panels. A strength reduction model for a larger panel could then be established.

In order to achieve better correlations between the impact-induced damage area and residual strength, impact tests could be conducted when only the edges of the specimen are constrained, giving the plate the ability to deflect out-of-plane. By conducting this kind of test, boundary effects as the steel substrate used in this thesis or other edge effects, would not affect the damage region. This might give a better correlation between the impact-induced damage area and the residual strength properties.

6.2   Conclusion

An analysis of the residual strength characteristics for glass-fiber reinforced plastics after impact has been studied by conducting different strength tests. Two laminates representative for marine hulls have been investigated. One cross-ply and a quasi-isotropic laminate with the layups $[0/90]_5$ and $[(0/90/\pm 45)_2/0/90]$ respectively. An equivalent hole to impact damage model has been utilized for predicting the residual strength for both laminates.

Drop weight impact tests with an impactor of a hemispherical tip, were conducted on specimen with the approximate dimensions, 244.0 mm x 27.5 mm and a thickness of 4.0 mm and 3.6 mm for the cross-ply laminate (Laminate A) and the quasi-isotropic laminate (Laminate B), respectively. The specimens were supported by a rigid substrate. By varying the height, different damages were produced in the range of 28-142 J.

Damage assessments methods were used to determine the extent of the impact-induced damages, including delamination, matrix cracking and fiber failure, through both nondestructive and destructive methods. Since the glass-fiber vinylester composites studied are translucent the damage could be inspected by the nondestructive method - strong backlighting. The extent of delaminations was possible to observe through backlighting, but other inspection methods were needed for damage modes through the thickness of the laminate, such as matrix cracking and fiber failure. Microscopic examinations and burn-off tests on specimen with different impact energies were done. The damage assessment techniques confirmed the presence of all damage modes. The extent of damage varied within each impact series, giving some variations in the residual strength.

The effect of the impact damages on residual strength properties were shown through tension, compression and flexural tests. It was shown an overall clear reduction with increasing impact energy for both Laminate A and B. The largest impact energy on Laminate A gave a reduction of 40% in tensile, 35% in compression and 30% in flexural tests. For laminate B the residual strength reduced by 30%, 25% and 25% in tension, compression and flexural, respectively. The damage initiation threshold for compressive

and tensile strength were relatively lower compared to the residual flexural strength. It was not a clear trend between the delamination area and residual strength, but a rather clear trend between impact energy and residual strength.

The residual strength after these impact damages show the same trend as for the through thickness clean hole strength reduction. A model has been utilized using the impact energy as an input and a dimension of a through thickness clean hole with its respective residual strength as an output. The model does not take into account the effects of flexural bending of the composite during impact.

The comparison of an impact induced damage with its complex nature to a simple clean hole will make it easy to perform numerical simulations and might be powerful in predicting the residual strength of a larger composite panel. This model could be used to set a damage tolerance for Norsafe's composite hulls.

Bibliography

[1]   Inc. Abaqus. *Abaqus Analysis User's Guide.* 2014.

[2]   Serge Abrate. *Impact on composite structures.* Cambridge university press, 1998.

[3]   FJ Bradshaw, G Dorey, and GR Sidey. *Impact resistance of carbon fibre reinforced plastics.* PlasticsInstitute, 1973.

[4]   WJ Cantwell and J Morton. "The impact resistance of composite materials—a review". In: *composites* 22.5 (1991), pp. 347–362.

[5]   G Caprino. "Residual strength prediction of impacted CFRP laminates". In: *Journal of Composite Materials* 18.6 (1984), pp. 508–518.

[6]   Giancarlo Caprino. "On the prediction of residual strength for notched laminates". In: *Journal of Materials Science* 18.8 (1983), pp. 2269–2273.

[7]   Pål Duus. "Low-velocity impact and residual strength analyses of glass reinforced composite laminates". In: (2015).

[8]   Brian Hayman. "Approaches to damage assessment and damage tolerance for FRP sandwich structures". In: *Journal of Sandwich Structures and Materials* 9.6 (2007), pp. 571–596.

[9]   J.M. Hodgkinson. *Mechanical Testing of Advanced Fibre Composites.* Woodhead Publishing Series in Composites Science and Engineering Series. CRC Press, 2000. ISBN: 9781855733121. URL: https://books.google.no/books?id=FLC3SBtEt1kC.

[10] Jae-Mean Koo, Jung-Hun Choi, and Chang-Sung Seok. "Evaluation for residual strength and fatigue characteristics after impact in CFRP composites". In: *Composite Structures* 105 (2013), pp. 58–65.

[11] Tom Mitrevski et al. "The effect of impactor shape on the impact response of composite laminates". In: *Composite Structures* 67.2 (2005), pp. 139–148.

[12] Researchgate.net. *Transverse force and moment diagrams for three point and four point bending*. URL: https://www.researchgate.net/profile/Ali_Amiri14/publication/276207310/figure/fig3/AS:294482911219712@1447221605146/Figure-3-Transverse-force-and-moment-diagrams-for-three-point-and-four-point-bending.png.

[13] MOW Richardson and MJ Wisheart. "Review of low-velocity impact properties of composite materials". In: *Composites Part A: Applied Science and Manufacturing* 27.12 (1996), pp. 1123–1131.

[14] V Silberschmidt. *Dynamic Deformation, Damage and Fracture in Composite Materials and Structures*. Elsevier Science, 2016.

[15] Martin Welle Skaar. "Modeling and Testing of Impact Damage in Composite Pressure Vessels". In: (2015), pp. 19–21.

[16] ASTM Standard. "3039/D 3039M-14". In: *Standard test method for tensile properties of polymer matrix composite materials* 10 (2014).

[17] ASTM Standard. "D6641/D6641M-14". In: *Standard test method for determining the compressive properties of polymer matrix composite laminates using a combined loading compression (CLC) test fixture* (2014).

[18] ASTM Standard. "D7264/D7264M-15". In: *Standard Test Method for Flexural Properties of Polymer Matrix Composite Materials* (2015).

[19] ASTM Standard. "D790-15". In: *Standard Test Methods for Flexural Properties of Unreinforced and Reinforced Plastics and Electrical Insulating Materials* (2015).

[20] J Ma Whitney and RJ Nuismer. "Stress fracture criteria for laminated composites containing stress concentrations". In: *Journal of composite materials* 8.3 (1974), pp. 253–265.

[21]   AS Yigit and AP Christoforou. "On the impact between a rigid sphere and a thin composite laminate supported by a rigid substrate". In: *Composite Structures* 30.2 (1995), pp. 169–177.

Appendix

Appendix A - Tables

Table 1: Variation of coefficient for damage size versus residual strength in section 5.2.

Coefficient of variation, R^2	Strength test
0.521	Tensile, Laminate A
0.114	Compression, Laminate A
0.404	Flexural, Laminate A
0.110	Tensile, Laminate B
0.269	Compression, Laminate B
0.520	Flexural, Laminate B

Table 2: Variation of coefficient for mechanical tests on specimen with holes of Caprino's model.

Coefficient of variation, R^2	Caprino's model
0.951	Tensile, Laminate A
0.979	Compression, Laminate A
0.941	Tensile, Laminate B
0.968	Compression, Laminate B

Table 3: Dimensions of a random selection from Laminate A.

#	Length (mm)	Thickness (mm)	Width at gauge (mm)
1	244	3.7	27.5
2	244.4	4	27.5
3	244.9	4.2	27.6
4	244	4.1	27.4
5	244.5	3.8	27.6
6	244.2	4	27.6
7	244	4.1	27.6
8	244.2	4	27.4
9	244.2	4.1	27.4
10	244.1	3.9	27.5
11	244.2	3.9	27.6
12	244.2	3.9	27.6
13	244.5	4.1	27.7
14	244	3.9	27.4
15	244.5	4	27.7
16	244	4	27.4
17	244	3.7	27.5
18	244.5	4	27.6
19	244.5	3.5	27.5
20	244.4	4.1	27.4
21	244.5	3.7	27.6
22	244.1	3.8	27.6
23	244.1	4	27.6
24	244.2	4	27.4
25	244.5	4.1	27.5
26	244	4	27.5
27	244	4	27.5
28	244.5	4	27.6
29	244	4	27.5
30	244.5	3.9	27.6

Table 4: Voids of coupons, Laminate A.

Voids	Number of coupons out of n
Bubbles	4
Drought	11
Damage top/bottom	27
Bumps	1

Table 5: Dimensions of a random selection from Laminate B.

#	Length (mm)	Thickness (mm)	Width at gauge (mm)
1	244.2	3.7	27.5
2	244.5	3.3	27.6
3	244.2	3.5	27.6
4	244.2	3.8	27.5
5	244.2	3.5	27.5
6	244.2	3.5	27.5
7	244.5	3.4	27.5
8	244.5	3.5	27.6
9	244.5	3.7	27.6
10	244.3	3.6	27.7
11	244.2	3.5	27.6
12	244.2	3.4	27.7
13	244.1	3.9	27.6
14	244	3.4	27.5
15	244.2	3.5	27.6
16	244.2	3.6	27.6
17	244.2	3.6	27.6
18	244.5	3.6	27.6
19	244	3.8	27.6
20	244.2	3.7	27.5
21	244.5	3.8	27.7
22	244	3.5	27.6
23	244.5	3.3	27.6
24	244.5	4	27.4
25	244.5	3.6	27.5
26	244.5	3.7	27.5
27	244	3.7	27.5
28	244.5	3.6	27.5
29	244.2	3.6	27.6
30	244.5	3.5	27.6

Table 6: Voids of coupons, Laminate B.

Voids	Number of coupons out of n
Bubbles	0
Dry zones	1
Damage top/bottom	29
Wrinkles	2

Appendix B - Stress-Displacement curves

Tensile tests
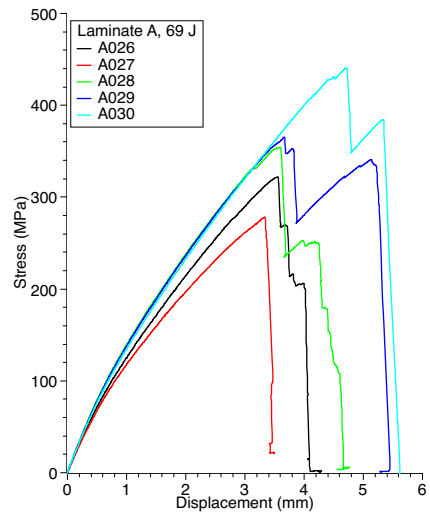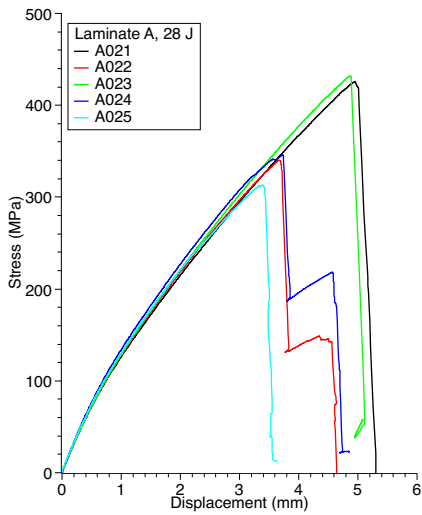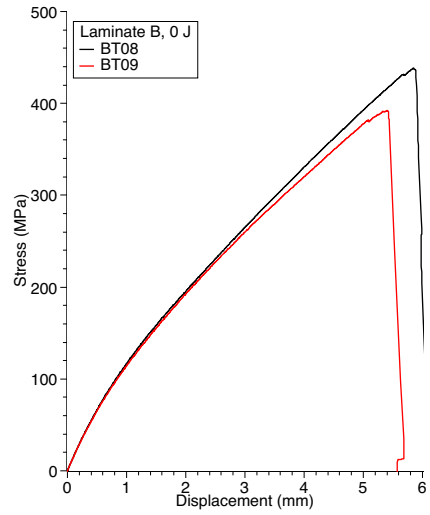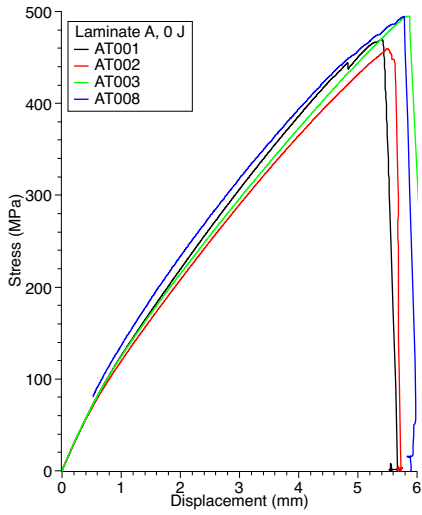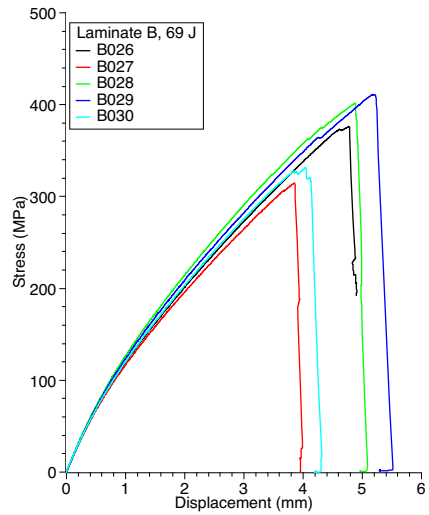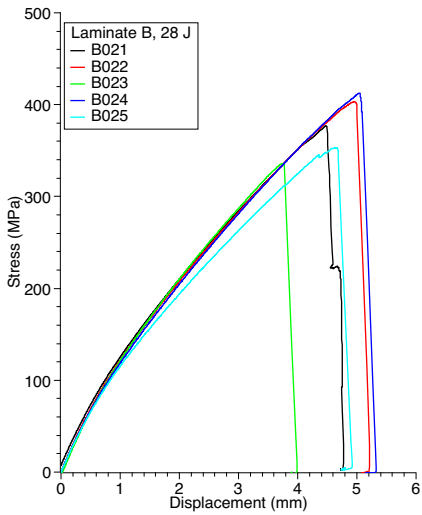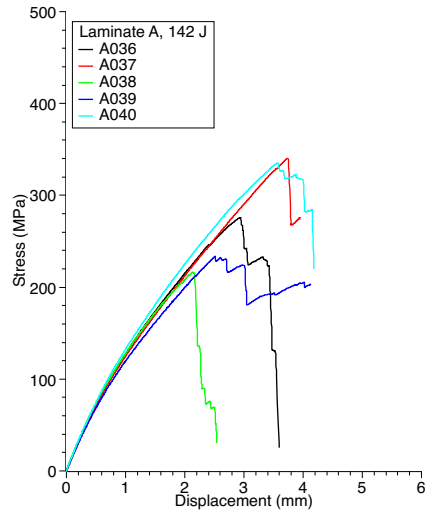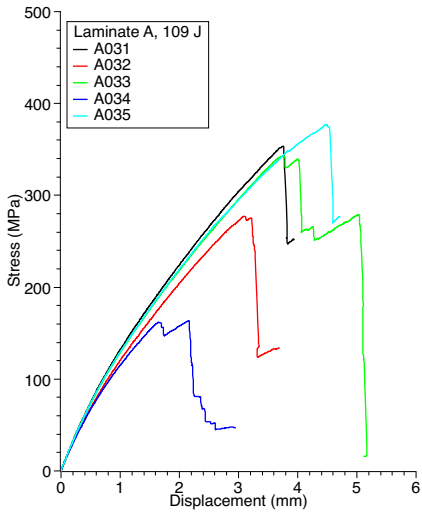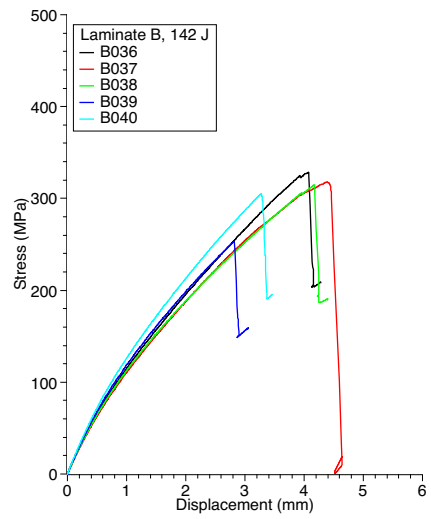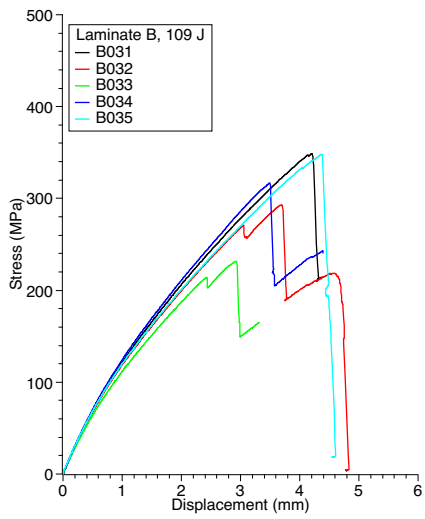
Compression tests
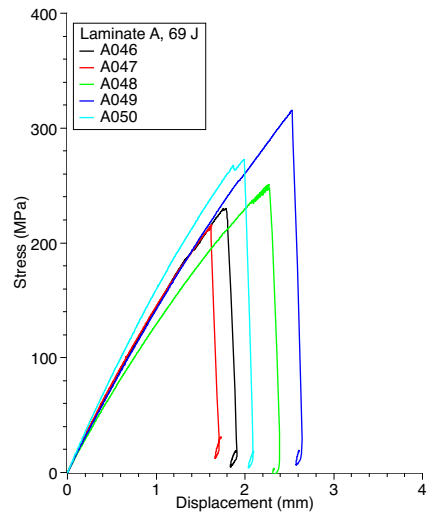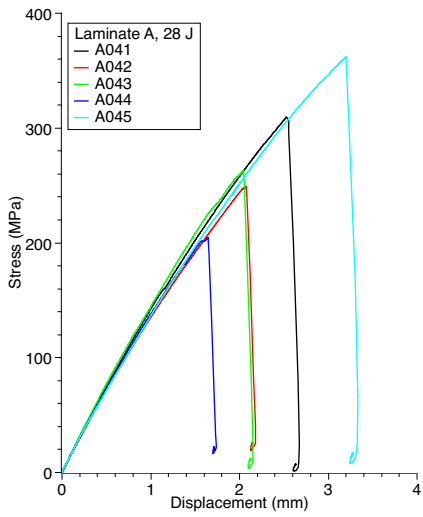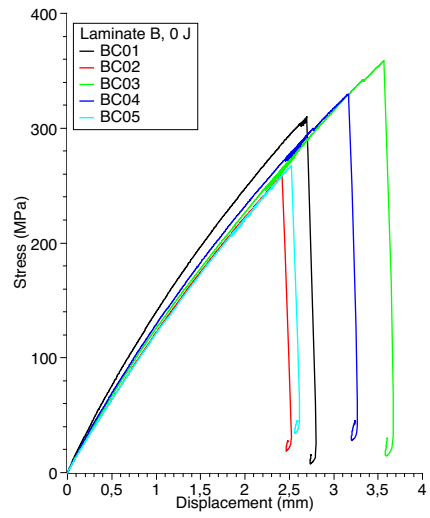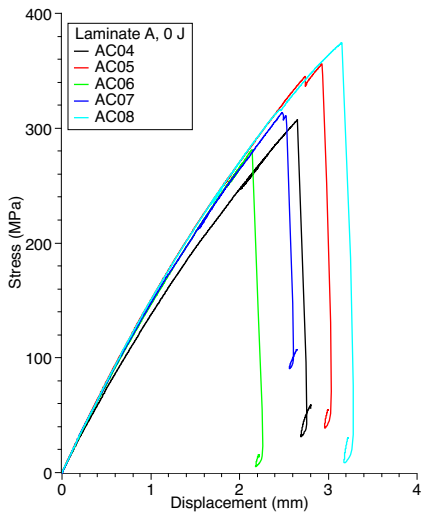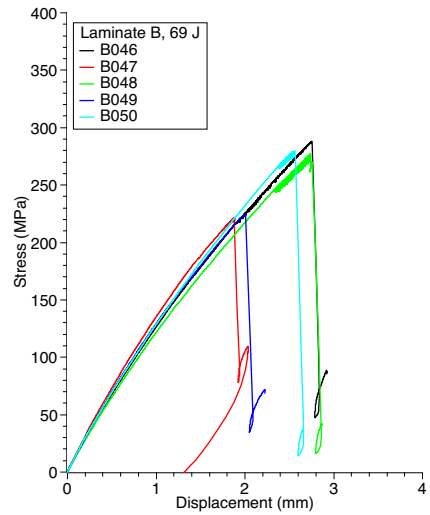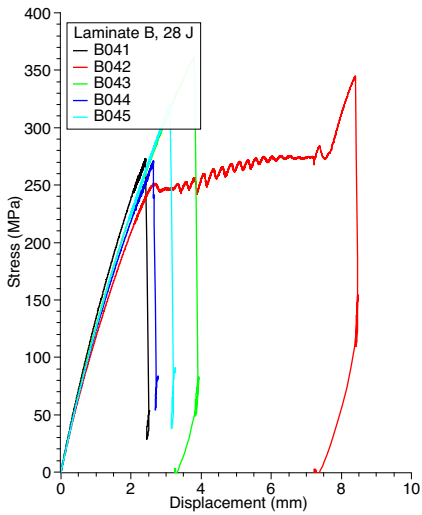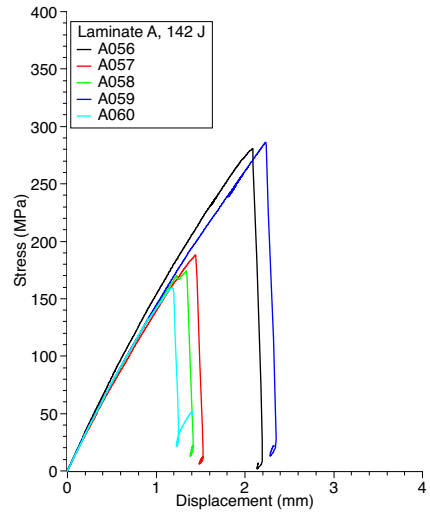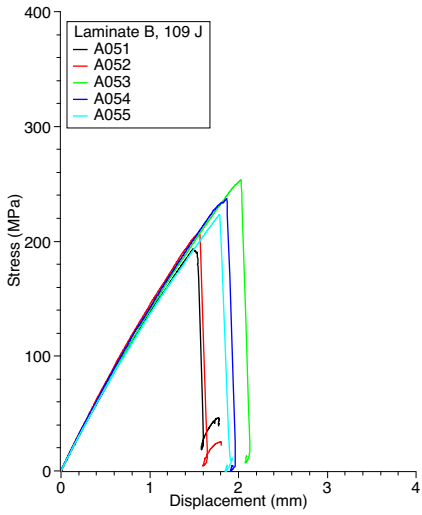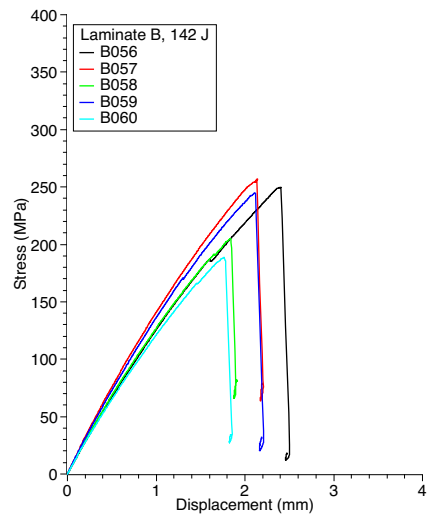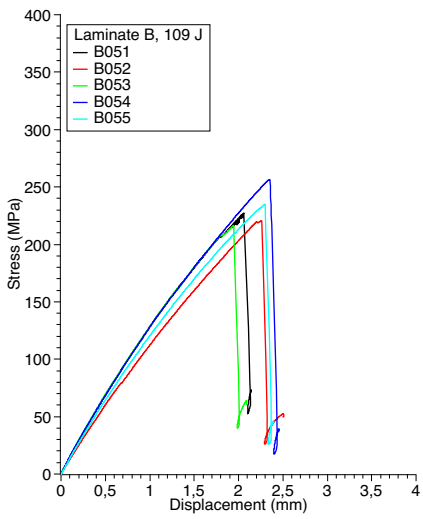
Flexural tests
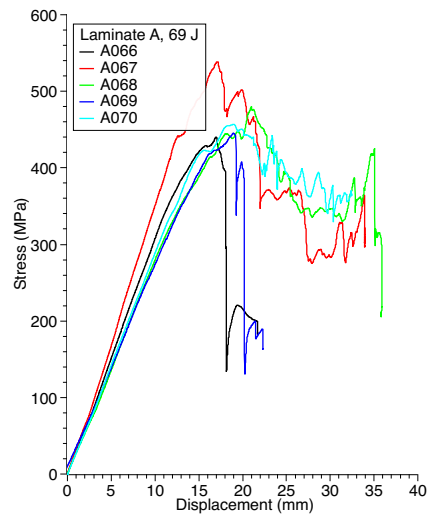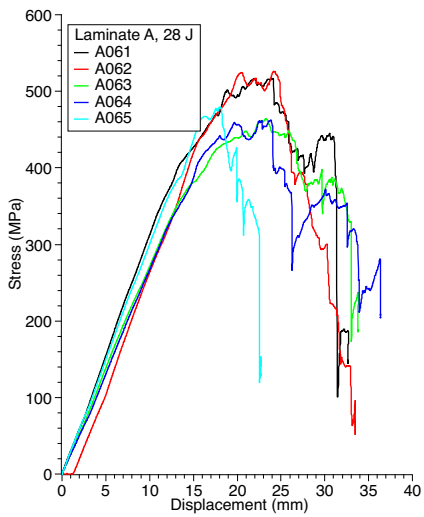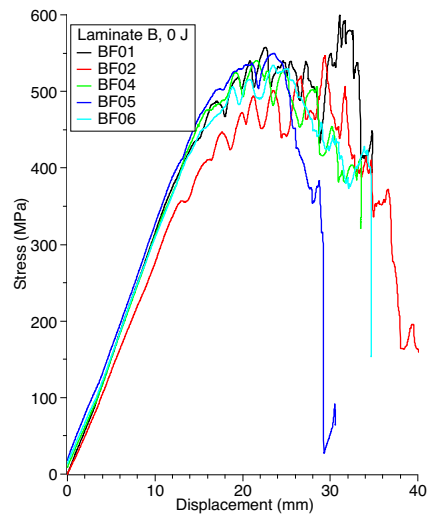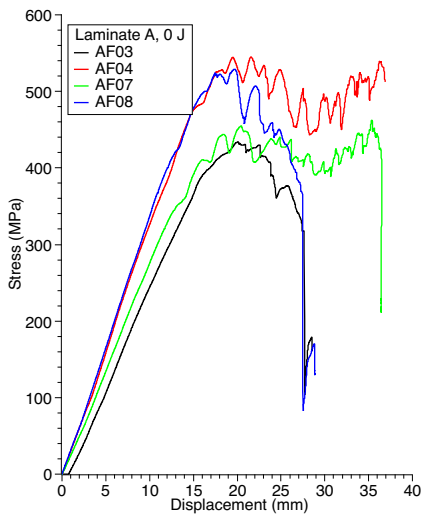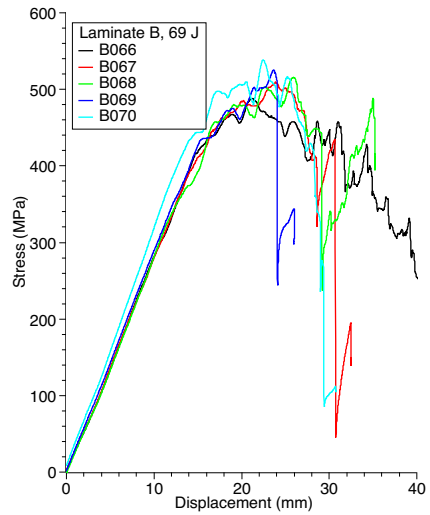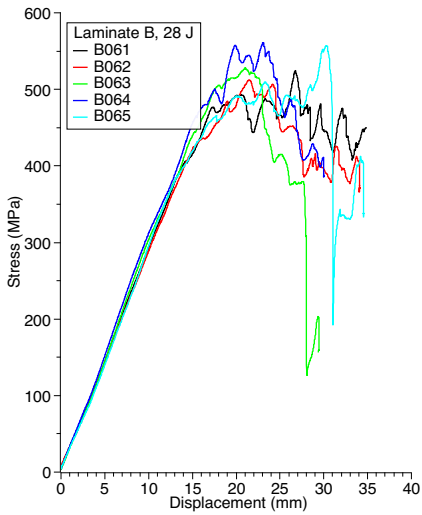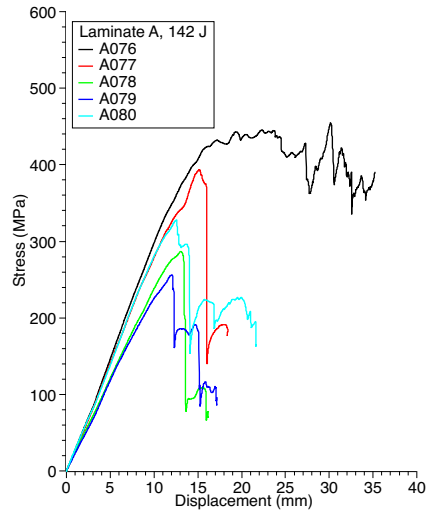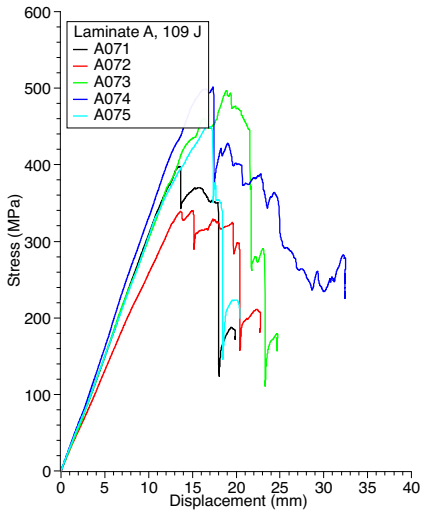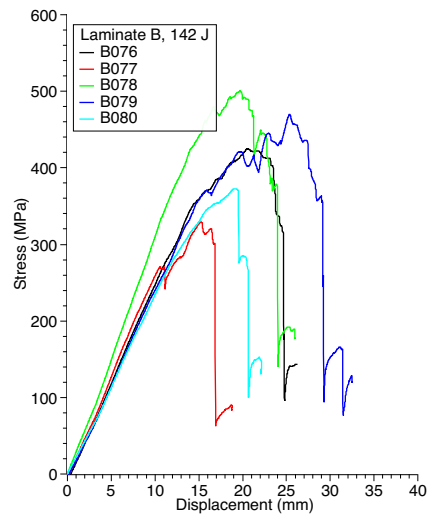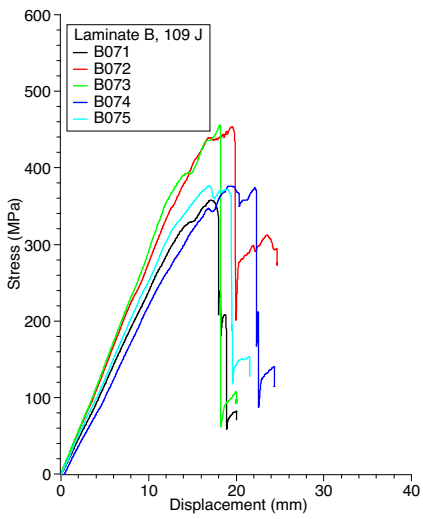
Appendix C - Technical data sheets

SELCOM SRL
via della Torre n. 17
31010 FREGONA (TV) ITALY
phone   +39 0438 585166
modem fax +39 0438 585172
manual fax +39 0438 916049

cap. soc. EURO 101490,00
cod. fisc. e p.i. IT 02369430265
trib. Treviso n. 33642 reg. soc.
c.c.i.a.a. Treviso n. 206094
M. estero TV 028944
E-mail: info@selcom-srl.com

MULTIAXIAL TECHNOLOGY (NCF)
unidirectional & stitched multiaxial fabrics in
glass, carbon, aramid... and hybrids for the
composite industry

internet: www.selcom-srl.com

Technical Data Sheet

PRODUCT NAME **EBXS900M100**	Code
Biaxial fabric 0º 90º in "E" glass stitched with chop strand mat	**01311000900**

layers	angle	fiber	plan	tex	areal weight	areal weight
	tolerance				gr/m²	tolerance
0º	± 1º	PPG Roving 2002	L4	1200 - 600	449	± 3 %
90º	± 1º	PPG Roving 2002	L4	1200	448	± 3 %
random	-	PPG "E" glass 7864	L4	2600 - 2400	100	± 3 %
0º	-	polyester	L4	7,8	9	± 3 %
		TOTAL gr/m²	-	-	1006	± 3 %

Characteristics for fabric

lunghezza rotolo - standard roll length:	mtl 50 ± 1 mtl
larghezza rotolo - standard roll width:	mm 1270 ± 10 mm
peso netto rotolo - net roll weight:	Kg. 64 ± 3 %
tolleranza sulla grammatura – areal weight tolerance:	± 3 % (± 30 gr/m²)
grammatura teorica - theoretical areal weight:	gr/m² 1006
identificazione rotolo - ident roll:	**EBXS900M100**
identification yarn:	two green yarns
tipo di legatura - knitting type:	tricot
filo di legatura – stitch yarn:	polyester, texturated, 7,8 tex

Characteristics for filament yarn

tipo fibra – type:	PPG Roving 2002
binder content:	0.55 – 0.65 % (nominal)
produttore – manufacturer:	PPG Industries
densità volumetrica – volumetric density:	gr/cm³ 2.59 – 2.62
diamentro filamento – filament diameter:	µm 12 - µm 17
resistenza a trazione – tensile strength:	Mpa 1900 – 2400 (ASTM D-2343) *
modulo a trazione – tensile modulus:	Gpa 69 – 76 (ASTM D-2343) *
allungamento a rottura – elongation at break:	3.5 - 4 %

* Determined from resin impregnated rovings according to ASTM D-2343
Fregona li   03/04/12

Quality Assurance
Ing. Giovanni Fardin

NB : THIS DOCUMENT IS COMPUTER GENERATED AND IT'S VALID WITHOUT SIGNATURE

DNV

TYPE APPROVED PRODUCT – CERTIFICATE NO. K-4016

Member of CISQ Federation

RINA
ISO 9001:2008
Certified Quality System

SELCOM SRL
via della Torre n. 17
31010 FREGONA (TV) ITALY
phone   +39 0438 585166
modem fax +39 0438 585172
manual fax +39 0438 916049

cap. soc. EURO 101490,00
cod. fisc. e p.i. IT 02369430265
trib. Treviso n. 33642 reg. soc.
c.c.i.a.a. Treviso n. 206094
M. estero TV 028944
E-mail: info@selcom-srl.com

MULTIAXIAL TECHNOLOGY (NCF)
unidirectional & stitched multiaxial fabrics in glass, carbon, aramid... and hybrids for the composite industry

internet: www.selcom-srl.com

Technical Data Sheet

PRODUCT NAME **EBX800M100**	Code
Biaxial fabric ±45º in "E" glass stitched with chop strand mat	01211000801

layers	angle		fiber	plan	tex	areal weight	areal weight
	tolerance					gr/m²	tolerance
0º	-		Polyester yarn	L6	8,3	7	± 3 %
+ 45º	± 1º		E glass : PPG Roving 2002	L6	600	397	± 3 %
- 45º	± 1º		E glass : PPG Roving 2002	L6	600	397	± 3 %
random	-		E glass : PPG Roving 7864	L6	2600	100	± 3 %
			TOTAL gr/m²	-	-	901	± 3 %

Characteristics for fabric

lunghezza rotolo - standard roll length:	mtl 50 ± 1 mtl
larghezza rotolo - standard roll width:	mm 1270 ± 10 mm
peso netto rotolo - net roll weight:	Kg. 57,5 ± 3 %
tolleranza sulla grammatura – areal weight tolerance:	± 3 % (± 27 gr/m²)
grammatura teorica - theoretical areal weight:	gr/m² 901
identificazione rotolo - ident roll:	**EBX800M100**
tipo di legatura - knitting type:	pillar
filo di legatura – stitch yarn:	polyester, texturated, 8,3 tex

Characteristics for filament yarn

tipo fibra – type:	PPG Roving 2002
binder content:	0.55 – 0.65 % (nominal)
produttore – manufacturer:	PPG Industries
densità volumetrica – volumetric density:	gr/cm³ 2.59 – 2.62
diamentro filamento – filament diameter:	µm 12
resistenza a trazione – tensile strength:	Mpa 1900 – 2400 (ASTM D-2343) *
modulo a trazione – tensile modulus:	Gpa 69 – 76 (ASTM D-2343) *
allungamento a rottura – elongation at break:	3.5 - 4 %

*Determined from resin impregnated rovings according to ASTM D-2343.These informations can be used for material selection purposes only.

Fregona li   19/03/13   Quality Assurance
NB : THIS DOCUMENT IS COMPUTER GENERATED AND IT'S VALID WITHOUT SIGNATURE   Ing. Giovanni Fardin

TYPE APPROVED PRODUCT – CERTIFICATE NO. K-4016

Member of CISQ Federation

RINA
ISO 9001:2008
Certified Quality System

Technical Datasheet
Ashland Performance Materials

AME™ 6001 INF-120 Premium Marine Resin / Infusion

AME 6001 INF-120 Infusion resin is a high performance 100% epoxy vinyl ester resin, that have both excellent processability and superior mechanical properties. AME 6001 INF-120 resin utilizes the proven history of resilience, blister resistance, excellent fatigue life and toughness of AME 6000 resins with new technology that further increases strength and improves surface profile for the boat builder that demands faultless, long lasting performance.

Greater Resistance to Fatigue Failure
Excellent Surface Profiles with Low Shrink
Increased Hydrolysis Resistance
Exceeds ISO 12215-1 Type "A" mechanical requirements
Exceeds DNV Grade "1" mechanical requirements

Typical liquid resin properties

Property at 25 °C	Value	Unit	Method
Viscosity, cone & plate	170	mPas	ISO 2884
Styrene content	39	%	SFS 4864
Geltime, 1,5% Norox MCP-75	120	min	D 006

Typical cured resin properties

Property	Value	Unit	Method
Postcured for 24h at 60 °C			
Tensile strength	79	MPa	ASTM D-638
Tensile modulus	3450	MPa	ASTM D-638
Elongation at break	5,2	%	ASTM D-638
Flexural strength	149	MPa	ASTM D-790
Flexural modulus	3620	MPa	ASTM D-790
Heat Deflection Temperature	91	°C	ASTM D-648
Ultimate Heat Deflection temperature*	111	°C	ASTM D-648
* postcured for 2h at 60°C + 3h at138°C			

Application and use

AME 6001 INF-120 resin is especially recommended for marine applications using the infusion process. AME 6001 INF-120 is designed as a premium resin for high performance off-shore motor and sailing yachts, that remain in the water for an extended period of time.

Remark: For more information on curing characteristics of AME 6001 INF-120 infusion resin and adjustments of inhibitor (NLC-10) and peroxide (MCP-75) levels for optimal curing, please contact your Ashland representative.

ASHLAND.
With good chemistry great things happen.™

Technical Datasheet
Ashland Performance Materials

AME™ 6001 INF-120 Premium Marine Resin / Infusion

Certificates and approvals

AME 6001 INF-120 resin is approved by Lloyd's Register for Special Service Craft.

The manufacturing, quality control and distribution of products, by Ashland Performance Materials, are complying with one or more of the following programs or standards: Responsible Care, ISO 9001, ISO 14001 and OHSAS 18001.

Handling and storage

It is highly recommended that all material is stored at stable temperature under 25 °C preferably indoors, and away from sunlight. Prolonged storage outside of recommended conditions can influence liquid resin properties like viscosity and gel time. It is also strongly recommended to mix resin thoroughly before use. Shelf life of AME 6001 INF-120 is three (3) months.

Notice

All information presented herein is believed to be accurate and reliable, and is solely for the user's consideration, investigation and verification. The information is not to be taken as an express or implied representation or warranty for which Ashland assumes legal responsibility. Any warranties, including warranties of merchantability or non-infringement of intellectual property rights of third parties, are herewith expressly excluded.

Since the user's product formulations, specific use applications and conditions of use are beyond the control of Ashland, Ashland makes no warranty or representation regarding the results which may be obtained by the user. It shall be the responsibility of the user to determine the suitability of any of the products mentioned for the user's specific application.

Ashland requests that the user reads, understands and complies with the information contained herein and the current Material Safety Data Sheet.

ASHLAND.
With good chemistry great things happen.™

Appendix D - Backlight inspection
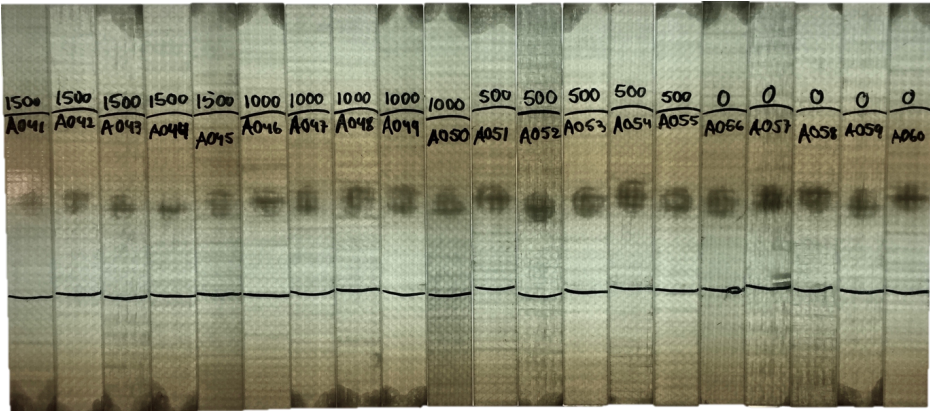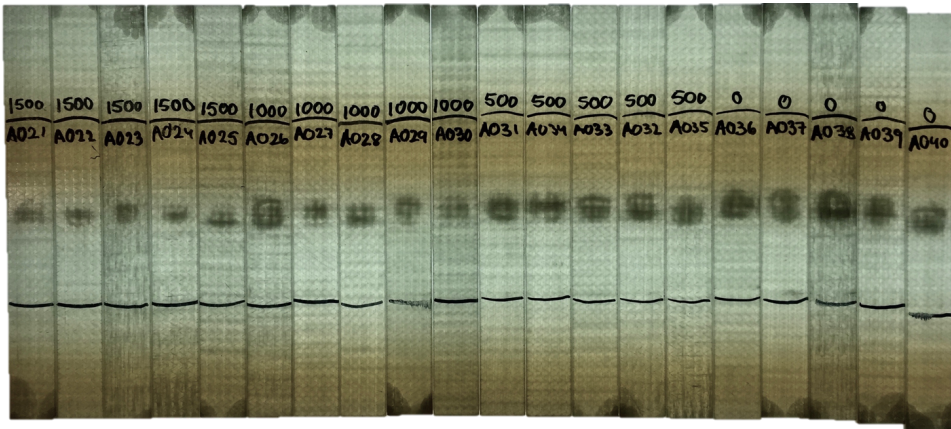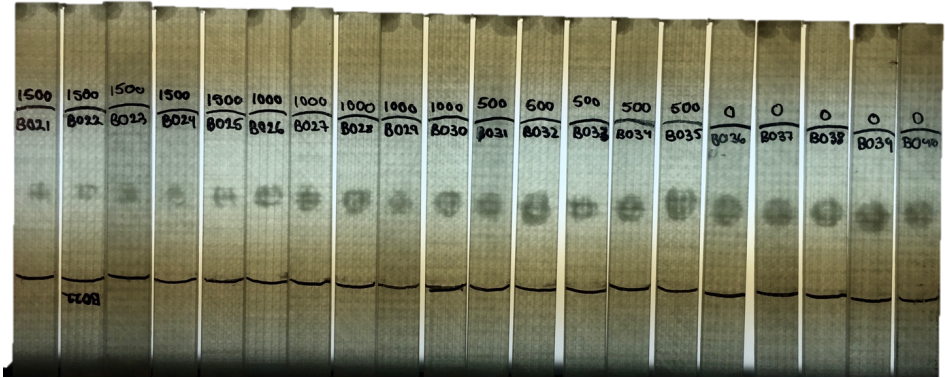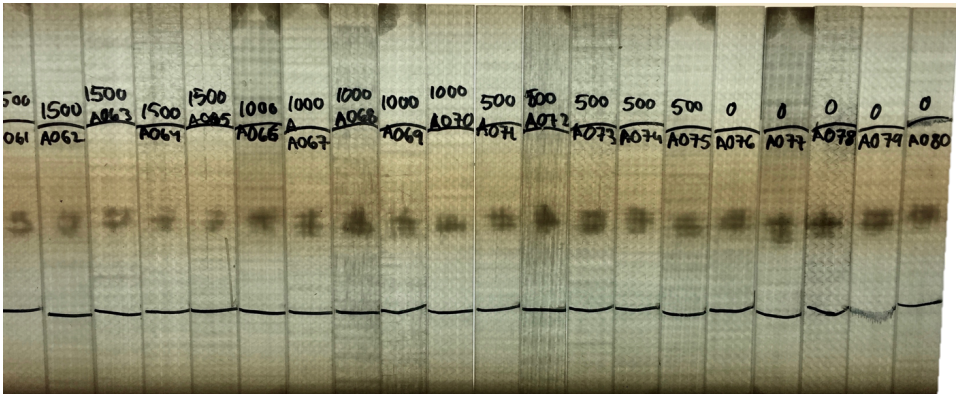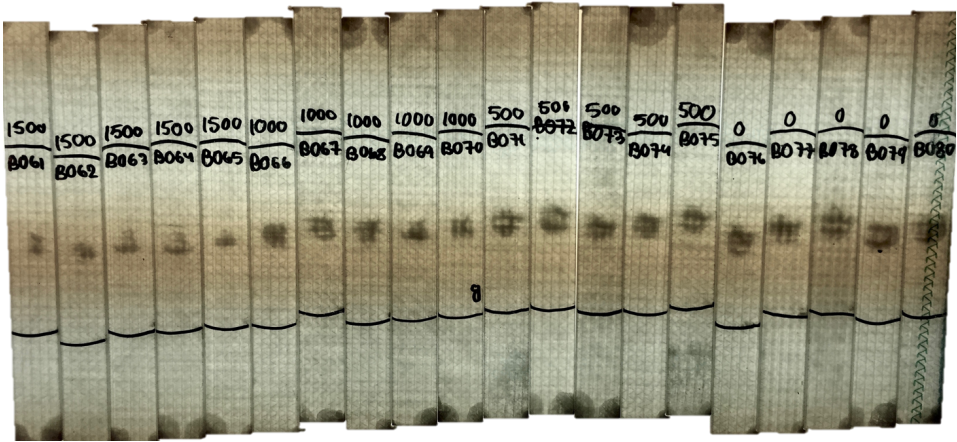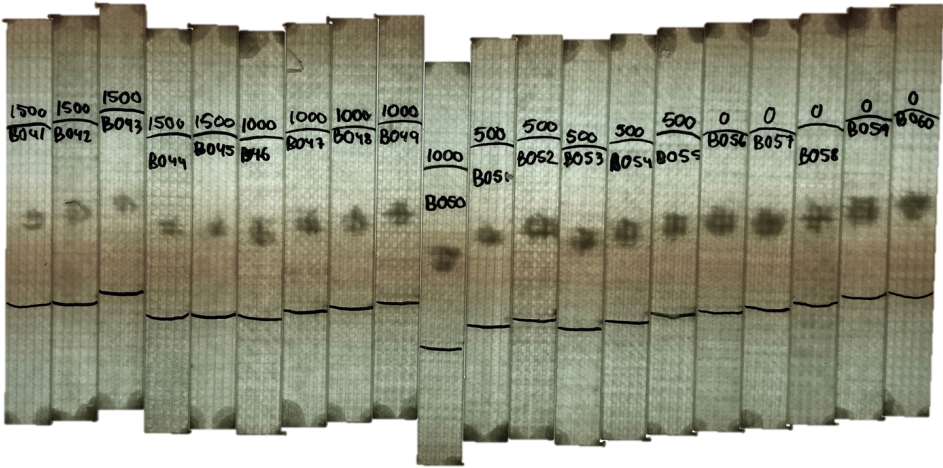
Appendix E - Master thesis assignment

NTNU - NORWEGIAN UNIVERSITY
OF SCIENCE AND TECHNOLOGY
DEPARTMENT OF ENGINEERING DESIGN
AND MATERIALS

MASTER THESIS SPRING 2016
FOR
STUD.TECHN. PÅL DUUS

Residual strength of composite hulls after impact

Reststyrke av kompositt skrog etter mekanisk slag

Composite laminates are used frequently in hulls of small to medium size ships. When these ships hit objects in the sea the hull may get some damage from the impact. This thesis shall measure and model the residual strength of the laminates in tension and compression after impact. Tests shall be done on coupons of hull materials with representative damage. Results shall be used to predict residual strength of full-scale hulls.

Formal requirements:

Three weeks after start of the thesis work, an A3 sheet illustrating the work is to be handed in. A template for this presentation is available on the IPM's web site under the menu "Masteroppgave" (https://www.ntnu.edu/web/ipm/master-thesis). This sheet should be updated one week before the master's thesis is submitted.

Risk assessment of experimental activities shall always be performed. Experimental work defined in the problem description shall be planed and risk assessed up-front and within 3 weeks after receiving the problem text. Any specific experimental activities which are not properly covered by the general risk assessment shall be particularly assessed before performing the experimental work. Risk assessments should be signed by the supervisor and copies shall be included in the appendix of the thesis.

The thesis should include the signed problem text, and be written as a research report with summary both in English and Norwegian, conclusion, literature references, table of contents, etc. During preparation of the text, the candidate should make efforts to create a well arranged and well written report. To ease the evaluation of the thesis, it is important to cross-reference text, tables and figures. For evaluation of the work a thorough discussion of results is appreciated.

The thesis shall be submitted electronically via DAIM, NTNU's system for Digital Archiving and Submission of Master's theses.

Torgeir Welo
Head of Division

Andreas Echtermeyer
Professor/Supervisor

NTNU
Norges teknisk-
naturvitenskapelige universitet
Institutt for produktutvikling
og materialer

Appendix F - Risk assignments

<table>
<tr><td colspan="3">Sikkerhets- og kvalitetsgjennomgang av laboratorietester og verkstedsarbeid
<i>Safety and Quality Evaluation of Activities in the Laboratory and Workshop</i></td><td>◉ NTNU

Perleporten</td></tr>
</table>

1 Identifikasjon - *Identification*	Dokumentnr. – *Document no.*:		
Kundenavn – *Customer name*	Prosjektnavn – *Project name* Residual strenght of composite hulls after impact		Projektnr. – *Project no.*
Beskrivelse av arbeid – *Description of job* Use of impact drop tower on composite coupons			Dato – *Date* 29.01.2016

2 Projekt - *Team*			
Prosjektleder og organisasjon – *Project manager and organisation*	Pål Duus (PD)	Ansvarlig for instrumentering – *Responsible for instrumentation.*	PD
Leiestedsansvarlig – *Laboratory responsible*	PD	Operatør – *Operator*	PD
Auditør for sikkerhets og kvalitetsgjennomgang – *Auditer for safety check*	PD	Ansvarlig for styring av forsøk – *Responsible for running the experiment.*	PD
Ansvarlig for eksperimentelt faglig innhold – *Responsible for experimental and scientific content*	PD	Ansvarlig for logging av forsøksdata – *Responsible for logging and storing experimental data*	PD
Ansvarlig for dimensjonering av last og trykkpåkjente komponenter – *Reponsible for dimensioning load bearing and pressurized components*	PD	Ansvarlig for montering av testrigg – *Responsible for building the rig*	PD

3 Viktig!! – *Important!!*	J: Ja – *Yes* / N: Nei - *No*
Er arbeidsordren signert? – *Is the work order signed?*	J
Har operatøren nødvendig kurs/trening i bruk av utstyret? - *Has the operator the required courses/training on the equipment?*	J
Har operatøren sikkerhetskurs? (påbudt) – *Has the operator followed the safety courses? (mandatory)*	J
Kan jobben gjøres alene? - *Can the work be done alone?*	N

- Dersom ja, er det med visse forbehold (for eksempel, må bruke alarm, ha avtale med noen som kommer innom med jevne mellomrom eller lignende). Dette må vurderes i Seksjon 5.
  If yes, the work may have to be done under special conditions (e. g. must use the alarm, have agreement with somebody coming back periodically or similar). This shall be evaluated in Section 5.

4.1 Sikkerhet – *Safety* (Testen medfører – *The test contains*)			J: Ja – *Yes* / N: Nei - *No*
Stor last – *Big loads*	N	Brannfare – *Danger of fire*	N
Tunge løft – *Heavy lifting*	N	Arbeid i høyden – *Working at heights*	N
Hengende last – *Hanging load*	Y	Hydraulisk trykk – *Hydraulic pressure*	N
Gasstrykk – *Gas pressure*	N	Vanntrykk – *Water pressure*	N
Høy temperatur – *High temperature*	N	Lav temperatur – *Low temperature*	N
Deler i høy hastighet – *Parts at high velocity*	Y	Farlige kjemikalier – *Dangerous chemicals*	N
Sprutakselerasjon ved brudd – *Sudden acceleration at fracture/failure*	N	Forspente komponenter – *Pre-tensioned components*	N
Farlig støv – *Dangerous dust*	N	Kraftig støy – *Severe noise*	N
Klemfare – *Danger of pinching*	N	Roterende deler – *Rotating parts*	N

4.2 Påkrevet verneustyr – *Required safety equipment*			J: Ja – *Yes* / N: Nei - *No*
Briller (påbudt) – *Glasses (mandatory)*	N	Vernesko – *Safety shoes*	N
Hjelm – *Helmet*	N	Hansker – *Gloves*	N
Skjerm – *Screen*	N	Visir – *Visir*	N
Hørselsvern – *Ear protection*	N	Løfteredskap – *Lifting equipment*	N
Yrkessele, fallsele, etc. – *Harness ropes, other measures to prevent falling down.*	N		

Sikkerhets- og kvalitetsgjennomgang av laboratorietester og verkstedsarbeid

NTNU

Perleporten

5.1 Beskrivelse av aktivitet – *Description of the activity (see Appendix)*

Vurdering skal være basert på en skriftlig prosedyre for bruk av maskinen. I enkelte tilfeller kan prosedyre bli beskrevet direkte i tabellen nedenfor.

The evaluation shall be based on a written operating procedure for the machine. For simple cases the procedure can be directly described in the tables below.

Nr.	Beskrivelse av aktivitet – *Description of activity*	Fare - *Danger*	Lov, forskrift o.l. – *Legal requirements*	Prosedyre nr. – *Procedure no.*	Sannsynlighet – *Probability*	Konsekvens – *Consequence*	Risiko – *Risk*
1	Using drop tower	Squeezing fingers/feet	HMS from NTNU	1	2	B	1B
2	Adjusting the drop tower tube	Squeezing fingers underneath the tube	HMS from NTNU	2	2	A	2A

5.2 Korrigerende Tiltak – *Corrective Actions*

Nr.	Korrigerende tiltak – *Corrective action*	Sannsynlighet – *Probability*	Konsekvens – *Consequence*	Risiko – *Risk*	Utført dato – *Date of action*
1	Only drop the dart when people are keeping distance	1	B	1B	29.01.2016
2	Keep fingers away from the tube bottom	1	A	1A	29.01.2016

112

Sikkerhets og kvalitetsgjennomgang av laboratorietester og verkstedsarbeid

◉ NTNU

Perleporten

5.3 Feilkilder – *Reasons for mistakes/errors*

Sjekkliste: Er følgende feilkilder vurdert? – Check list: Is the following considered?   J: Ja – *Yes* / N: Nei - *No*

Tap av strøm – *Loss of electricity*	Y	Overspenning – *Voltage surge*	Y
Elektromagnetisk støy – *Electromagnetic noise*	Y	Manglende aggregatkapasitet av hydraulikk – *Insufficient power of the machine*	Y
Jordfeil – *Electrical earth failure*	Y	Vannsprut – *Water jet*	Y
Ustabilt trykk av hydraulikk/kraft – *Unstable pressure or hydraulic force*	Y	Tilfeldig avbrudd av hydraulikk/kraft – *Unintended interruption of power supply*	Y
Last-/ forskyvnings grenser etablert ? – *Are load and displacement limits established?*	Y	Lekkasjer (slanger/koblinger, etc.) – *Leakage of pipes, hoses, joints, etc.*	Y
Mulige påvirkninger fra andre aktiviteter – *Possible interference from other activities*	Y	Mulige påvirkninger på andre aktiviteter – *Possible interference towards other activities*	Y
Problemer med datalogging og lagring – *Troubles in loading and storage*	Y	Brann i laboratoriet – *Fire in the laboratory*	Y

6 Kalibreringsstatus for utstyr – *Calibration of equipment*

(ex: load cell, extensometer, pressure transducer, etc)

I.D.	Utstyr - *Equipment*	Gyldig til (dato) – *Valid until (date)*
–	–	–

7 Sporbarhet – *Tracebility*

Eksisterer – *Is there*   J: Ja – *Yes* / N: Nei - *No*

Er alle prøvematerialene kjente og identifiserbare? – *Are all experimental materials known and traceable?*	Y
Eksisterer det en plan for markering av alle prøvene? – *Is there a plan for marking all specimens?*	Y
Er dataloggingsutstyret identifisert? – *Is the data aquisition equipment identified?*	Y
Er originaldata lagret uten modifikasjon? – *Are the original data stored safely without modification?*	Y
Eksisterer det en backup-prosedyre? – *Is there a back-up procedure for the data (hard disk crash)?*	Y
Eksisterer det en plan for lagring av prøvestykker etter testing? – *Is there a plan for storing samples after testing?*	Y
Eksisterer en plan for avhending av gamle prøvestykker? – *Is there a plan for disposing of old samples?*	Y

8 Kommentarer – *Comments*

–

9 Signaturer – *Signatures*

Godkjent (dato/sign) – Approved (date/signature)

Prosjektleder – *Project leader*	Verifikatør – *Verifier*	Godkjent – *Approved by*
		Carl-Magnus Midtbø

Rev. 09 – Nov 2013

Page 3 of 7

<table>
<tr><td colspan="2">Sikkerhets- og kvalitetsgjennomgang av laboratorietester og verkstedsarbeid
Safety and Quality Evaluation of Activities in the Laboratory and Workshop</td><td>☐ NTNU

Perleporten</td></tr>
</table>

1 Identifikasjon - *Identification*	**Dokumentnr.** – *Document no.*:	
Kundenavn – *Customer name*	Prosjektnavn – *Project name* Residual strenght of composite hulls after impact	Projektnr. – *Project no.*
Beskrivelse av arbeid – *Description of job* Use of test machines to measure tension/compression/flexural		Dato – *Date* 03.02.2016

2 Projekt - *Team*

Prosjektleder og organisasjon – *Project manager and organisation*	Pål Duus (PD)	Ansvarlig for instrumentering – *Responsible for instrumentation.*	PD
Leiestedsansvarlig – *Laboratory responsible*	PD	Operatør – *Operator*	PD
Auditør for sikkerhets og kvalitetsgjennomgang – *Auditer for safety check*	PD	Ansvarlig for styring av forsøk – *Responsible for running the experiment.*	PD
Ansvarlig for eksperimentelt faglig innhold – *Responsible for experimental and scientific content*	PD	Ansvarlig for logging av forsøksdata – *Responsible for logging and storing experimental data*	PD
Ansvarlig for dimensjonering av last og trykkpåkjente komponenter – *Reponsible for dimensioning load bearing and pressurized components*	PD	Ansvarlig for montering av testrigg – *Responsible for building the rig*	PD

3 Viktig!! – *Important!!* — J: Ja – *Yes* / N: Nei - *No*

Er arbeidsordren signert? – *Is the work order signed?*	J
Har operatøren nødvendig kurs/trening i bruk av utstyret? - *Has the operator the required courses/training on the equipment?*	J
Har operatøren sikkerhetskurs? (påbudt) – *Has the operator followed the safety courses? (mandatory)*	J
Kan jobben gjøres alene? - *Can the work be done alone?*	N

- Dersom ja, er det med visse forbehold (for eksempel, må bruke alarm, ha avtale med noen som kommer innom med jevne mellomrom eller lignende). Dette må vurderes i Seksjon 5.
  If yes, the work may have to be done under special conditions (e. g. must use the alarm, have agreement with somebody coming back periodically or similar). This shall be evaluated in Section 5.

4.1 Sikkerhet – *Safety* (Testen medfører – *The test contains*) — J: Ja – *Yes* / N: Nei - *No*

Stor last – *Big loads*	Y	Brannfare – *Danger of fire*	N
Tunge løft – *Heavy lifting*	N	Arbeid i høyden – *Working at heights*	N
Hengende last – *Hanging load*	N	Hydraulisk trykk – *Hydraulic pressure*	Y
Gasstrykk – *Gas pressure*	N	Vanntrykk – *Water pressure*	N
Høy temperatur – *High temperature*	N	Lav temperatur – *Low temperature*	N
Deler i høy hastighet – *Parts at high velocity*	N	Farlige kjemikalier – *Dangerous chemicals*	N
Sprutakselerasjon ved brudd – *Sudden acceleration at fracture/failure*	Y	Forspente komponenter – *Pre-tensioned components*	Y
Farlig støv – *Dangerous dust*	N	Kraftig støy – *Severe noise*	N
Klemfare – *Danger of pinching*	Y	Roterende deler – *Rotating parts*	N

4.2 Påkrevet verneustyr – *Required safety equipment* — J: Ja – *Yes* / N: Nei - *No*

Briller (påbudt) – *Glasses (mandatory)*	Y	Vernesko – *Safety shoes*	N
Hjelm – *Helmet*	N	Hansker – *Gloves*	N
Skjerm – *Screen*	Y	Visir – *Visir*	N
Hørselsvern – *Ear protection*	N	Løfteredskap – *Lifting equipment*	N
Yrkessele, fallsele, etc. – *Harness ropes, other measures to prevent falling down.*	N		

Rev. 09 – Nov 2013   Page 1 of 7

114

Sikkerhets- og kvalitetsgjennomgang av laboratorietester og verkstedsarbeid

NTNU — Perleporten

5.1 Beskrivelse av aktivitet – *Description of the activity (see Appendix)*

Vurdering skal være basert på en skriftlig prosedyre for bruk av maskinen. I enkelte tilfeller kan prosedyre bli beskrevet direkte i tabellen nedenfor.

The evaluation shall be based on a written operating procedure for the machine. For simple cases the procedure can be directly described in the tables below.

Nr.	Beskrivelse av aktivitet – *Description of activity*	Fare - *Danger*	Lov, forskrift o.l. – *Legal requirements*	Prosedyre nr. – *Procedure no.*	Sannsynlighet – *Probability*	Konsekvens – *Consequence*	Risiko – *Risk*
1	Mounting the coupon	Sqeezing fingers	HMS NTNU	1	3	B	3B
2	Stretching the coupon	Sudden acceleration at fracture/failure	HMS NTNU	2	4	C	4C

5.2 Korrigerende Tiltak – *Corrective Actions*

Nr.	Korrigerende tiltak – *Corrective action*	Sannsynlighet – *Probability*	Konsekvens – *Consequence*	Risiko – *Risk*	Utført dato – *Date of action*
1	Keep fingers away from grips	2	C	2C	01.02.2016
2	Use screen and glasses	2	A	2A	01.02.2016

Sikkerhets og kvalitetsgjennomgang av laboratorietester og verkstedsarbeid

⬛ **NTNU**

Perleporten

5.3 Feilkilder – *Reasons for mistakes/errors*
Sjekkliste: Er følgende feilkilder vurdert? – Check list: Is the following considered?   J: Ja – *Yes* / N: Nei - *No*

Tap av strøm – *Loss of electricity*	Y	Overspenning – *Voltage surge*	Y
Elektromagnetisk støy – *Electromagnetic noise*	Y	Manglende aggregatkapasitet av hydraulikk – *Insufficient power of the machine*	Y
Jordfeil – *Electrical earth failure*	Y	Vannsprut – *Water jet*	Y
Ustabilt trykk av hydraulikk/kraft – *Unstable pressure or hydraulic force*	Y	Tilfeldig avbrudd av hydraulikk/kraft – *Unintended interruption of power supply*	Y
Last-/ forskyvnings grenser etablert ? – *Are load and displacement limits established?*	Y	Lekkasjer (slanger/koblinger, etc.) – *Leakage of pipes, hoses, joints, etc.*	Y
Mulige påvirkninger fra andre aktiviteter – *Possible interference from other activities*	Y	Mulige påvirkninger på andre aktiviteter – *Possible interference towards other activities*	Y
Problemer med datalogging og lagring – *Troubles in loading and storage*	Y	Brann i laboratoriet – *Fire in the laboratory*	Y

6 Kalibreringsstatus for utstyr – *Calibration of equipment*
(ex: load cell, extensometer, pressure transducer, etc)

I.D.	Utstyr - *Equipment*	Gyldig til (dato) – *Valid until (date)*
–	–	–

7 Sporbarhet – *Tracebility*

Eksisterer – Is there   J: Ja – *Yes* / N: Nei - *No*

Er alle prøvematerialene kjente og identifiserbare? – *Are all experimental materials known and traceable?*	Y
Eksisterer det en plan for markering av alle prøvene? – *Is there a plan for marking all specimens?*	Y
Er dataloggingsutstyret identifisert? – *Is the data aquisition equipment identified?*	Y
Er originaldata lagret uten modifikasjon? – *Are the original data stored safely without modification?*	Y
Eksisterer det en backup-prosedyre? – *Is there a back-up procedure for the data (hard disk crash)?*	Y
Eksisterer det en plan for lagring av prøvestykker etter testing? – *Is there a plan for storing samples after testing?*	Y
Eksisterer en plan for avhending av gamle prøvestykker? – *Is there a plan for disposing of old samples?*	Y

8 Kommentarer – *Comments*

–

9 Signaturer – *Signatures*
Godkjent (dato/sign) – Approved (date/signature)

Prosjektleder – *Project leader*	Verifikatør – *Verifier*	Godkjent – *Approved by*
[signature]	*[signature]*	Carl-Magnus Midtbø *[signature]*

Rev. 09 – Nov 2013   Page 3 of 7

Sannsynlighet vurderes etter følgende kriterier:
Probability shall be evaluated using the following criteria:

Svært liten Very unlikely 1	Liten Unlikely 2	Middels Probable 3	Stor Very Probable 4	Svært stor Nearly certain 5
1 gang/50 år eller sjeldnere – *Once per 50 years or less*	1 gang/10 år eller sjeldnere – *Once per 10 years or less*	1 gang/år eller sjeldnere – *Once a year or less*	1 gang/måned eller sjeldnere – *Once a month or less*	Skjer ukentlig – *Once a week*

Konsekvens vurderes etter følgende kriterier:
Consequence shall be evaluated using the following criteria:

Gradering – *Grading*	Menneske – *Human*	Ytre miljø, Vann, jord og luft – *Environment*	Øk/materiell – *Financial/Material*	Omdømme – *Reputation*
E **Svært Alvorlig** – *Very critical*	Død – Death	Svært langvarig og ikke reversibel skade – *Very prolonged, non-reversible damage*	Drifts- eller aktivitetsstans >1 år. – *Shutdown of work >1 year.*	Troverdighet og respekt betydelig og varig svekket – *Trustworthiness and respect are severely reduced for a long time.*
D **Alvorlig** – *Critical*	Alvorlig personskade. Mulig uførhet. – *May produce fatality/ies*	Langvarig skade. Lang restitusjonstid – *Prolonged damage. Long recovery time.*	Driftsstans > ½ år Aktivitetsstans i opp til 1 år – *Shutdown of work 0,5-1 year.*	Troverdighet og respekt betydelig svekket – *Trustworthiness and respect are severely reduced.*
C **Moderat** – *Dangerous*	Alvorlig personskade. – *Permanent injury, may produce serious health damage/sickness*	Mindre skade og lang restitusjonstid – *Minor damage. Long recovery time*	Drifts- eller aktivitetsstans < 1 mnd – *Shutdown of work < 1 month.*	Troverdighet og respekt svekket – *Troverdighet og respekt svekket.*
B **Liten** – *Relatively safe*	Skade som krever medisinsk behandling – *Injury that requires medical treatment*	Mindre skade og kort restitusjonstid – *Minor damage. Short recovery time*	Drifts- eller aktivitetsstans < 1uke – *Shutdown of work < 1 week.*	Negativ påvirkning på troverdighet og respekt – *Negative influence on trustworthiness and respect.*
A **Siker** - Safe	Injury that requires first aid	Insignificant damage. Short recovery time	Shutdown of work < 1day	

Risikoverdi = **Sannsynlighet X Konsekvenser**
Beregn risikoverdi for menneske. IPM vurderer selv om de i tillegg beregner risikoverdi for ytre miljø, økonomie/ material og omdømme. I så fall beregnes disse hver for seg.

Risk = **Probability X Consequence**
Calculate risk level for humans. IPM shall evaluate itself if it shall calculate in addition risk for the environment, economic/material and reputation. If so, the risks shall be calculated separately.

Risikomatrisen

Risk Matrix

I risikomatrisen er ulike grader av risiko merket med rød, gul eller grønn:

Rød: Uakseptabel risiko. Tiltak skal gjennomføres for å redusere riskoen.

Gul: Vurderingsområde. Tiltak skal vurderes.

Grønn: Akseptabel risiko. Tiltak kan vurderes ut fra andre hensyn.

Når risikoverdien havner på rødt felt, skal altså enheten gjennomføre tiltak for å redusere risikoen. Etter at tiltak er iverksatt, skal dere foreta ny risikovurdering for å se om risikoen har sunket til akseptabelt nivå.

For å få oversikt over samlet risiko: Skriv risikoverdi og aktivitetens IDnr. i risikomatrise (docx) / risikomatrise (odt). Eksempel: Aktivitet med IDnr. 1 har fått risikoverdi 3D. I felt 3D i risikomatrisen skriver du IDnr. 1. Gjør likedan for alle aktiviteter som har fått en risikoverdi. En annen måte å skaffe oversikt på, er å fargelegge feltet med risikoverdien i skjemaet for risikovurdering. Dette tydeliggjør og gir samlet oversikt over riskoforholdene. Ledelse og brukere får slik et godt bilde av risikoforhold og hva som må prioriteres.

In the risk matrix different degrees of risk are marked with red, yellow or green;

Red: Unacceptable risk. Measures shall be taken to reduce the risk.

Yellow: Assessment Area . Measures to be considered.

Green: Acceptable risk. Measures can be evaluated based on other considerations.

When a risk value is red, the unit shall implement measures to reduce risk. After the action is taken, you will make a new risk assessment to see if the risk has decreased to acceptable levels.

To get an overview of the overall risk: Write the risk value and the task ID no . the risk matrix (docx) / risk matrix (odt) . Example : Activity with ID no . 1 has been risk value 3D. In the field of 3D risk matrix type ID no . 1 Do the same for all activities that have been a risk . Another way to get an overview is to color the field of risk value in the form of risk assessment . This clarifies and gives overview of the risk factors . Management and users get such a good picture of the risks and what needs to be prioritized.

KONSEKVENS	Svært alvorlig	E1	E2	E3	E4	E5
	Alvorlig	D1	D2	D3	D4	D5
	Moderat	C1	C2	C3	C4	C5
	Liten	B1	B2	B3	B4	B5
	Svært liten	A1	A2	A3	A4	A5
		Svært liten	Liten	Middels	Stor	Svært stor
		SANNSYNLIGHET				

Prinsipp over akseptkriterium. Forklaring av fargene som er brukt i risikomatrisen.

Farge	Beskrivelse
Rød	Uakseptabel risiko. Tiltak skal gjennomføres for å redusere risikoen.
Gul	Vurderingsområde. Tiltak skal vurderes.
Grønn	Akseptabel risiko. Tiltak kan vurderes ut fra andre hensyn.

Til Kolonnen "Korrigerende Tiltak":
Tiltak kan påvirke både sannsynlighet og konsekvens. Prioriter tiltak som kan forhindre at hendelsen inntreffer, dvs sannsynlighetsreduserende tiltak foran skjerpende beredskap, dvs konsekvensreduserende tiltak.

For Column "Corrective Actions"
Corrections can influence both probability and consequence. Prioritize actions that can prevent an event from happening.

Oppfølging:
Tiltak fra risikovurderingen skal følges opp gjennom en handlingsplan med ansvarlige personer og tidsfrister.

Follow Up
Actions from the risk evaluation shall be followed through by an action plan with responsible persons and time limits.

Etterarbeid #

- Gå gjennom aktiviteten/prosessen på nytt.
- Foreta eventuell ny befaring av aktiviteten/prosessen for enten a) å få bekreftet at risikoverdiene er akseptable eller b) for å justere risikoverdiene.
- Gå gjennom, vurder og prioriter tiltak for å forebygge uønskede hendelser. Først skal dere prioritere tiltak som reduserer sannsynlighet for risiko. Dernest skal dere ta for dere tiltak som reduserer risiko for konsekvenser.
- Tiltakene skal føres inn i handlingsplanen. Skriv fristen for å gjennomføre tiltaket (dato, ikke tidsrom) og navn på den / de som har ansvar for tiltakene.
- Foreta helhetsvurdering for å avgjøre om det nå er akseptabel risiko.
- Ferdig risikovurdering danner grunnlag for å utarbeide lokale retningslinjer og HMS-dokumenter, opplæring og valg av sikkerhetsutstyr.
- Ferdig risikovurdering og eventuelle nye retningslinjer gjøres kjent/tilgjengelig for alle involverte.
- Sett eventuelt opp kostnadsoverslag over planlagte tiltak.

120